POLYCONDUCTOR THERMAL WATTMETER

A Thesis

Presented to

The Faculty of Graduate Studies

University of Manitoba

In Partial Fulfillment

of the Requirements for the Degree

Master of Science

Electrical Engineering Department

---

by

James Gordon Maciejko

March 1975

POLYCONDUCTOR THERMAL WATTMETER

BY

JAMES GORDON MACIEJKO

A thesis submitted to the Faculty of Graduate Studies of
the University of Manitoba in partial fulfillment of the requirements
of the degree of

MASTER OF SCIENCE

ACKNOWLEDGEMENT

I would like to especially thank Dr. M. A. K. Hamid, my advisor, the staff of the Electrical Engineering Department, Mr. C. Ward, Mr. J. Taylor and my friends and associates for their unyeilding assistance without which this thesis would not be possible,

Thanks are due to Manitoba Hydro for their financial assistance.

Particular thanks to Diann Dyck, Mrs. Chris Hulse and Donavan Hulse for their cooperation in typing this thesis.

ABSTRACT

The thesis presents a thermal wattmeter which using a new matal oxide type of polyconductor (Moxie) for the sensing elements and which could be incorporated in a watthour meter for remote reading of on line energy consumption of a load. The basic feature of this semiconductor is that its terminal resistance can vary by many orders of magnitude for a small change in input power during transition, thus accounting for the high sensitivity of the wattmeter. The sensing circuit makes use of the approximate square law characteristics of two polyconductors to provide the necessary multiplication of the instantaneous current and voltage required in wattmeter operation. In order to correct for ambient temperature fluctuations in the wattmeter circuit investigated,a novel temperature compensation network is incorporated and which generates heating pulses with frequency determined by the ambient temperature. The main drawback associated with the accuracy of the experimental meter is due to the hysteresis phenomenon inherent in the polyconductor used and is partially overcome by the manner in which the pair of polyconductors are used resulting in a uncertainty of 1.0%. Other factors are also investigated such as

transient power pulse, step temperature fluctuations and harmonic content of the line power.

TABLE OF CONTENTS

LIST OF FIGURES

LIST OF TABLES

CHAPTER I

INTRODUCTION

Many electrical engineers are constantly engaged in a struggle to improve existing electrical equipment with newly developed devices and novel ideas. Their efforts have led to many intriguing developments in electromagnetic field, control, satellite and space communication and telemetry technology. Inspite of these advances it is astonishing to realize how electric power is metered in domestic and industrial installations. Current meters require the employment of manually recorded readouts to control and monitor power flows. In addition, these power recordings serve no value as real time information sources. Any effort to economically solve this problem will be of great interest to those engaged in power generation, distribution, and consumer billing industry.

The first universal application automatic remote meter reading and load control system was developed by the Plessey Electronics Group (1). The system alters the existing induction type watthour meter with a mechanical to electrical device which changes state after a "unit" of energy has been consumed. The state of the

device is interrogated regularly, and frequently enough to count every unit consumed. Louisiana Power and Light Company have an experimental residential load control system (2) AMRAC (acronym for automatic meter reading and control) similiar to the Plessey Group system. Steps are taken in converting to remotely read meters but an average annual meter-reading cost of one dollar per meter per year is too small a quarry to justify only automatic power meter reading (3), as was the economic situation fourteen years ago but with time the economics will overrule the meter man in favour of automatic remote meter reading (18).

The scope of this thesis is to investigate the use of a new device in a power metering instrument. The new wattmeter in this study was investigated in hopes of developing a meter which would easily lend itself to remote meter reading applications. In this case, the output of the meter is to be already in a electrical form thus not necessitating the use of mechanical to electrical convertors currently employed. The new device investigated has associated problems with which original designs and ideas were needed to complete the study. The philosophy employed in this thesis is to utilize a semiconductor device (Moxie,Metal-Oxide) to sense a portion of the power flowing in the line. In this sense it is

similiar to the transformerless and transformer type thermal wattmeters developed by Hagan (4) and Lincoln Electric (5) which are discussed in Chapter 3.

The device used is a Moxie, which is a trade name for a polyconductor (vanadium dioxide, VO_2) film which undergoes a change of several orders of magnitude in its terminal resistance for typically a few degrees °C. change from ambient temperature. The device is non-linear but its terminal resistance vs temperature characteristic can be approximated piecewise to exhibit three logarithmically linear ranges, the second of which gives the square law response required in a wattmeter. The basic characteristics of Moxie devices are discussed in Chapter 2.

The original design details incorporated in this study include a novel method of ambient temperature fluctuation compensation and utilization of the polyconductor in a thermal wattmeter which are presented in Chapter 4.

The device has an approximate square law response which is also found in other thermoelements currently manufactured. Substitution of this device for the others mainly stems from the large sensitivity as discussed in Chapter 3.

To date there has been no other attempt to employ Moxies in a thermal wattmeter but numerous thermal watt-

meters employing conventional thermoelements have been investigated and a brief summary is also presented in Chapter 3.

The instrument presented in Chapter 4 and results of which we presented in Chapter 5 is designed and constructed by the author in search of a meter which would solve some of the problems inherent in present meters and one which unfortunately introduces new problems not realized with conventional instruments. The problems related to accuracy and their suggested solutions are discussed in Chapter 6 and Chapter 7. Some of these could not be overcome due to the present inadequate technological state of manufactured Moxies. The Moxie devices employed were far from ideal but nevertheless were utilized in the testing of the instrument.

CHAPTER 2

TRANSITION METAL POLYCONDUCTORS

2.1 General Characteristics

Transition Metal Polyconductors, more commonly called Moxies, are solid state devices (see Fig. 2.1) which exhibit changes in physical properties due to a phase change in the polyconductor crystal structure (6). The physical property which has been exploited is that of resistance, specifically, the resistance of a typical device which will switch from 200KΩ to 300Ω when subjected to thermal energy. An ideal terminal resistance vs temperature characteristic is shown in Fig. 2.2. The three logarithmically linear regions (pre-transition, transition post transition) are clearly illustrated. The region of most interest is the transition region where a linear relationship is evident. The value R_b is the resistance value before transition and R_c is the value after transition. T_b and T_c are the temperatures at which switching from a low conductivity state to a high conductivity state begins and ends respectively. These four values (R_b, R_c, T_b, T_c) can be controlled by commercial manufacturing processes.

FIGURE 2.1

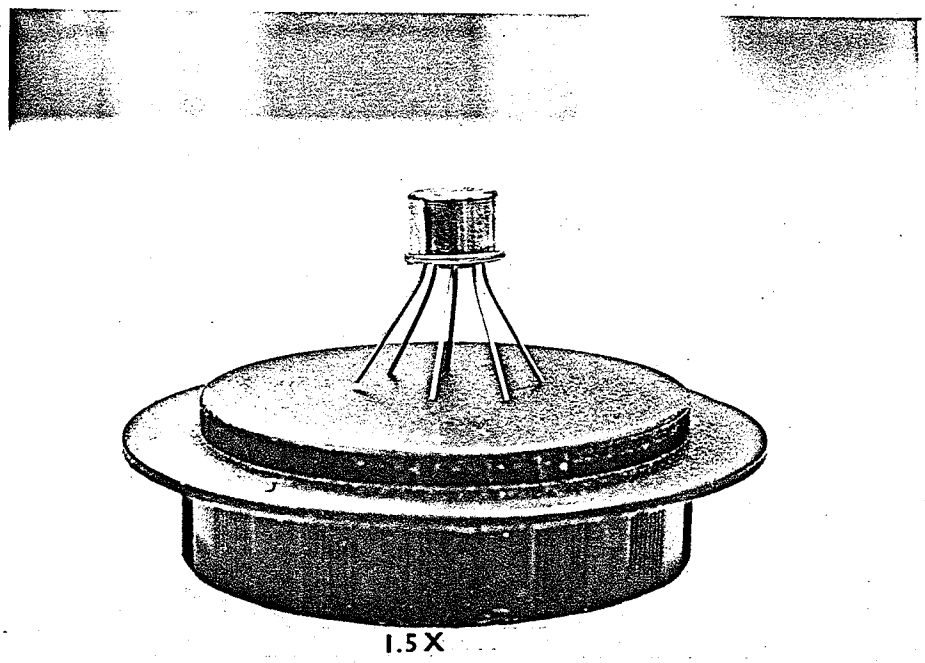

1.5X

DUAL TC1-F 5v MOXIE

FIGURE 2.2

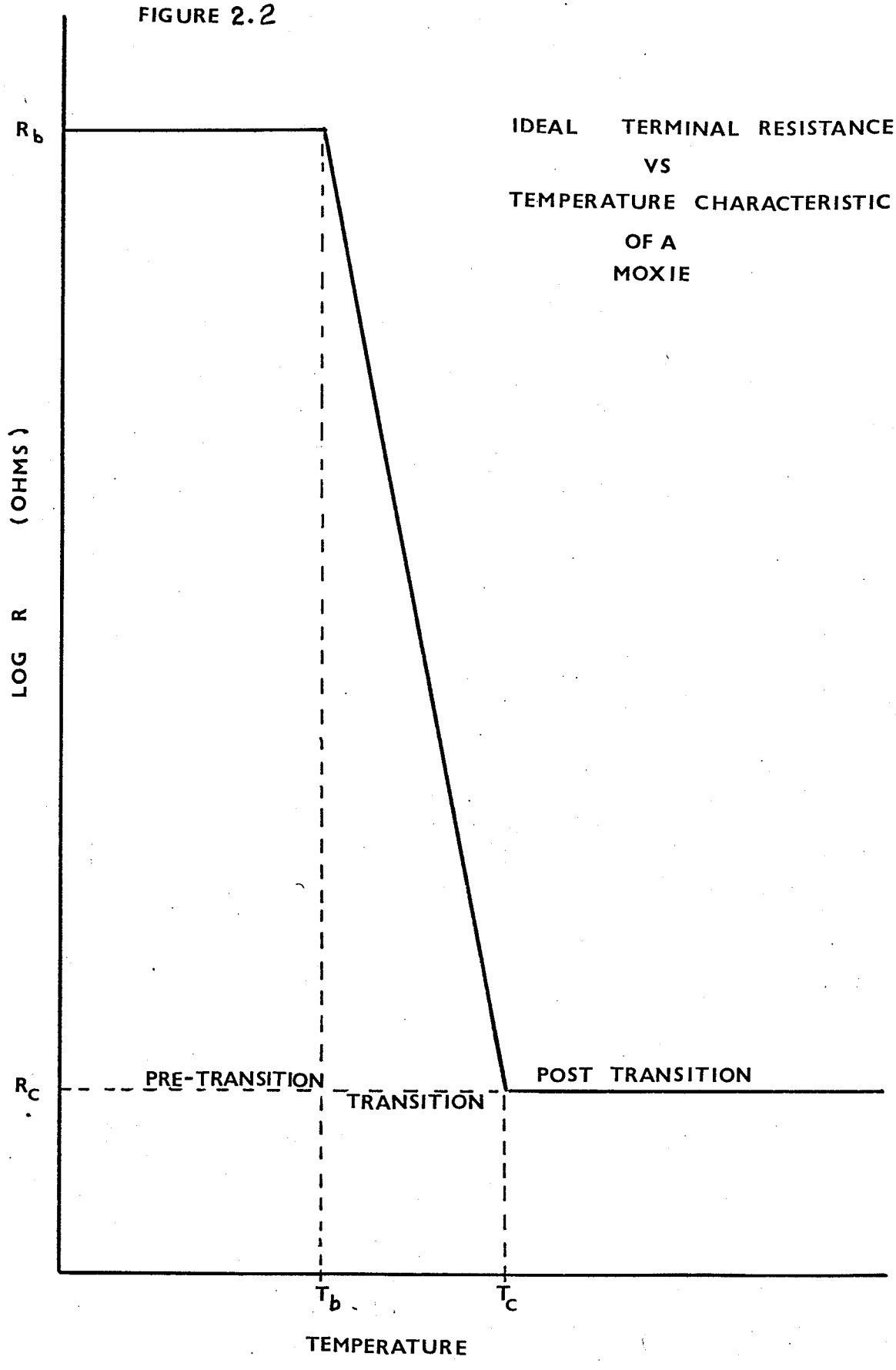
IDEAL TERMINAL RESISTANCE
VS
TEMPERATURE CHARACTERISTIC
OF A
MOXIE
R_b
R_c
LOG R (OHMS)
PRE-TRANSITION
TRANSITION
POST TRANSITION
T_b
T_c
TEMPERATURE

The power required for switching a Moxie device is approximately 150 mw (7) when the Moxie chip is the 65 °C. switching temperature type and ambient air is at room temperature. When the air temperature increases the input power required decreases as the Moxie is "pushed" further towards total transition.

The Moxies are currently being manufactured with transition temperatures of 57,65,75,85 and 140 °C. The switching from a low to high conductivity varies from a high speed "on-off" action to a slow transition requiring substantially longer switching time. As the device returns to low conductivity state (after being switched), it does so by tracing a hysteresis (temperature lag) as illustrated by the typical plot of terminal resistance vs temperature curve shown in Fig. 2.3, (6). This graph illustrates a high speed polyconductor with its transition from high to low, or viceversa, requiring only a few degrees C to complete.

The commercial fabrication of the device involves deposition of the polyconductor, in the form of a thin film onto a suitable substrate (Fig. 2.4) as sapphire, protection of the film by means of a passivation layer of silicon dioxide, the attachment of contacts (Fig. 2.5) and final packaging in either a hermetically sealed tin header or ceramic package. The sensitivity of such a device to changes in temperature is dependent on the combined heat

FIGURE 2.3 TYPICAL TERMINAL RESISTANCE VS TEMPERATURE CHARACTERISTIC OF A MOXIE

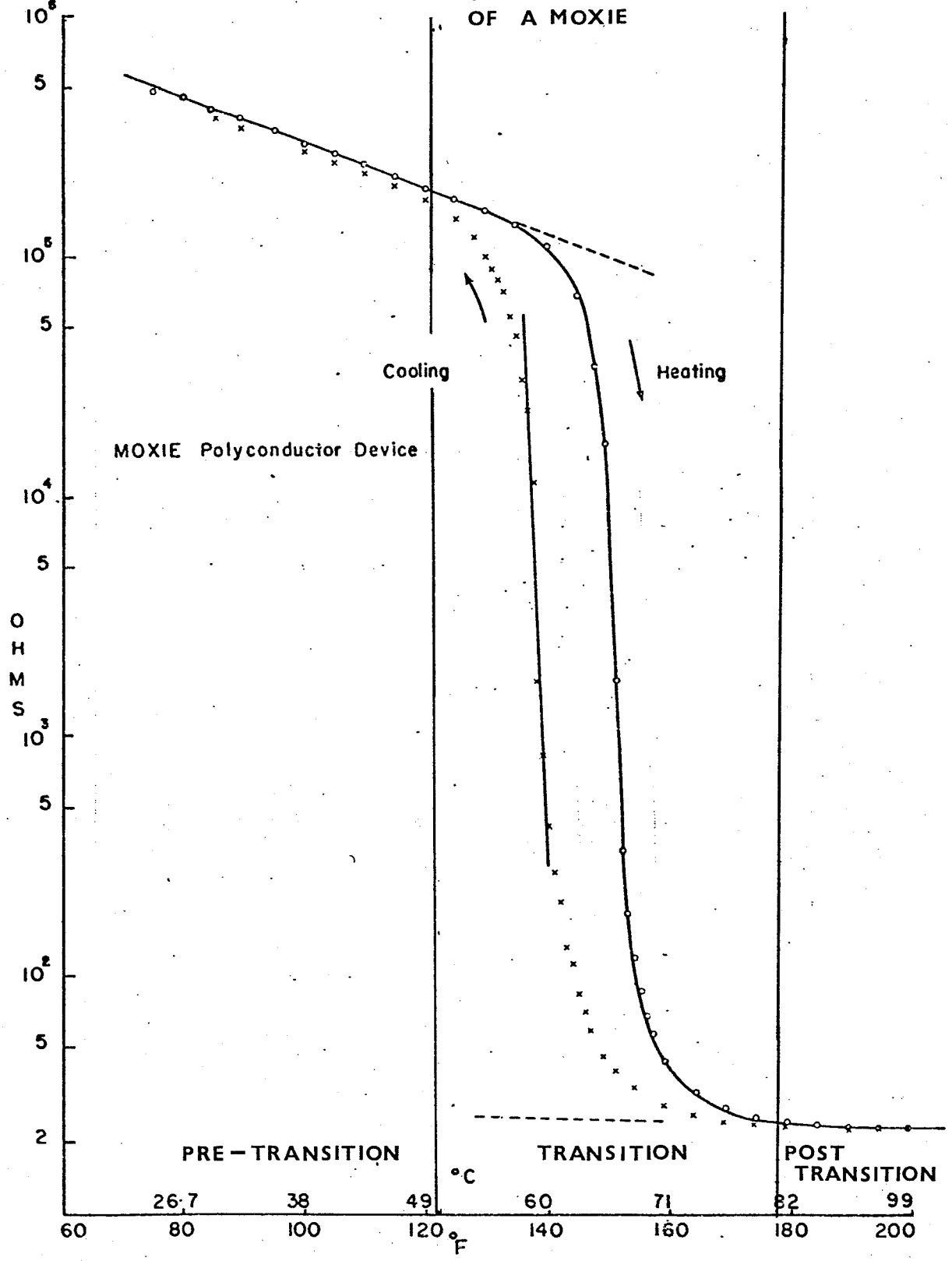

FIGURE 2.4

VO2 POLYCONDUCTOR FILMS

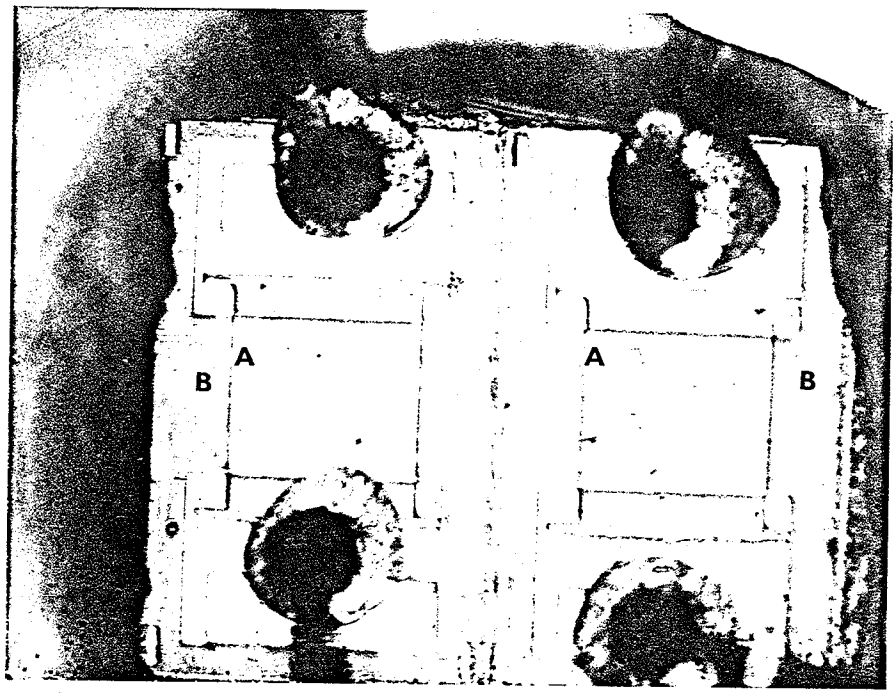

170 X

A - VO2 FILMS
B - SUBSTRATE

FIGURE 2.5

DUAL TCIF-5V MOXIE

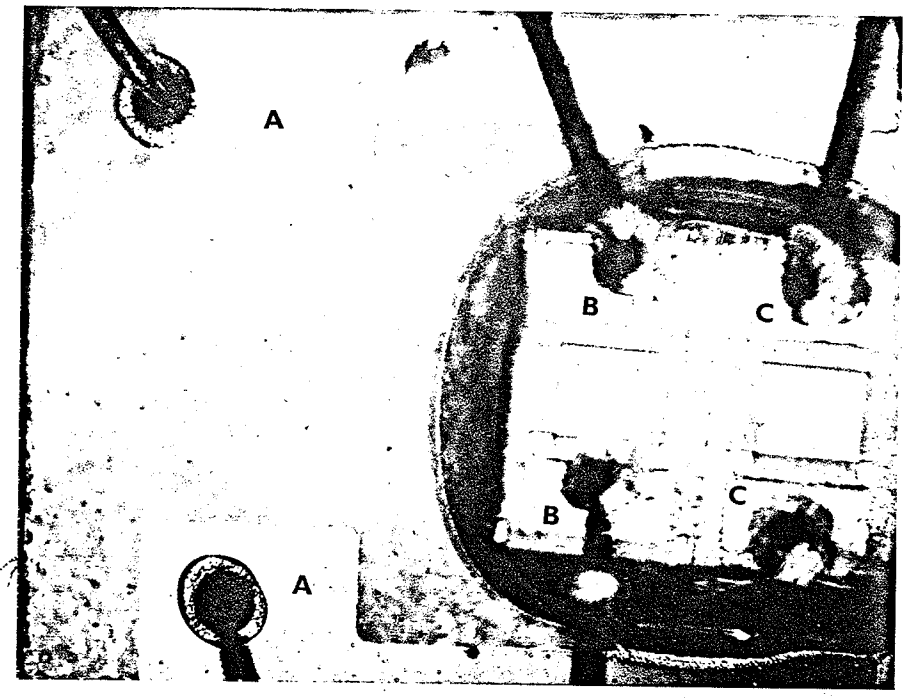

101 X

A- HEATER CONTACTS
B- VO2 FILM CONTACTS
C- VO2 FILM CONTACTS

capacity and thermal conductivity of the film, the substrate, the contact leads and the mass of the package with which the substrate is in intimate contact. The switching speed of the polyconductor is dependent on heat flow through and heat loss by the various materials used in mounting and packaging the film. Thermal coupler Moxie devices have heaters in contact with the substrate to provide the thermal energy required for a state change. In this case, because the heater and the substrate are in immediate contact, the speed of response of the film depends mainly on heat flow through the substrate. The extremely fast switching thermal couplers have a thin film resistive heating element deposited directly on top of the very thin silicon dioxide passivation layer covering the polyconductor. Switching speeds in the low microsecond range have been observed with high peak pulse power supplied to the heater. Various heater resistances can be obtained from the manufacturer, but are typically manufactured for 5,12, and 24V operation.

One of the fundamental drawbacks of Moxie devices is the hysteresis effect previously mentioned which limits its application in precision instrumentation. A linear axis plot of the polyconductor temperature hysteresis graph is shown in Fig. 2.6. This graph was experimentally obtained from the dual TCl-F 5V Moxies employed in this

FIGURE 2.6 TEMPERATURE HYSTERESIS CURVE

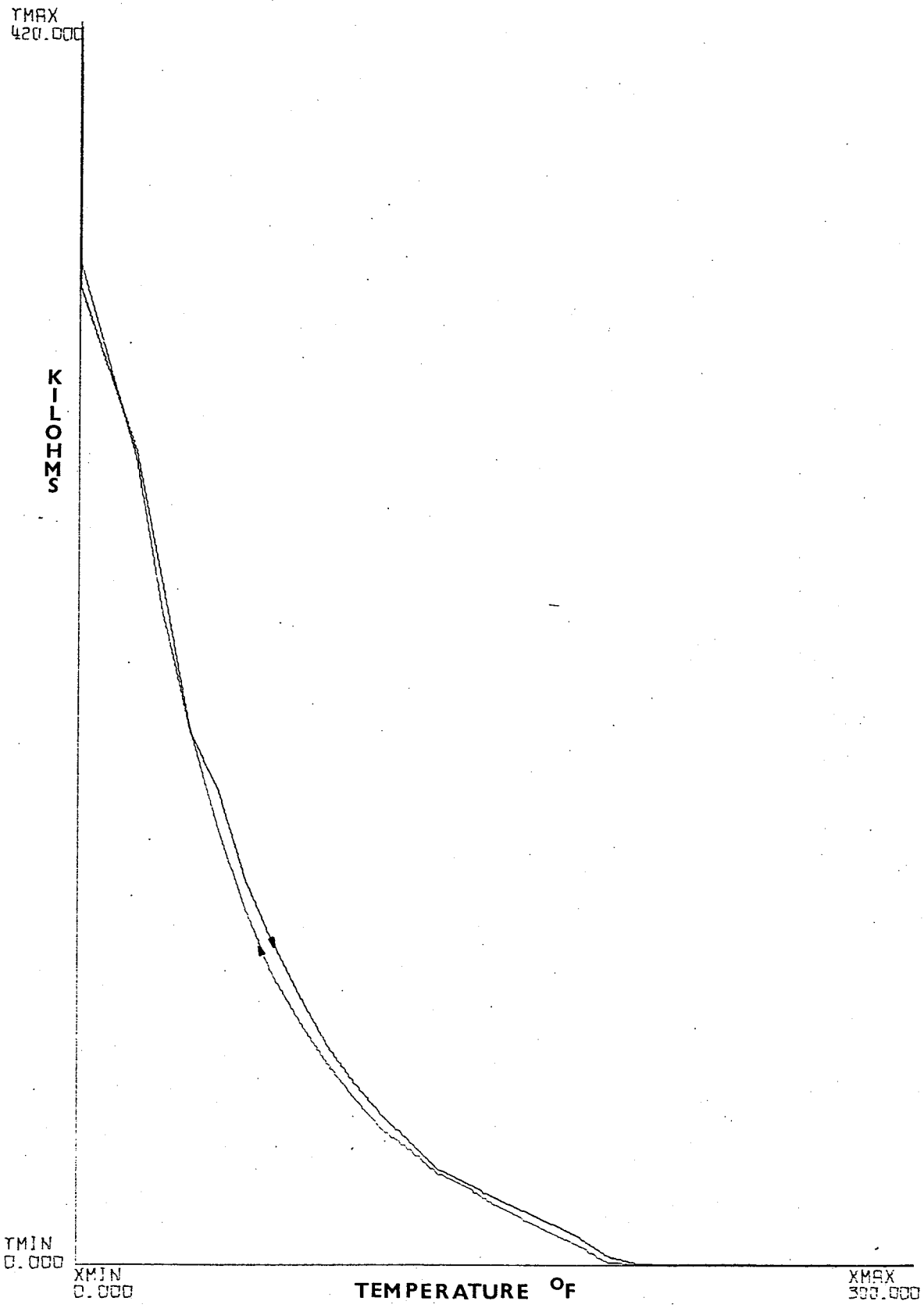

investigation. The upper curve illustrates the heating portion and the lower the cooling portion. The extreme lower portion of the curve is narrow. The transition region is stretched out as it goes through a greater order of magnitude change in this region. The main requirement of the Moxie device in this investigation is a slow switching characteristic which will produce an expanded transition region, thus enlarging the monitoring range available for instrument operation. The peak value reached for the dual TC1-F 5V Moxie tested is 420 KΩ at 0°F and the minimal value of 60Ω is reached at 300°F. This device therefore goes through an enormous magnitude change when exposed to a few hundred °F temperature variation.

The hysteresis curve of interest would naturally be the portion corresponding to above room temperature. This part of the curve is shown in Fig. 2.7 with the hysteresis curve plotted against the power applied to the heater of the Moxie device. The useful range is from 90 KΩ to 1 KΩ where the device still exhibits a substantial magnitude of transition.

2.2 Typical Applications

Most of the existing applications of Transition

FIGURE 2.7 HYSTERESIS CURVE OF MOXIE

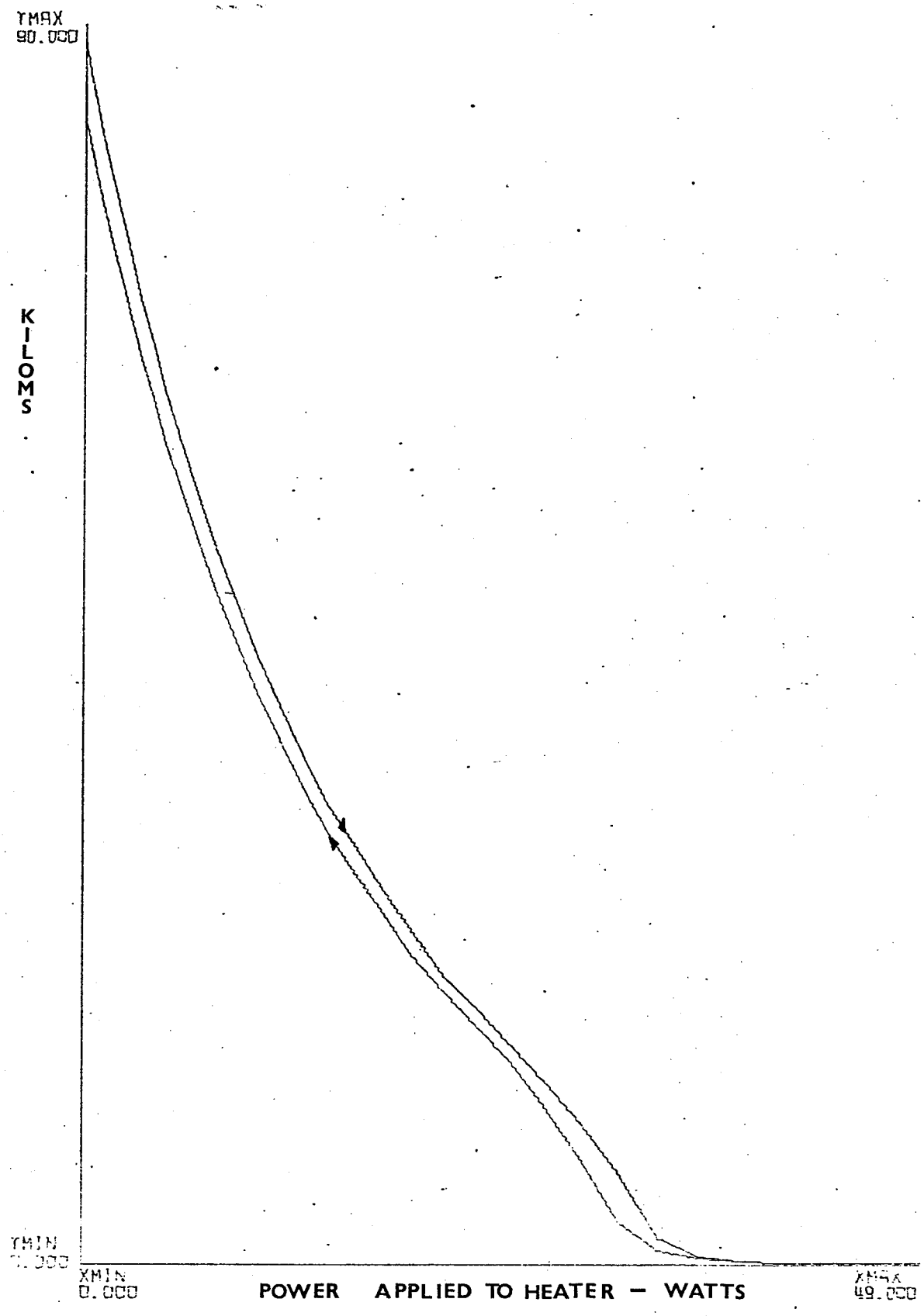

Metal Polyconductors exploit the indirect heating feature of Moxies. Here the device is on a substrate and senses temperature variations due to electric power applied to a heater (Thermal Coupler) or direct heating of the enclosed air (tin header type) or the ceramic package. Fig. 2.1 shows the TC1-F 5V utilized in this study. An enlargement of the VO_2 polyconductor films and substrate on which they are mounted is shown in Fig. 2.4.

The Thermal Sensor is best suited for detecting thermal overloads and applying a suitable feedback network to correct the overload condition or disconnect its source. Some of the configuration in which Moxie devices have been used in this manner are lamp dimmer protection, power supply protection, temperature stabilized operational amplifiers, and fire detectors (12).

Thermal Coupler Moxies have been utilized to convert electrical overloads to thermal energy and thus initiate the transition of the polyconductor to apply suitable corrective or interruptive feedback. Existing application of this type are fast charging of nickel cadium batteries with automatic shut down, current overload protection and electronic rate of battery charge control.

The Moxies have been applied in other forms of energy conditions as the acoustic, optical, microwave, and nuclear have been reported utilizing suitable modifications of the physical structure of the device (8).

CHAPTER 3

INDUCTION TYPE WATTHOUR METER

3.1 General Description

Although electronic watthour meters have been designed, their complexity explains why the induction type integrating meters remain in use (9). The induction type meter is operated by the action of alternating magnetic fluxes on the eddy currents produced by them, it is braked by eddy currents in the field of a permanent magnet. Rotational equilibrium is set up with a permanent magnet brake so that the number of revolutions performed by the induction meter is a measure of the electrical energy consumed by the load and registered by a revolution counter.

3.2 Advantage of Induction Type Energy Meter

The main advantages of the induction type meter is its simplicity and low cost. Induction type watthour meters are built to withstand specification of 1% error almost throughout the rated current and rated voltage. (This is in accordance to international IEC recommend-

ations, the error should not exceed ±2% for either unity or .5 lagging power factor from 10% basic current to maximum overload current.)

3.3 Operational Errors

The main types of errors associated with the implementation of the commercially manufactured induction watthour meters are of human, mechanical, electrical, and enviromental origin.

The main cause of error is the human oriented type which includes improperly made connections during the installation of the meter or poor workmanship during the manufacturing of the meter (14). Some mechanical associated errors result from friction and bearing wear from vibration. The frictional torque is compensated by an equal and opposite constant excess torque generated by the line voltage. The bearings are spring loaded to overcome vibrational effects.

The electrical associated error arise from variations in frequency, voltage and waveform (harmonics). An increase in frequency decreases flux density, exciting current and iron losses, thus producing an erronious torque. Variations from the voltage causes a change in the friction compensating torque and also the flux density in the voltage core. The error associated with flux density

in voltage core increases with decreasing power factor. The waveform variation can cause an increase or decrease in the flux density thus increasing or decreasing the magnetizing component of exciting currents and affecting the torque produced.

The enviromental associated errors are lightning and atmospheric conditions as dust, humidity and bacteria. Lightning destroys the braking action of the permanent magnet brake. The atmospheric impurities and particles attack the mechanical structure but protection from these is easily attained with air tight seals.

3.4 Proposed Wattmeter

The wattmeter in this study was built in an attempt to overcome some of the basic problems of induction type meters mentioned in the previous section. The device used is of the Moxie type and consists of a heater and a sensor used in the basic thermal wattmeter philosophy as discussed in the next section. Although the meter built is a wattmeter there are integrating schemes available for conversion to a watthour meter. This watthour meter could lend itself to the remote meter applications referred to in Chapter 1 or a more recent scheme employed in Edmonton which is read by a helicopter (14).

The expected advantages of the proposed meter once

developed commercially are the small size, possible lower cost, easily adapted to remote meter reading schemes, and possible higher accuracy.

3.5 Basic Thermal Wattmeters

Most existing types of thermal wattmeters incorporate two basic types of circuitry. One type uses transformers to do the required mathematical manipulation while the other type uses a resistive bridge network.

The basic principle of a thermal wattmeter was first published in 1903 by Bauch (10), according to whom the instaneous values of currents through the heating branches (Fig. 3.1) should be expressed in the form

$$i1=C1v + C2i \qquad (3.1)$$

$$i2=C1v - C2i \qquad (3.2)$$

where v and i are the instantaneous load voltage and current and C1 and C2 are constants. Since these currents are squared (ideally) in the heaters, the outputs M1 and M2 of the two thermoelements will be of the form:

$$M1=(C1v)^2 + 2C1C2vi + (C2i)^2 \qquad (3.3)$$

$$M2=(C1v)^2 - 2C1C2vi + (C2i)^2 \qquad (3.4)$$

If the difference between the two outputs is taken, the desired quantity of instantaneous power emerges in the form

$$M1 - M2 = 4C1C2vi \qquad (3.5)$$

FIGURE 3.1

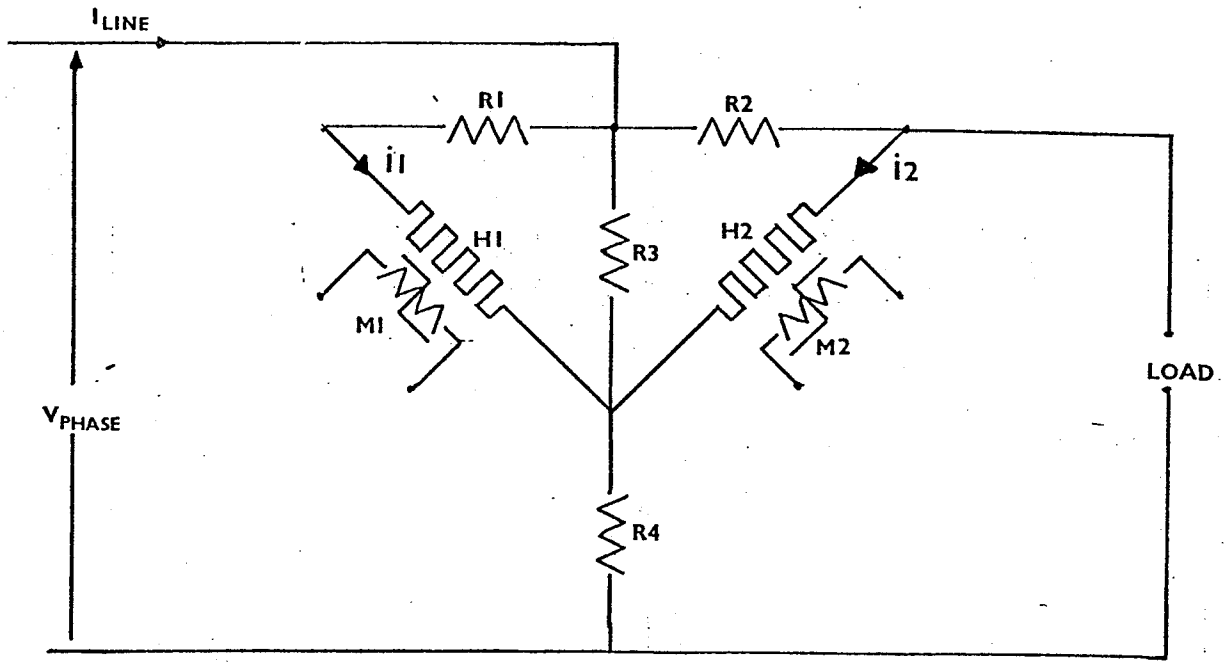

TRANFORMERLESS TYPE

WATTMETER

or alternately

$$M1 - M2 = 4C1C2VI\cos\phi \qquad (3.6)$$

where V and I are the rms values of load voltage and current respectively and $\cos\phi$ represents the load power factor. The constant 4C1C2 can be replaced by a single constant K and equation (3.6) becomes

$$M1 - M2 = KP\cos\phi \qquad (3.7)$$

where P is the volt ampere load consumption.

The transformerless type wattmeter is shown in Fig. 3.1. In this case the currents in the two heating branches can be expressed in the form

$$i1 = \frac{v}{2(R4+H2)} + i\frac{R2}{2(R4+H1)} \qquad (3.8)$$

$$i2 = \frac{v}{2(R4+H2)} - i\frac{R2}{2(R4+H1)} \qquad (3.9)$$

where H1 and H2 are the resistances of the heaters. Since the response of the thermoelements corresponds to the average power dissipated in the heaters, the differential output will be of the form

$$M1 - M2 = \frac{K}{T}\int_0^T vidt \qquad (3.9)$$

or alternately

$$M1 - M2 = KP\cos\phi \qquad (3.10)$$

which is the desired power response. The thermo-element illustrated is a Thermal Coupler and the difference between the resistances of the two Moxies M1 and M2 in ohms.

The transformer type wattmeter is illustrated in Fig.3.2. In this case the mathematical manipulation takes place in the split secondary winding of the potential transformer. Assuming the two Moxies identical, the heater resistance values are represented by the value H. The currents flowing through the two heaters are represented by

$$i1 = \frac{i}{2} + \frac{e}{2H} \qquad (3.11)$$

$$i2 = \frac{i}{2} - \frac{e}{2H} \qquad (3.12)$$

where i and e are values proporational to the instantaneous current and voltage of the metered load. As before the currents are squared when converted to thermal energy and the differential output is

$$M1 - M2 = ei \qquad (3.13)$$

and again due to the fact that Moxie devices respond to the average power dissipated in the heaters, equation (3.13) becomes

$$M1 - M2 = \frac{K}{T}\int_0^T eidt \qquad (3.14)$$

FIGURE 3.2

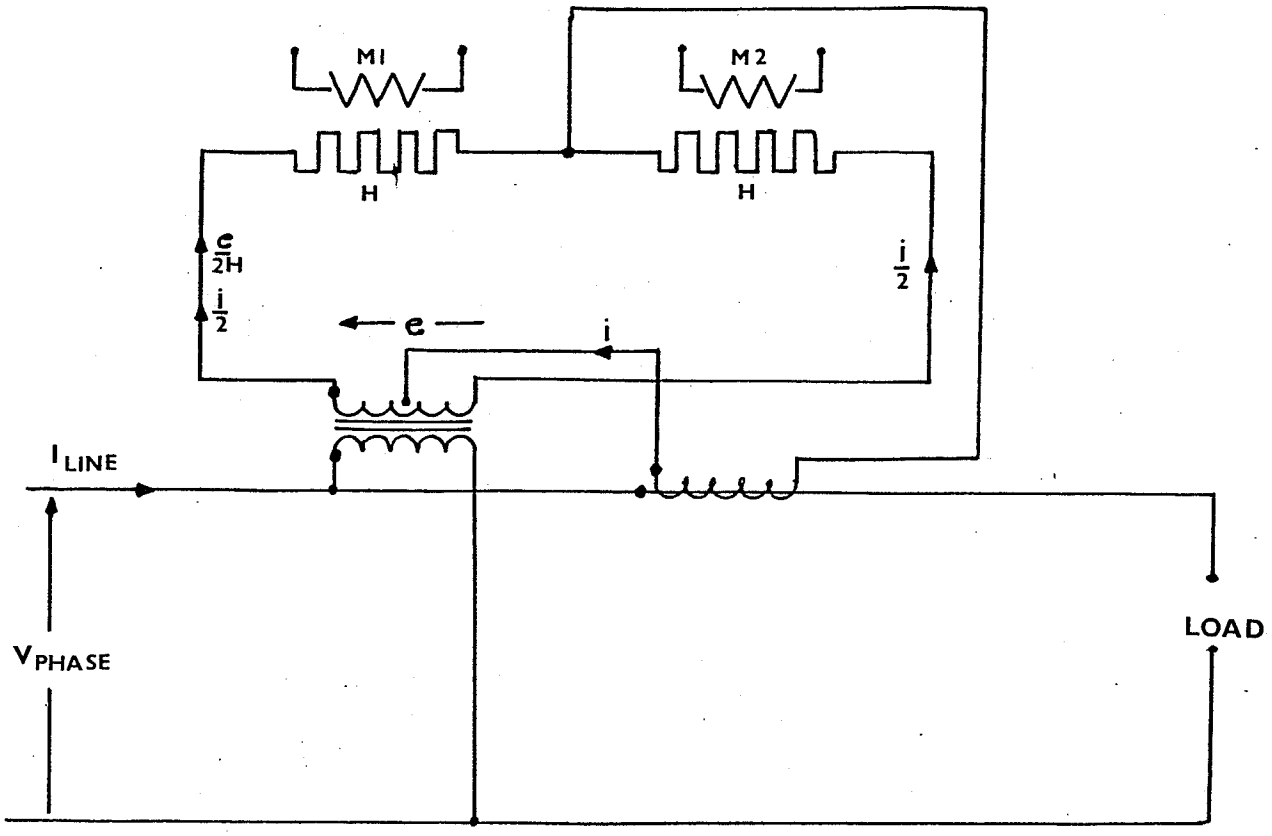

TRANSFORMER TYPE

WATTMETER

which after integration becomes

$$M1 - M2 = V_{phase} I_{line} \cos\phi \qquad (3.15)$$

which again is the desired power responsive output with V_{phase} being rms phase voltage, I_{line} the rms line current and $\cos\phi$ the load power factor. Since, as in the transformerless case, the thermoelements are Moxies and the output is expressed in ohms.

These two main types of wattmeters (transformerless and transformer) have distinct advantages and disadvantages associated with each. The transformer type wattmeter has good isolation from high current and voltage sources but high quality voltage and current transformers must be used for good accuracy and these transformers are designed for a particular frequency range and generally have poor frequency response. The transformerless type wattmeter avoids the intrinsic errors associated with the transformer type wattmeter but instead places high requirements on balancing conditions and quality of resistors. Wattmeters of this type have been developed with frequency range of 20Hz to 20KHz (4). This bridge type circuit was originally developed with a hot-wire instrument where the generated effect was the lengthening of a heated wire. The wattmeter indicated the difference between linear expansions of two hot-wires (11).

CHAPTER 4

THERMAL WATTMETER LAYOUT

In this chapter the proposed wattmeter is presented as a composite of two basic circuits, one for signal processing and the other for compensating the effect of ambient temperature fluctuations. The first circuit makes use of active elements to achieve addition and subtraction of signals proportional to the instantaneous load voltage and current. The second circuit maintains a reference Moxie at a quiescent temperature, meters the power required to maintain this constant temperature, introduces this power to the power sensing Moxies, and thus achieving a temperature compensated quiescent point for these sensing Moxies.

4.1 Signal Processing Circuit

Based on the review of the basic thermal wattmeter designs in Chapter 3 it can be concluded that the mathematical manipulation described should be implemented.

Two voltages, one proportional to the load voltage and the other proportional to the load current were added, subtracted, squared and finally averaged inorder to

produce the desired output. To attain an adequate frequency response for harmonics and transients the wattmeter of Fig. 4.1 was designed and partially developed.

The mathematical operations (ie. addition and subtraction) are achieved with an operational amplifier adder and subtractor. This technique offers low cost components and good frequency and temperature response. The open loop frequency response of the amplifiers used was flat to 10KHz and had a temperature range from 0°C to 75°C. If higher frequency or larger temperature range is desirable, there are commercial amplifiers available and the meter range could be extended by replacement and minor adjustment.

4.1.1 Circuit Description and Operation

The power measurement made by assuming a square law relationship between the input and output characteristics of the sensing Moxie devices MX2 and MX3. These Moxies have heaters H2,H3 with terminal resistances M2,M3,respectively. These two Moxies, MX2 and MX3, were closely matched and have a terminal resistance hysteresis curve as illustrated in Fig. 4.2. Here, as before, the upper curve illustrates increasing voltage applied to the heater and the lower curve decreasing applied voltage. A quiescent

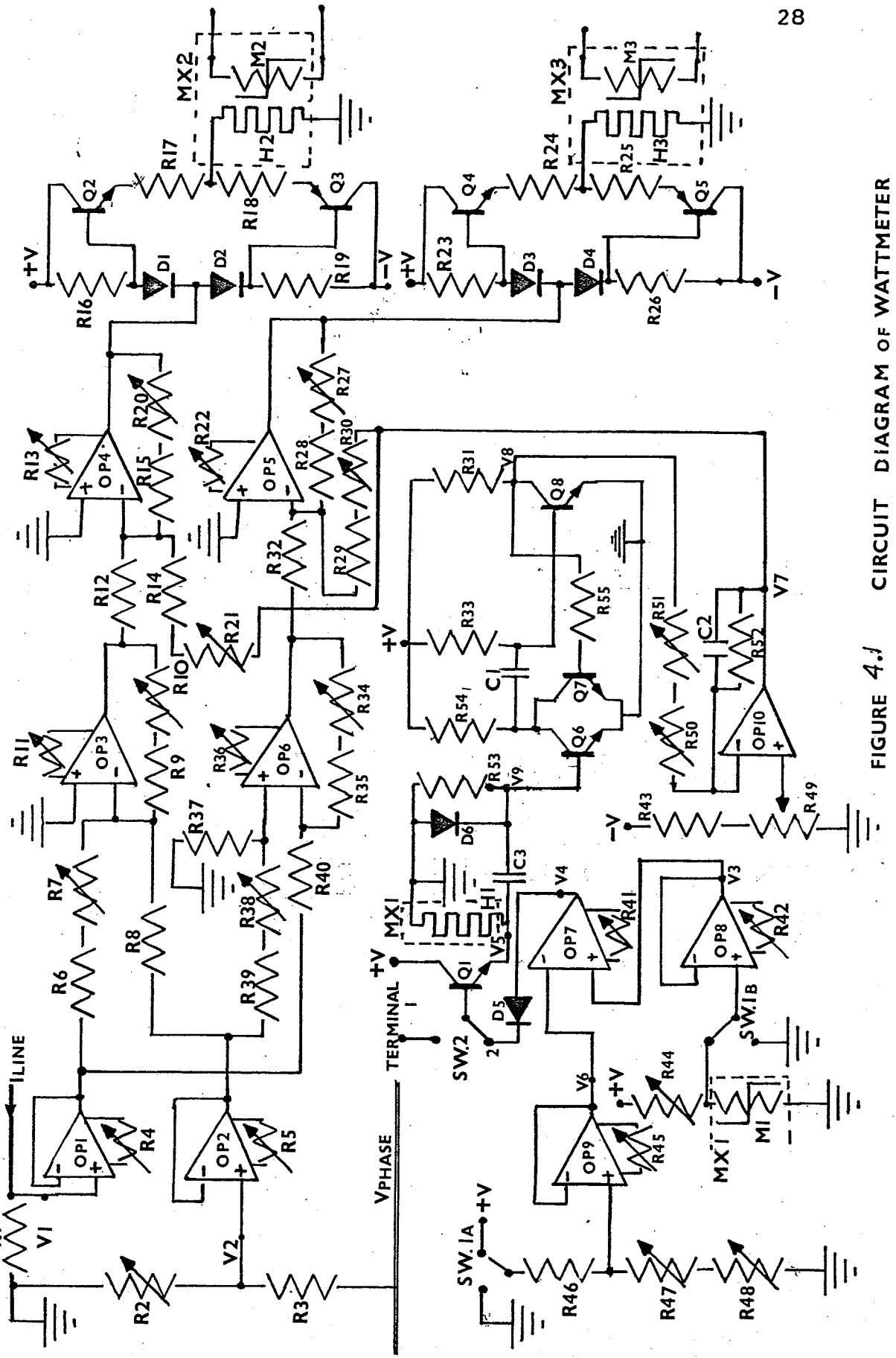

FIGURE 4.1 CIRCUIT DIAGRAM OF WATTMETER

FIGURE 4.2 HYSTERESIS CURVE OF MOXIE

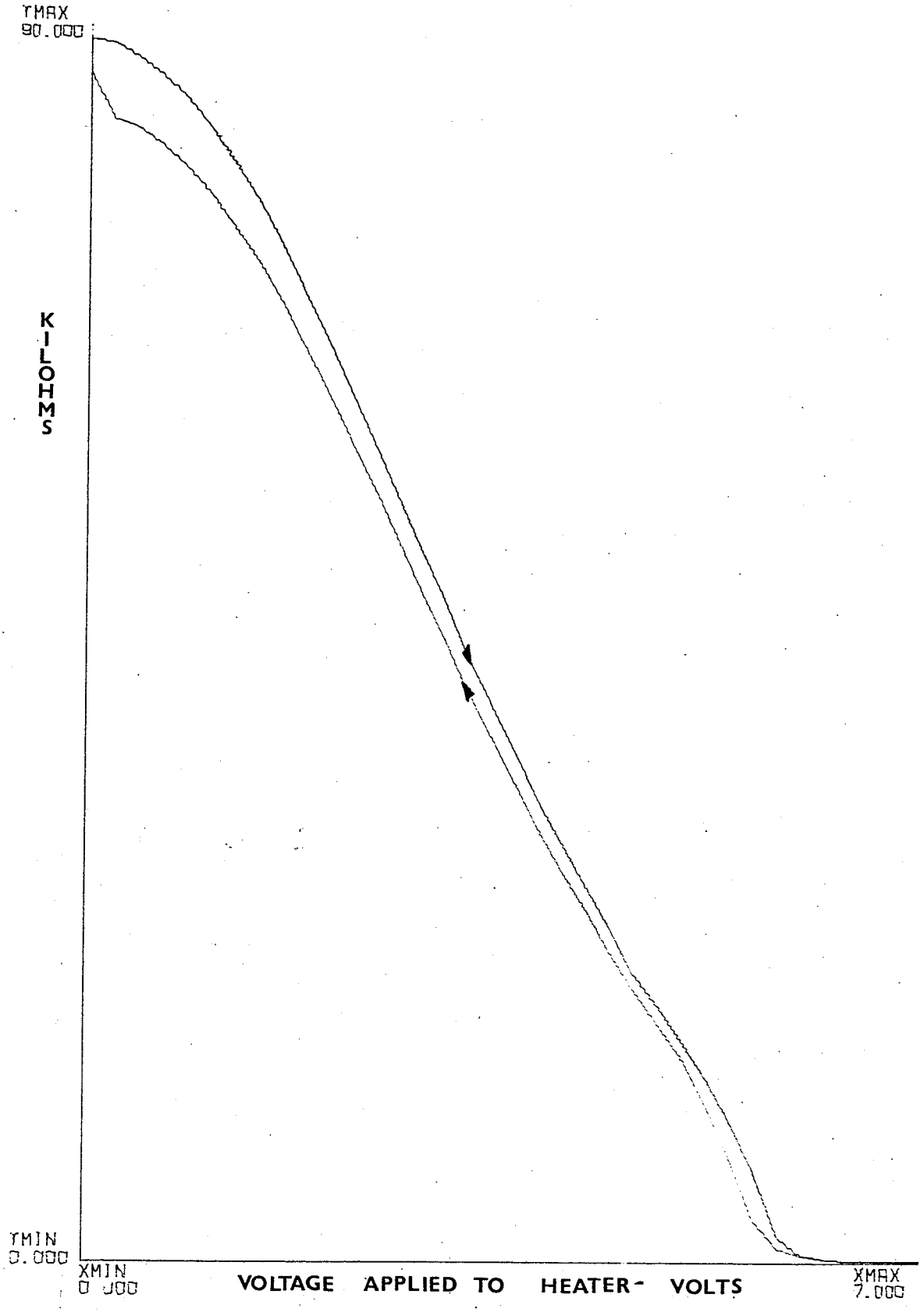

point (T_q,M_q where T_q is quiescent temperature and M_q the associated terminal resistance value) was chosen to place the meter in higher than ambient conditions to allow for a working range for the temperature compensator. This quiescent point was chosen at M_q = 60 KΩ and produced by the ambient temperature T and the power supplied to the heater (P_q) by the dc temperature compensator level which was added on to the processed signal voltages by adders OP4 and OP5. A dc signal was added to determine a monitoring region for dc conditions and the hysteresis graph of Fig. 4.3 was obtained. When an ac signal was added to the dc operating point, the transition curves do not coincide voltagewise with the dc curve as illustrated in Fig. 4.4 (hysteresis graph of MX2) and Fig. 4.5 (hysteresis graph MX3). This phenomenon is explained in appendix A. The two biased hysteresis curves associated MX2 and MX3 form the monitoring region of the wattmeter. Inorder to make equal the contributions of the load voltage and current proportional signals, each signal is rated at 2.75 volts full scale at unity power factor. Thus when these two contributions are added, a full transition is obtained. This operating transition region is ideally represented by a square law relationship and the output is represented as

FIGURE 4.3 DC-BIASED DC-HYSTERESIS CURVE

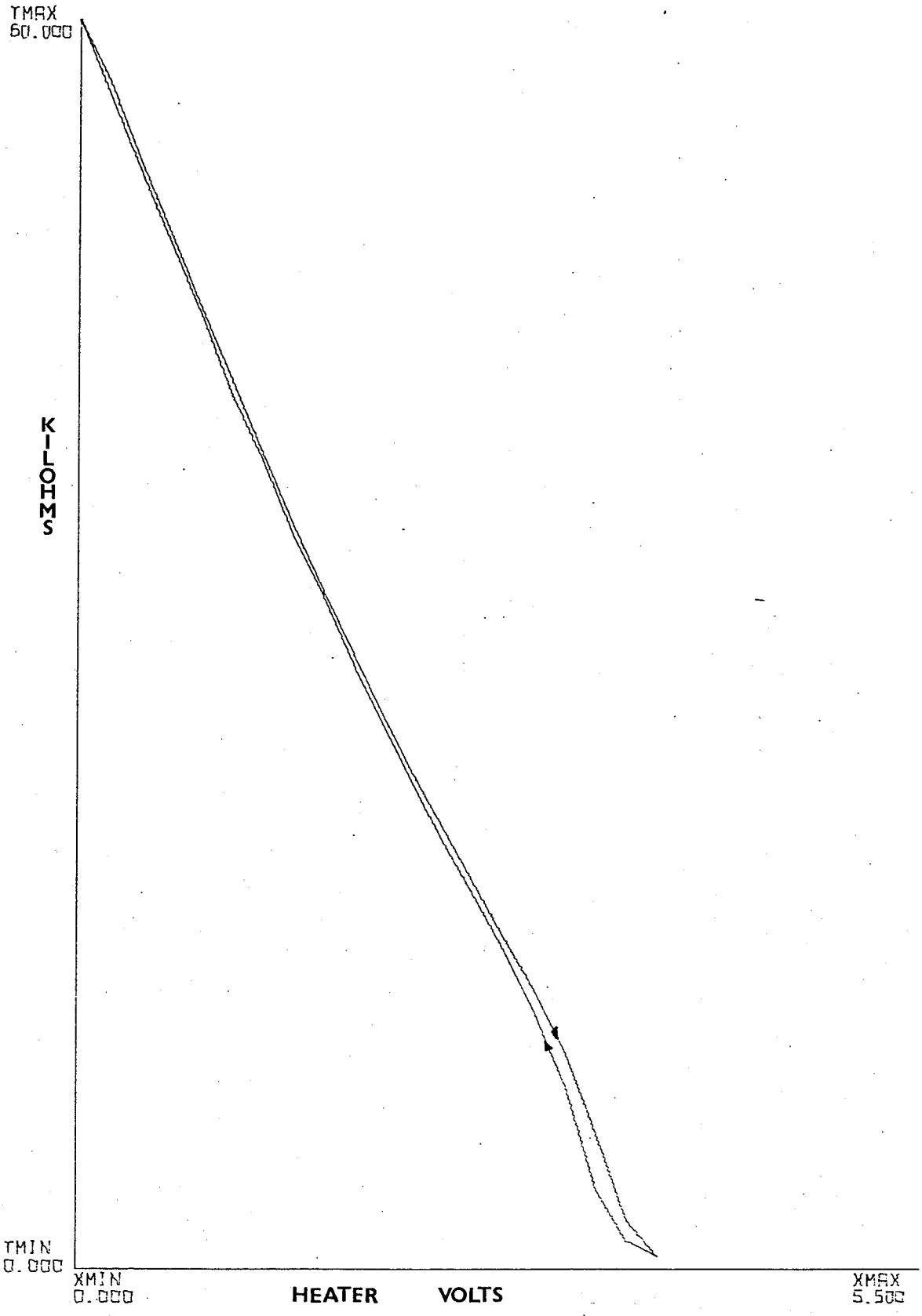

FIGURE 4.4 DC-BIASED AC-HYSTERESIS CURVE

-M2-

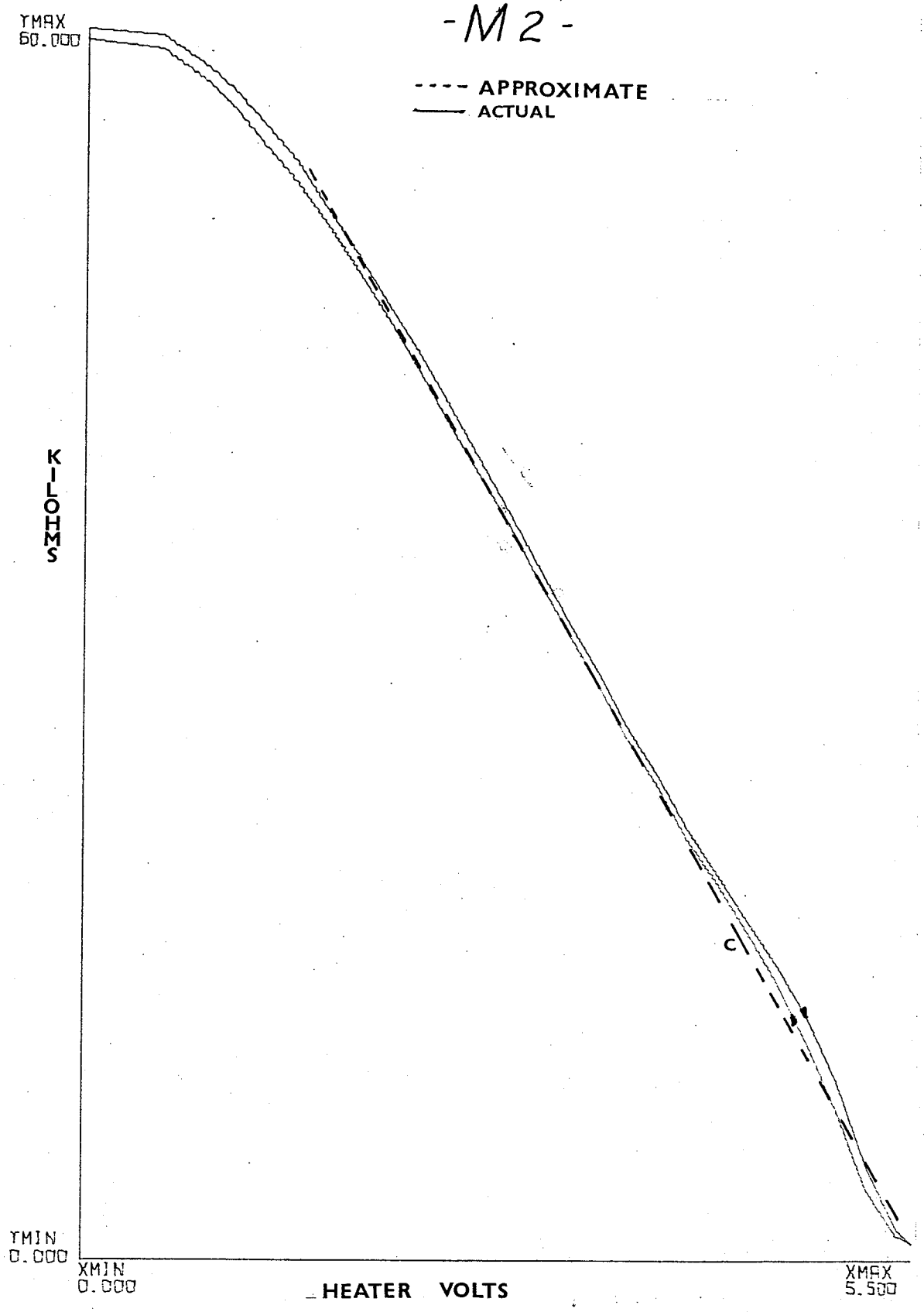

FIGURE 4.5 DC-BIASED AC-HYSTERESIS CURVE

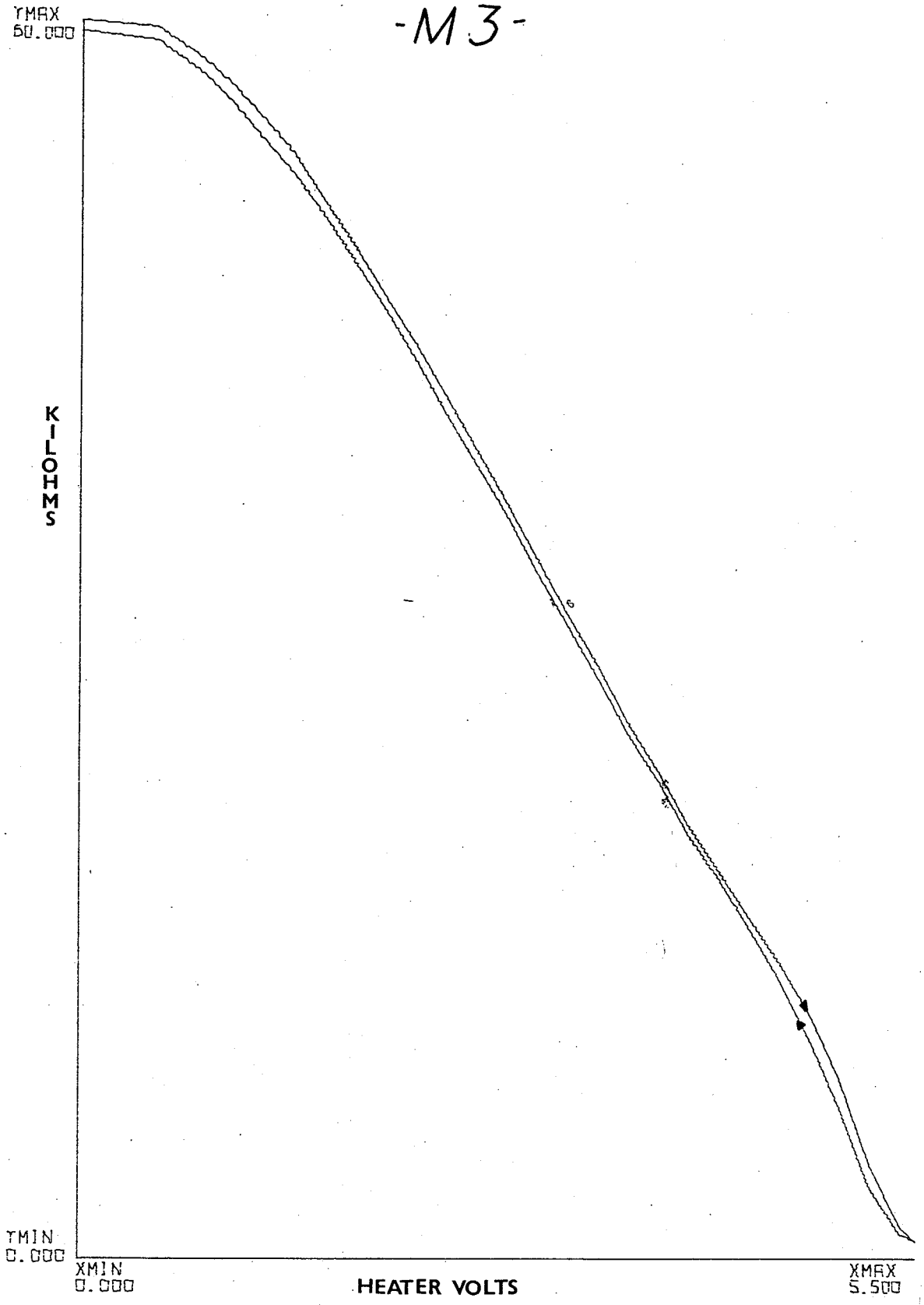

$$R = K \frac{V^2}{H} \qquad (4.1)$$

where H is the resistance of the heater, V is the voltage applied, K is a constant of proportionality and R the terminal resistance change due to the applied voltage.

The line current flowing through current shunt resistor R1 produces the required voltage V1 proportional to the instantaneous current in the load. The voltage divider between R2 and R3 produces the voltage V2 proportional to the voltage applied to the load. The voltage followers OP1 and OP2 isolate these voltages from the rest of the measuring circuit. The voltage follower OP1 could be converted to a difference amplifier if the shunt resistor was to be placed in the "hot" instead of "neutral" line as would be the case for polyphase power measurements. These two voltages (V1 and V2) are added in the adder OP3. Trimmer resistance R10 is used to match R8 to R39 and trimmer resistance R7 is used to match R9 and R10. This matching is necessary to provide a highly accurate addition function. The output of OP3 is therefore

$$VOP3 = -(V1 + V2). \qquad (4.2)$$

The two voltages are simultaneously subtracted by the

subtractor OP6. Similiarily R34 matches feedback resistor R35 to R40. Trimmer resistor R38 matches R39 to feedback resistors R34 and R35. This matching is necessary to provide an extremely accurate subtraction function. The output of OP6 is therefore

$$VOP6 = V2 - V1. \qquad (4.3)$$

The sum and difference of the two voltages are the values which are to be squared in the polyconductor and give a set of resistive output values proportional to the instantaneous power flowing in the line. The temperature compensated operating point of the polyconductors is added to the sum and difference voltages by adders OP4 and OP5, respectively. The adder OP4 feeds the push - pull power amplifier created with Q2 and Q3. The adder has trimmer pots R20 and R21 to match resistances in the feedback network. Matched diodes D1 and D2 are forward biased diodes to match the base to emitter junction of Q2 and Q3, respectively. The dc offset control resistor R13 is adjusted to give zero voltage across H2 with zero input to the adder. This is required since the diodes are not perfectly matched to emitter-base junction of the transistor. The gain of the adder is adjusted to provide a unity

voltage gain across the heater H2. R17 and R18 are two 5Ω resistors placed in the circuit to prevent the push - pull pair from "running away". Any unwarranted changes in the collector current will change the emitter current of the transistor. This change in emitter current increases the voltage drop across the feedback resistor which in turn decreases the base to emitter voltage and pulls the transistor back to its operating point. The voltage across heater H2 is given by

$$VH2 = -V3 + (V1 + V2). \qquad (4.4)$$

The quantity of interest is the resistive excursion from the operating point and thus the voltage of interest is

$$VH2' = V1 + V2. \qquad (4.5)$$

The difference voltage output of OP6 is fed through adder OP5 which is identical to OP4. In this case R30 matches R29 to R32 and, R27 and R28 provides the necessary gain to give the required summation to appear across heater H3. Forward biased diodes D3 and D4 match the base to emitter junction of the push - pull transistor pair Q4 and Q5, respectively. R24 and R25 provide the same negative feedback which

was accomplished by R17 and R18. The voltage appearing across heater H3 is given by

$$VH3 = -V3 + V1 - V2. \tag{4.6}$$

The resistance excursion from the operating point is again the voltage of interest and equals

$$VH3' = V1 - V2.$$

The voltages VH2' and VH3' cause further heating of the polyconductors and the output differential of the polyconductors is

$$M2 - M3 = K \frac{I}{T} \int_0^T \left(\frac{VH2'^2}{H2} - \frac{VH3'^2}{H3} \right) dt \tag{4.7}$$

This is true only if we assume that the period during which e and i go through a complete cycle of values is short compared to the response time of the Thermal Couplers (i.e. The Thermal Coupler response is a measure of the average square of the heater voltage.). If the respective values for VH2' and VH3' are substituted and assuming the heater is to have equal resistive values, (4.7) is rewritten

$$M2 - M3 = \frac{K}{H} \cdot \frac{I}{T} \int_0^T (V1\ V2)dt \tag{4.8}$$

and since

$$V2 = \frac{R2}{R2 + R3} V_{phase} \tag{4.9}$$

and also

$$V1 = R1 \quad I_{line} \tag{4.10}$$

where V_{phase} and I_{line} are instantaneous voltage and current values, the result becomes

$$M2 - M3 = \frac{K}{H} \quad \frac{R2}{R2 + R3} \quad R1 \frac{I}{T} \int_{o}^{T} I_{line} \, V_{phase} \, dt \tag{4.11}$$

By defining a total proportionality constant K, we obtain

$$M2 - M3 = K \cdot \frac{1}{H} \int_{o}^{T} I_{line} \quad V_{phase} \tag{4.12}$$

and using the definition of power in a circuit as

$$\text{Power} = \frac{K}{T} \int_{o}^{T} I_{line} \quad V_{phase} \quad dt \tag{4.13}$$

the final and desired expression is

$$M2 - M3 = K \cdot \text{Power}. \tag{4.14}$$

4.2 Temperature Compensation Principle

In order to accurately sense the load power consumption at a domestic or industrial installation

using a polyconductor wattmeter, the Moxies must be compensated for any changes in the ambient temperature at which the initial calibration was made (T_o). If such compensation is not supplied, a temperature fluctuation ($\triangle To$) could cause the Moxies to deviate from the monitoring region associated with them (see Section 4.1) and produce an erroneous output.

Temperature compensation at the sensing Moxies could be achieved by either of two ways:

1. the sensors could be placed in a constant temperature chamber and therefore would never experience any temperature variation, or
2. by choosing a quiescent point (Tq Mq) and increasing or decreasing power Pq in order to maintain Tq (where Pq is an additional power supplied to the heater to go from To to Tq).

The first method was easily discarded as a constant temperature chamber would be quite bulky, expensive and somewhat impractical. The second method has a theoretically infinite means of compensation as long as the ambient temperature T remains below Tq and the power supplies to the heater are capable of providing the required Pq without overloading. In this sense an

"oven" effect or constant temperature chamber is created within the Moxie device until the ambient temperature T equals Tq at which point all the heating required to maintain the "oven" at Tq is supplied from the surrounding air (ie Pq = 0), resulting in no available electrical power Pq to be withdrawn for any cooling action. Temperatures exceeding Tq are uncompensated for as no conventional cooling can be simulated with this method and thus an operating region's boundaries are defined by Tq and the power rating of the Pq supply.

The "oven" effect in this study was accomplished by allowing a reference Moxie device (MX1) to fluctuate between an upper and lower temperature limit around Tq. Thus fluctuation is generated by applying a heating pulse whenever the device cools to the lower temperature limit, the duration of which (pulse width) is controlled by the upper temperature limit at which point the pulse is removed. The power Pq associated with the heating pulse train V5 is metered and introduced to the sensing Moxies MX2 and MX3 in order to generate a constant temperature quiescent point. A detailed explanation of this scheme is offered in the next section.

4.2.1 Circuit Description And Operation

The electronic components and the desired operational characteristic of the temperature compensating scheme are presented in Fig. 4.1 and Fig. 4.6, respectively. The "oven" condition is set within Moxie MX1, which has associated heater and terminal resistance H1 and M1, respectively, by an applied pulse train V5 to heater H1 maintaining the quiescent temperature Tq and is representative of Pq. This power Pq is applied to the heaters H2 and H3 of the sensing Moxies MX2 and MX3, respectively, thus generating a temperature compensated quiescent point for each.

The pulse train is generated by operation amplifiers OP7, OP8, OP9 and transistor Q1. OP7 is in an open loop mode (voltage gain of 50,000 typically) thus being extremely sensitive to the voltage differences (V3 - V6) which determines the output voltage, +V or -V. The underlying concept is that a constant number of pulses is generated depending upon the time the Moxie requires to cool to generate a voltage V3 larger than V6 and thus generate a heating pulse to heat the Moxie MX1 back to the quiescent temperature. Once V3 drops below V6, V4 becomes negative (i.e. quiescent temperature is reached) and the cooling process is

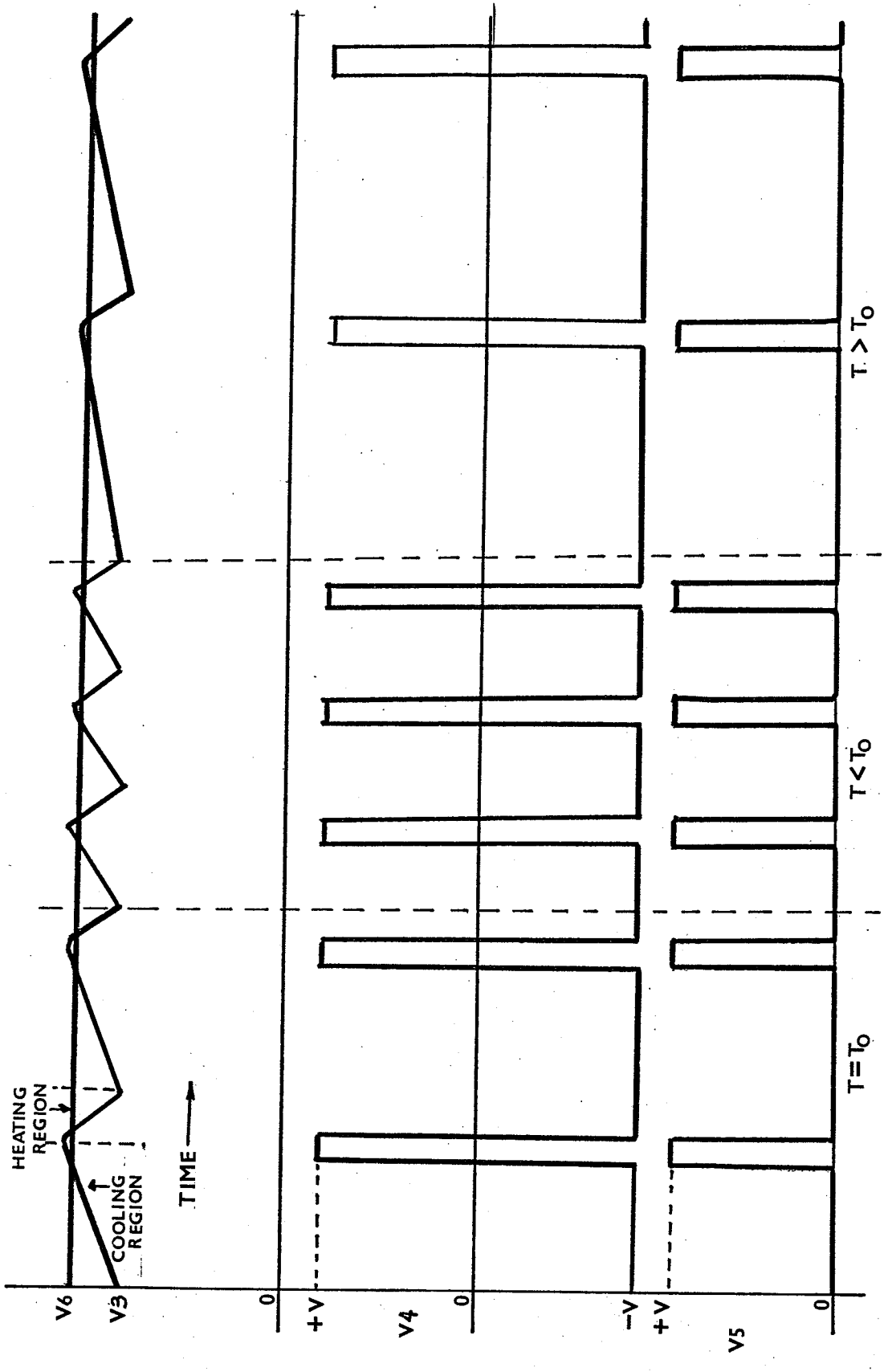

FIGURE 4.6 OPERATIONAL CHARACTERISTICS OF TEMPERATURE COMPENSATOR

initiated. The constant pulse frequency fp generates approximately constant value for the quiescent point Tq. When a temperature fluctuation occurs, the cooling period is mainly affected (heating period only slightly affected due to close proximity of heater to VO_2 films - see Fig. 2.4) and it either requires longer time for V3 to reach V6 (a condition of temperature T higher than ambient temperature To) resulting in fewer pulses and thus a reduction in Pq or a quicker cooling time (a condition of temperature T lower than ambient temperature To) resulting in more pulses and higher Pq. In this way Pq is increased or decreased to provide a relatively constant temperature within the Moxie device. The quiescent "oven" temperature Tq can be adjusted to lie in with the pre-transition, transition or post transition range of the Moxie as long as Tq lies above room temperature. Furthermore Tq is established by a suitable combination of the two voltages V6 and V3. To illustrate this, assume that V6 is adjusted to $\frac{1}{2}$ + V (i.e. R47 + R48 is made equal to R46) and thus V4 will be either +V or -V if V3 is greater or less than $\frac{1}{2}$ + V, respectively. The quiescent point Tq can now be controlled by the adjustment of R44 as it dictates where Tq of MX1 will lie as MX1 will be heated until V3 becomes less than V6 at which R44

approximately equals M1 (i.e. V3 is slightly smaller than V6). When this occurs, the heating pulse terminates, the cooling process begins and the temperature of MX1 will fluctuate about the Tq value so established. In actual practice R44 is adjusted to approximately equal to Mq of M1 required for the quiescent operating point while a coarse and fine adjustment of V6 is accomplished through R48 and R47, respectively. Using this method, R47 and R48 could be selected to give a accurate Tq keeping in mind that R44 has only to approximately coincide with Mq. In this manner variations in the ambient temperature (ΔTo) result in corresponding variations in frequency of the heating pulses (Δfp) wherefp is dictated by Mq for a fixed ambient temperature To. Although a heating signal proportional to fp is fed into the sensing Moxies (analogue to digital and back to analogue) the value of fp is a digital indication of the ambient temperature (i.e. a digital thermometer), or similiarly used to indicate quantitatively the degree of overloading of a circuit. The value of an unknown current could be determined by sensing the thermal power it produces (i.e. a digital type Moxie ammeter) or the value of an unknown resistance, as will be described later. These schemes represent potential

analogue to digital converters using Moxie devices and frequency counters which may replace existing more expensive, less accurate instruments presently used.

Photographs of the pulse train V5 and fluctuating voltage V3 are shown in Fig. 4.7. Here V3 continues to decrease after the V5 pulse is removed. This is due to the fact that heat flow from the heater to the VO_2 film does not stop instantaneously thus the heating rate gradually decreases before cooling begins. This thermal overshoot creates the upper temperature limit in relation to the lower limit determined by V6 and R44 and hence affecting the pulse frequency Pq. Since the thermal overshoot is generated by the thermal time constant of the polyconductor, there could be some associated errors which will be discussed in Chapter 6.

To calibrate the compensator, switch SW2 is placed to number 1 position and an external voltage is applied to terminal 1. This will cause MX1 to heat to the desired Tq. R44 is then adjusted until V3 approximately equal $\frac{1}{2}$+ V (i.e. R44 approximately equals Mq). R47 and R48 are then adjusted until slightly greater than V3, thus causing V4 to be -V as OP7 acts as a switch having either +V or -V output due to the extremely high gain.

The scheme can be described with reference to

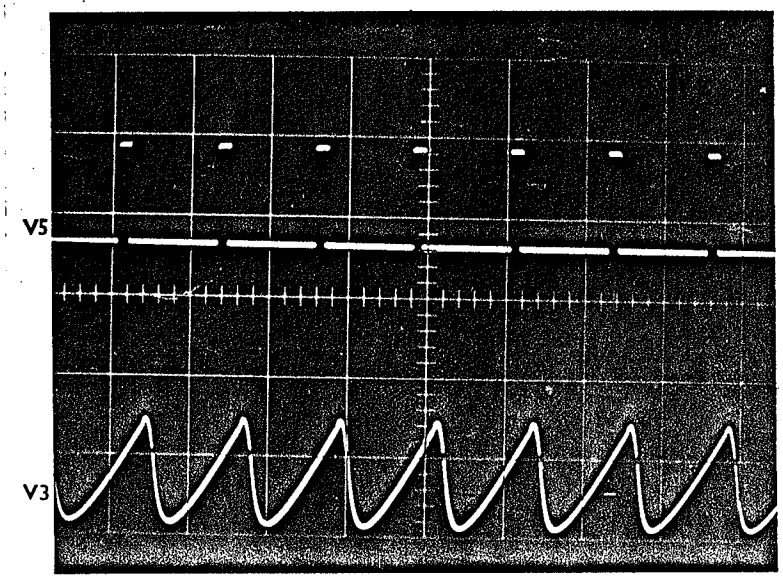

FIGURE 4.7

ACTUAL

TEMPERATURE COMPENSATION

Fig. 4.6. SW2 is moved to position 2 and the external bias is removed. H1 has no applied voltage as V4 is -V and Q1 is turned off (reverse voltage breakdown across base to emitter junction of Q1 is prevented by D5). MX1 then cools, as illustrated by the cooling region of V3. V3 increases (MX1 cools as M1 increases in value) until it exceeds V6 in value at which time V4 equals +V and correspondingly V5 also equals +V. The heating region is then initiated as power is applied to H1 and V3 decreases (i.e. M1 decreases in value) until reaching a level which makes V6 greater than V3 at which point V4 becomes -V and V5 zero volts. Since V6 and R44 remained fixed, the only quantity able to increase or decrease the pulse frequency (fp) is the temperature of the surrounding medium, thus temperature compensation is achieved with an increase or decrease in ambient temperature. The $T < To$ section of Fig. 4.6 illustrates the increase in fp to supply more power Pq to MX1 when a decrease in temperature occurs. The heating region is relatively unchanged (due to close proximity of the heater to the VO_2 film) with respect to the cooling region which is substantially shorter. This condition produces more pulses per unit time thus maintaining the quiescent ambient temperature within MX1. The following section

(T > To) illustrates a condition of higher than quiescent ambient temperature. In this case the time required for cooling is increased with the heating time remaining relatively unchanged as before. With the condition of a longer heating period, the number of pulses in a given time is reduced and correspondingly is the power Pq applied to the heater and thus temperature compensation for above quiescent temperature condition is achieved.

If a Thermal Coupler Moxie device with two heaters was available at the time of the design of this circuit these pulses could have been fed into one heater and the processed signal to the other. Since only single heater Thermal Couplers were available, the pulses were converted to a dc level and then fed into the adders OP4 and OP5. In order to determine which type of conversion would be most suitable, the curves of Fig. 4.8 and Fig. 4.9 were plotted and analyzed. These two graphs show how the pulse frequency varies throughout the available temperature range. One curve is plotted at an ambient temperature Tq corresponding to an Mq of 60 KΩ and other corresponding to 40 KΩ. Both graphs show that the pulse frequency changed non linearly with temperature, the upper curve being the cooling curve while the lower

PULSE FREQUENCY VS TEMPERATURE-60K

FIGURE 4.8

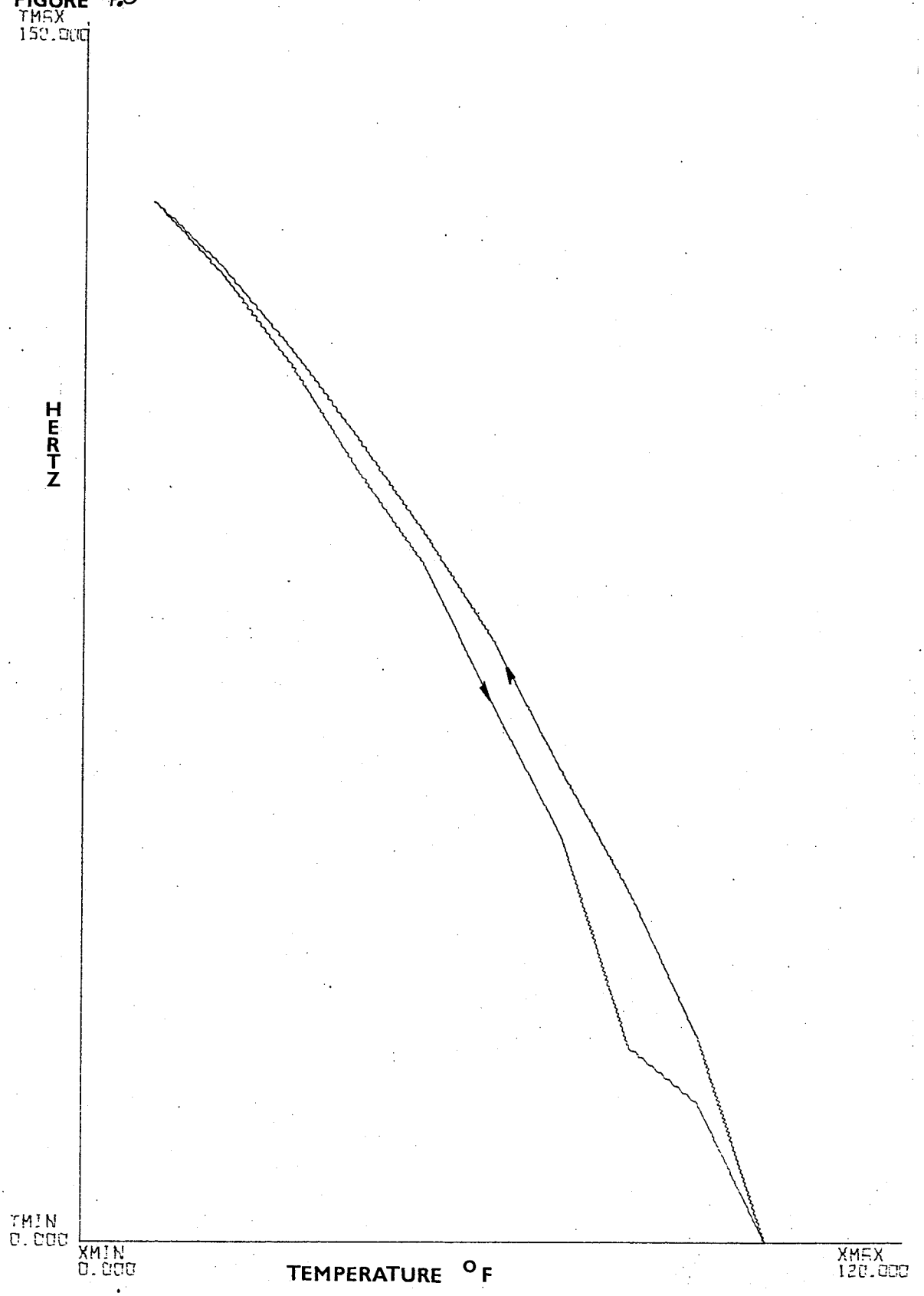

PULSE FREQUENCY VS TEMPERATURE-40K

FIGURE 4.9

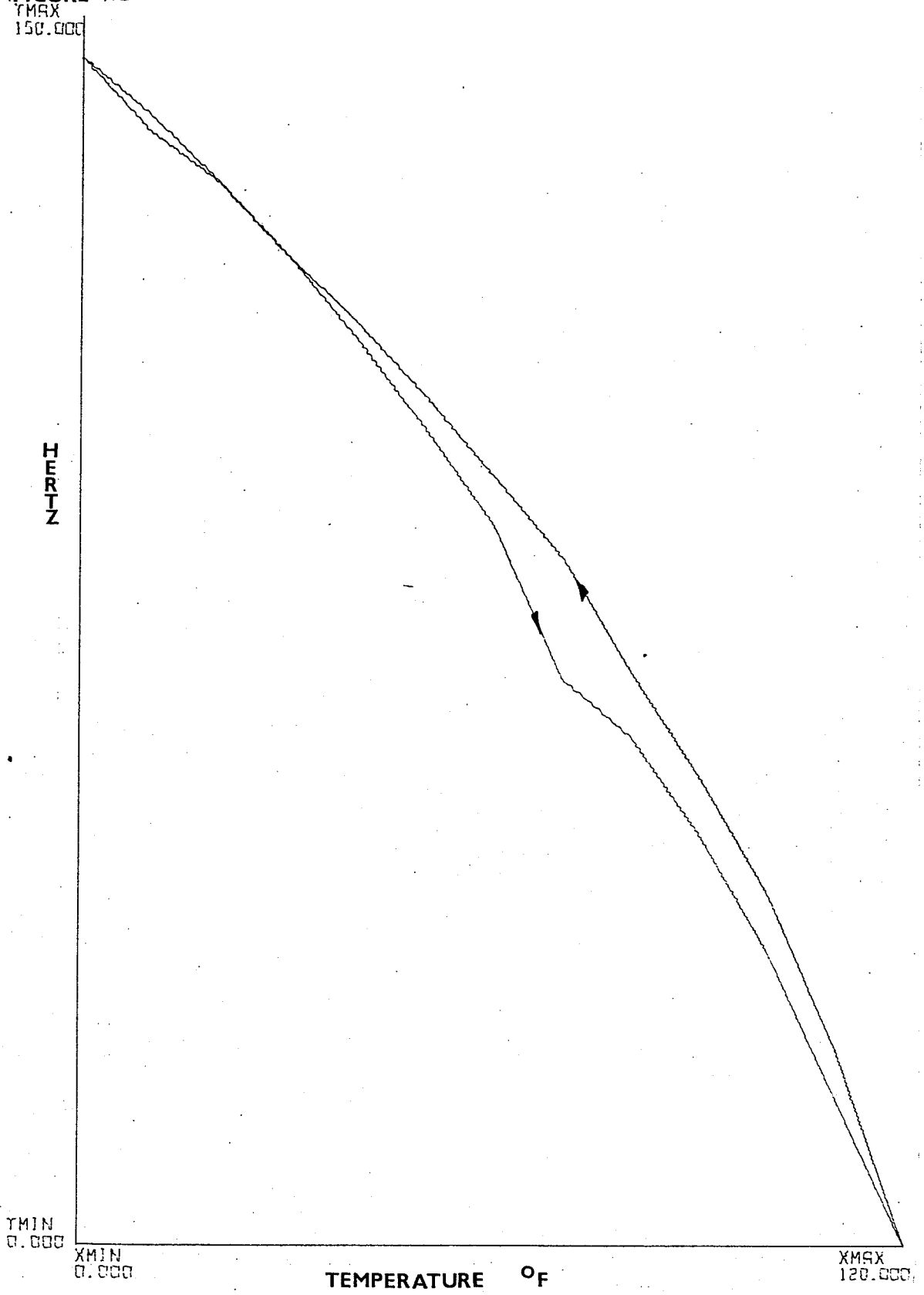

curve the heating one. This nonlinear phenomenon indicates that the pulse width changes with varying temperature. This means the effective dc voltage of the pulses must be determined and fed into the adders OP4 and OP5. A low pass filter approximates an averager if the pulse width change is negilable. The low pass filter OP10 was tried but proved ineffective by itself since the gain of the device not only changed the slope du/dfp, but also the dependence of pulse width. The pulse to dc scheme is incorporated in order to reduce the dependence of pulse width and consists of a frequency to voltage converter. This converter was achieved by first feeding the pulses into a monostable multivibrator and then feeding the output of the multivibrator to the low pass filter OP10. It should be noted that OP10 was designed with a 1.0 second electrical time constant in order to minimize the ripple voltage produced at its output (see Fig. 4.10). The multivibrator is formed by transistors Q6, Q7 and Q8 with R31 and R55 controlling the pulses height and R33 and C1 controlling the pulse width. The multivibrator output is a pulse of constant width and height once triggered. The design of the circuit must insure that if the input pulse width (trigger pulse) increases, the input pulse should not control

FIGURE 4.10

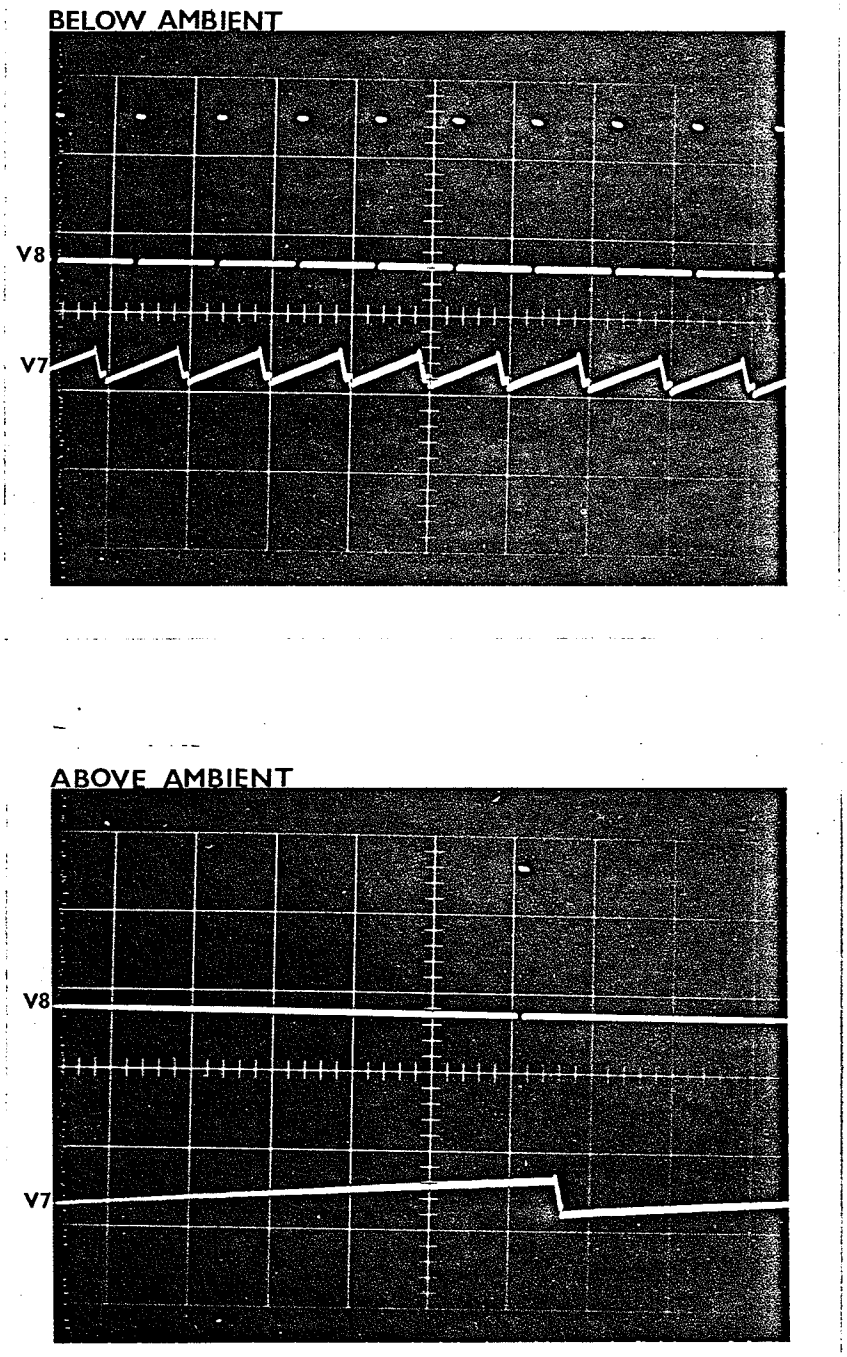

RIPPLE VOLTAGE

the output pulse width. The temperature compensator pulse train (V5) is then converted to an impulse train through differentation by C3 and R53 with D6 preventing reverse voltage breakdown from occuring at Q6 (see Fig. 4.11). In order to get as close as possible to a perfect conversion, the gain of the low pass filter is varied with a coarse adjuster R50 and a fine adjustment R51. These two trimmers control the slope dv/dfp and R43 and R49 control the dc offset. The output of the frequency to voltage converter is shown in Fig. 4.12. The output of the low pass filter is then fed into adders OP4 and OP5 to accomplish final temperature compensation for the sensing Moxies. R12 is matched to R14 and R21 in order to compensate for losses across feedback resistor R17 and R18. Similiarly, R32 is matched to R29 and R30 to attain the proper gain. It should be noted that SW1 is used in zeroing all voltage output in the temperature compensation.

FIGURE 4.11

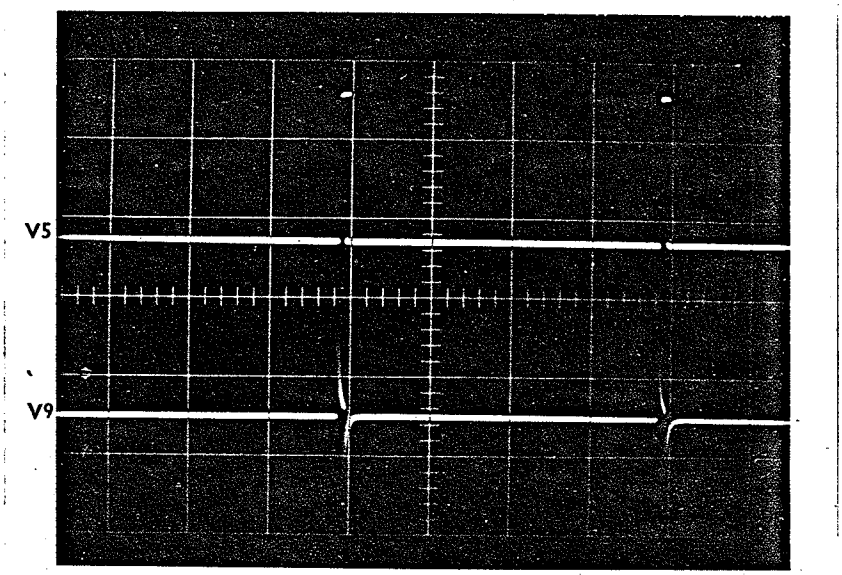

DIFFERENTIATED PULSES

FIGURE 4.12 FREQUENCY TO VOLTAGE CONVERTER

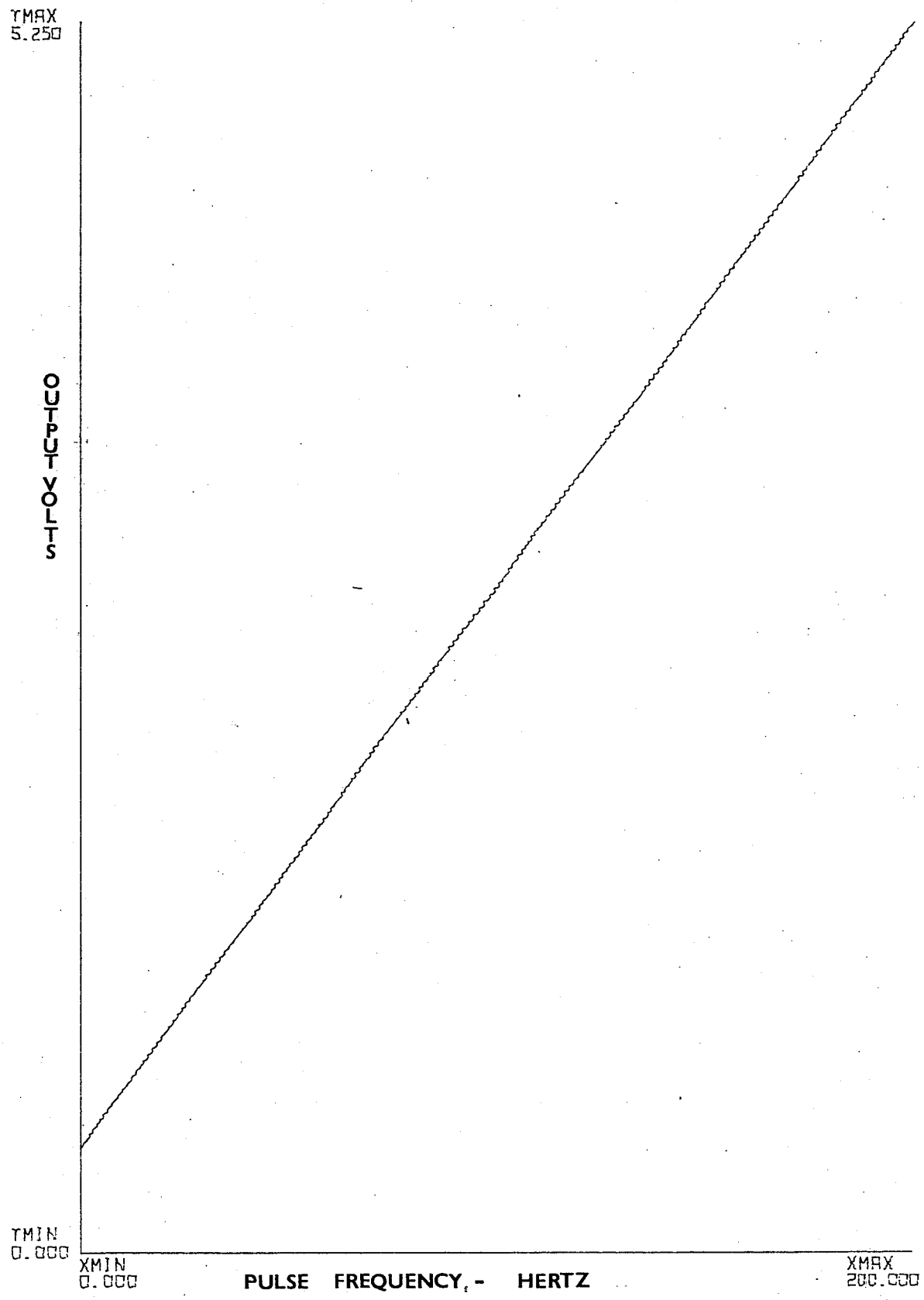

CHAPTER 5

EXPERIMENTAL PROCEDURE AND RESULTS

The experimental results presented in this chapter were obtained to determine the performance of the polyconductor wattmeter discussed earlier. The temperature compensation method was tested with the original pulsed scheme and also the "trade off" frequency to voltage converter, and led to temperature compensation curves which were obtained by placing the biased Moxies in a controlled temperature chamber, varying the chamber temperature and recording the terminal resistance. The power response curves were obtained by simulating various load power factors and magnitude conditions with a variable phase signal generator.

5.1 Temperature Compensation Circuit

5.1.1 Experimental Layout

The effectiveness of both the temperature compensation schemes (pulsed and dc) were tested by placing the reference and sensing Moxies in a constant temperature chamber, varying the chamber temperature and

recording the terminal resistance and pulse frequency fp V5 temperature characteristic. The laboratory set up is shown schematically in Fig. 5.1.

The oscilloscope used to observe the various waveforms of interest associated with the wattmeter (V3, V5, V7 and V9) was a Type 516A Tektronix Oscilloscope. All frequency measurements were made by a Hewlett Packard 53064A Multimeter/Counter and all voltage and resistance measurements were made with a Fluke Model 8000-A Digital Multimeter. The two power supplies used in conjunction with the polyconductor wattmeter were Lambda regulated power supplies, model LP411-FM. The temperature chamber used for testing the pulsed temperature compensation scheme was an Associated Testing Laboratories, Inc. which used CO_2 for cooling and electricity for heating. The use of CO_2 resulted in step changes in temperatures around lower than ambient thermostat settings and, since the dc temperature compensator has an 1.0 second time lag (due to low pass fitter OP10), a smooth slow temperature variation was unattainable and thus a chamber Inreco Model 13-81 was used to test the dc type "trade off" temperature compensator scheme. The pulsed temperature changes, as described in a later chapter and thus the Associated Testing Laboratories chamber

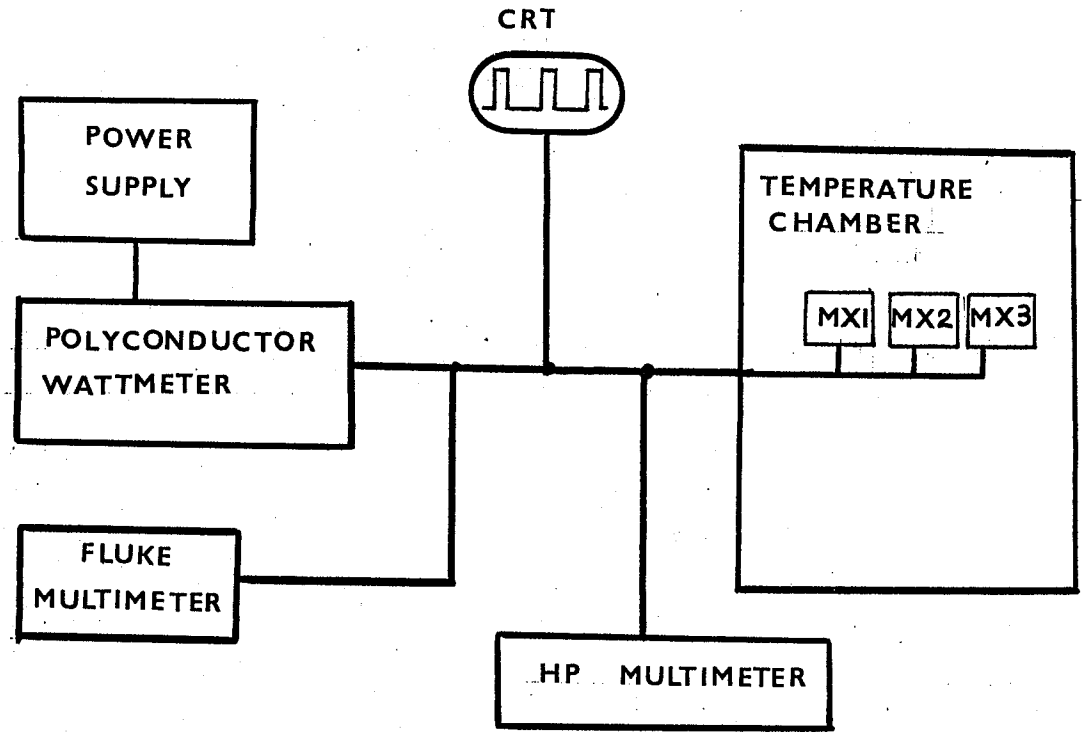

FIGURE 5.1 CIRCUIT DIAGRAM FOR TESTING PERFORMANCE OF TEMPERATURE COMPENSATION

was used. The Inreco chamber provided a very slow temperature variation (30 minutes to decrease from 70 to 20°F) and thus provided a slow, smooth transition for the dc type scheme. The results obtained from these layouts are given next.

5.1.2 Laboratory Procedure And Results

As stated earlier, the commercially available temperature compensator requires a very steep switching characteristic to operate satisfactorily, thus proving to be insufficient since the moxies used have a slow transition. The temperature compensation was measured by varying the chamber temperature and recording the change in resistance of the second polyconductor chip M1 in MX1. The bias points Mq chosen were 60, 40 and 10 KΩ. The plot shown in Figs. 5.2, 5.4 and 5.6 have two curves each, one with a bias point chosen with temperature compensation applied (B) and the other without (A).

Fig. 5.2 displays the two curves of M1 with a bias point of 60 KΩ. The temperature was varied from 20°F to 100°F at which the compensator reached its upper limit (no electrical energy applied, i.e. Pq = 0). M1 illustrated by curve A varied from 285 KΩ to 48 KΩ,

FIGURE 5.2 TEMPERATURE COMPENSATION-60K

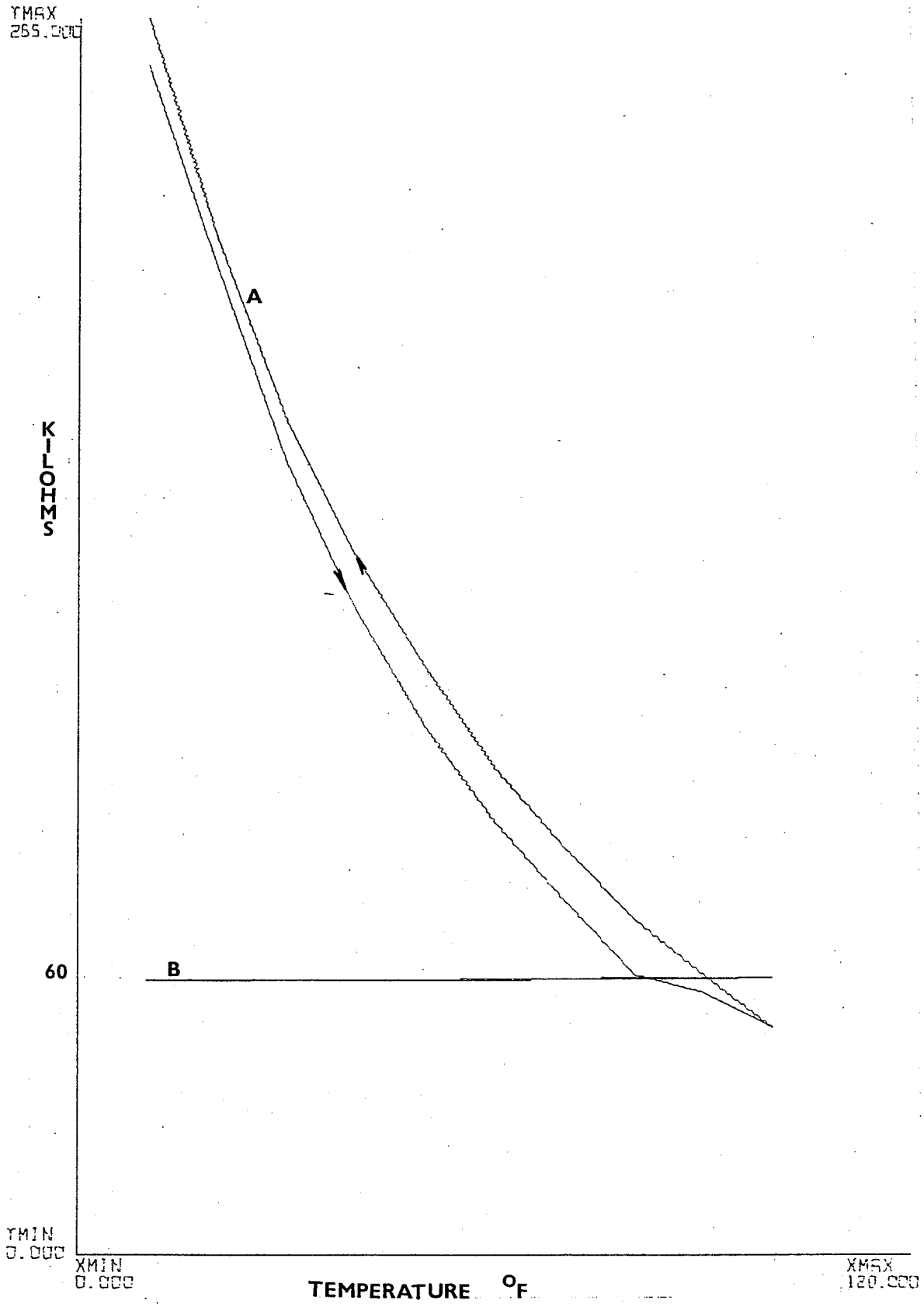

a resistance change of 217 KΩ. The compensated curve designated as B and expanded in Fig. 5.3 shows variations of Ml from 60.2 KΩ down to 59.1 KΩ, a Mq of 1.1 KΩ as compared to 217 KΩ of the uncompensated curve.

Fig. 5.4 shows the two curves associated with a Mq of 40 KΩ. In this case the temperature is varied from 0 °F to 120 °F, a higher upper temperature limit due to the higher temperature corresponding in Mq. Ml in curve A varies from 200.0 KΩ down to 22.0 KΩ, a change of 178.0 KΩ which is lower because MXl is biased in a different part of the transition curve corresponding to a lower $d\overline{Ml}/dT$. Curve B varies from 40.1 KΩ down to 39.4 KΩ, Mq of 700 Ω as shown in Fig. 5.5

Fig. 5.6 shows the temperature compensation curves for an Mq of 10 KΩ. The temperature was varied from 0 °F to 175 °F, again a higher temperature range due to the higher bias point. Curve A varies from 56.5 KΩ to 71 Ω, a smaller excursion again due to the smaller value of dM dt. Curve B is expanded in Fig. 5.7 and varies from 10.5 KΩ to 9.1 KΩ, a Mq of 1.4 KΩ. The much smaller reduction in the uncompensated case is due to the increase in Tq corresponding to Mq while the bias point of the compensated case still

FIGURE 5.3 TEMPERATURE COMPENSATION-60K

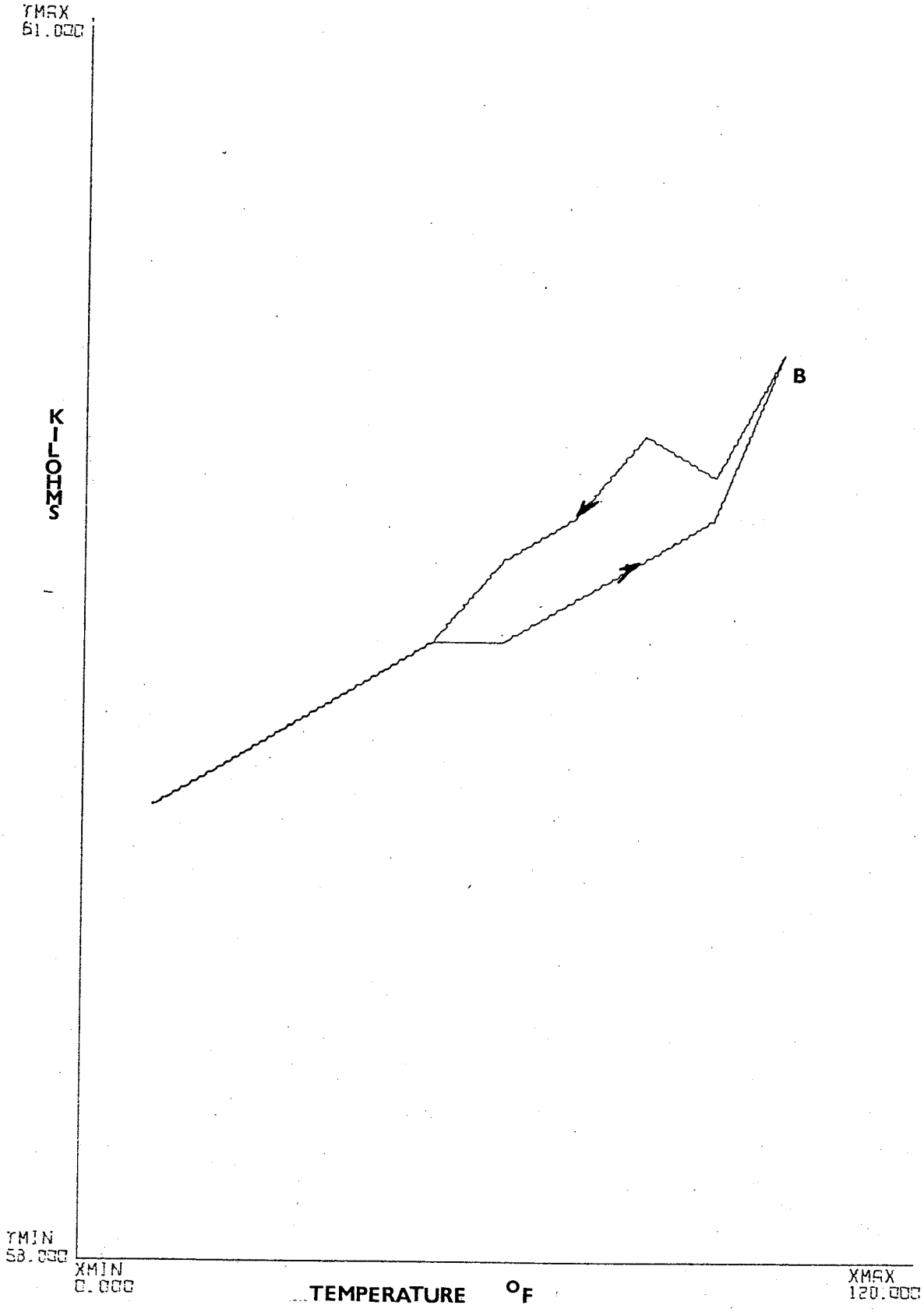

FIGURE 5.4 TEMPERATURE COMPENSATION-40K

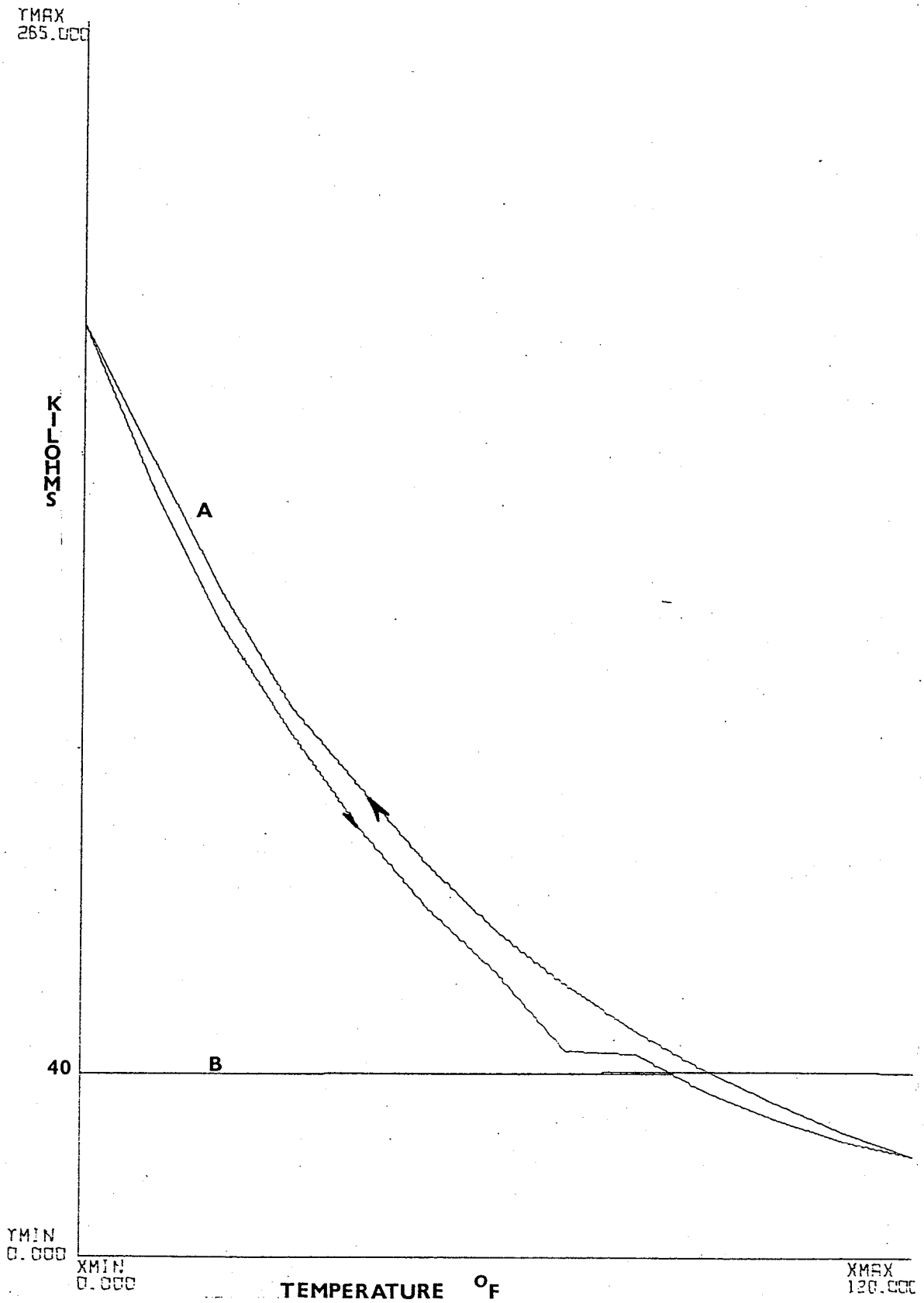

FIGURE 5.5 TEMPERATURE COMPENSATION-40K

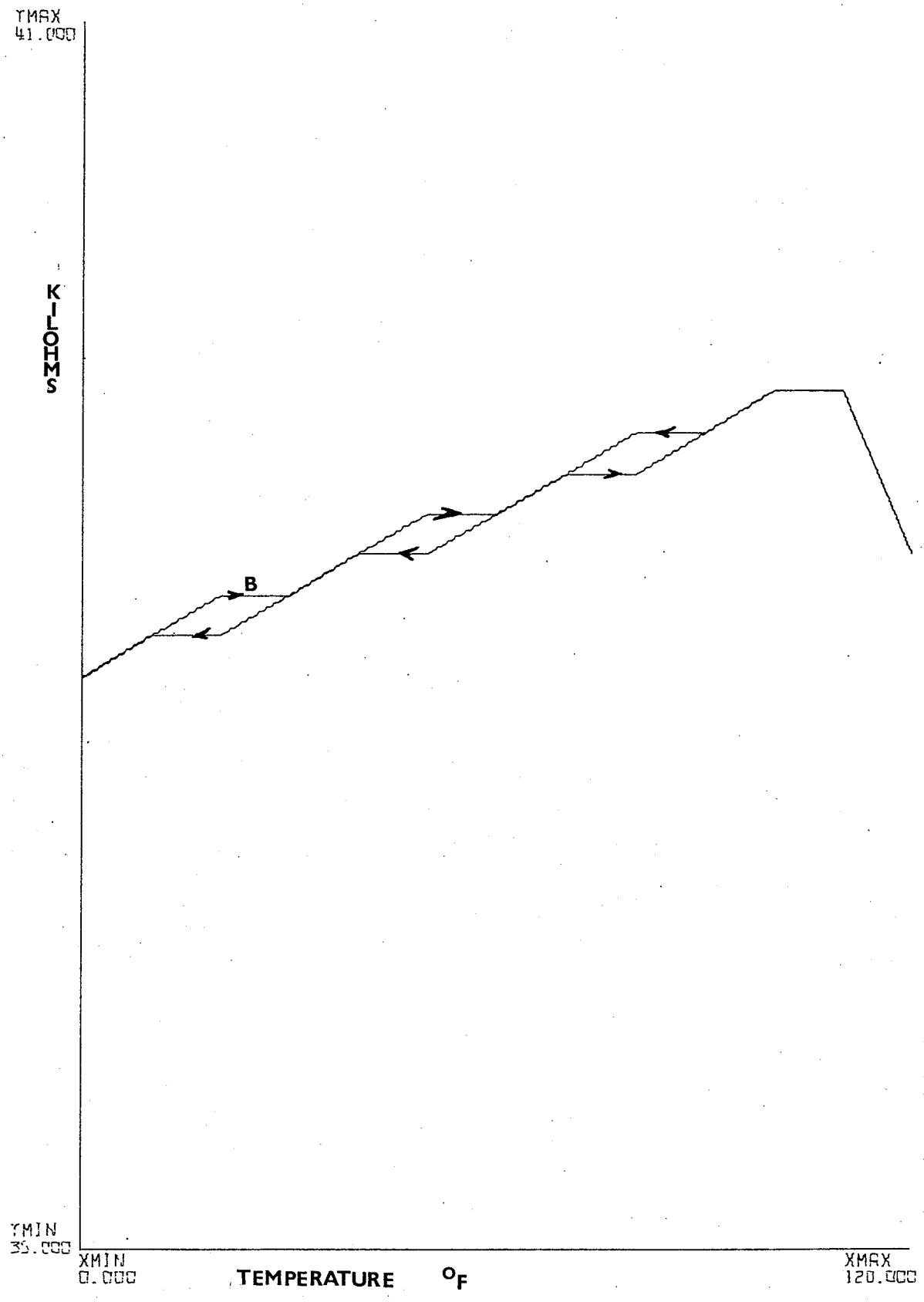

FIGURE 5.6 TEMPERATURE COMPENSATION-10K

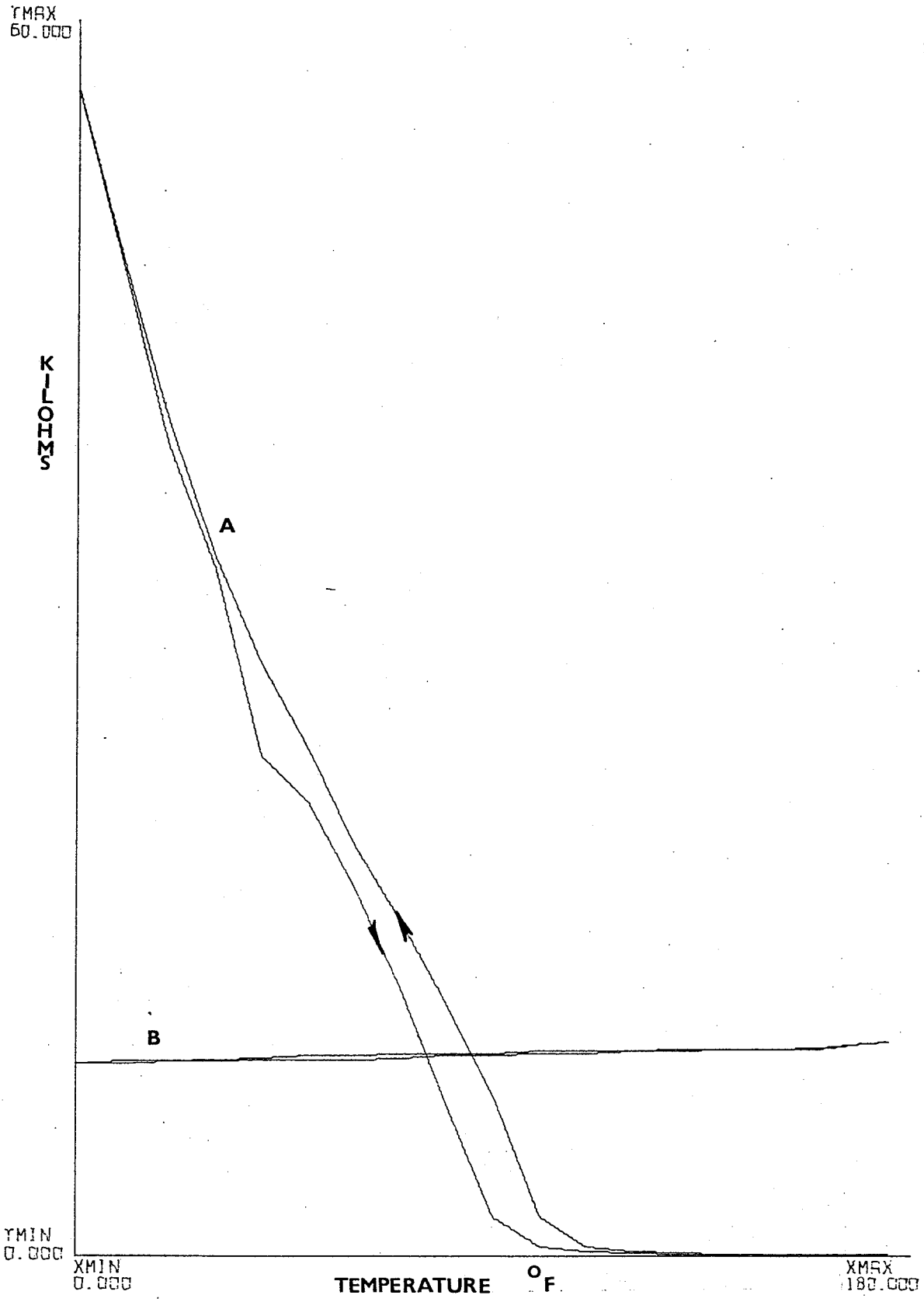

FIGURE 5.7 TEMPERATURE COMPENSATION-10K

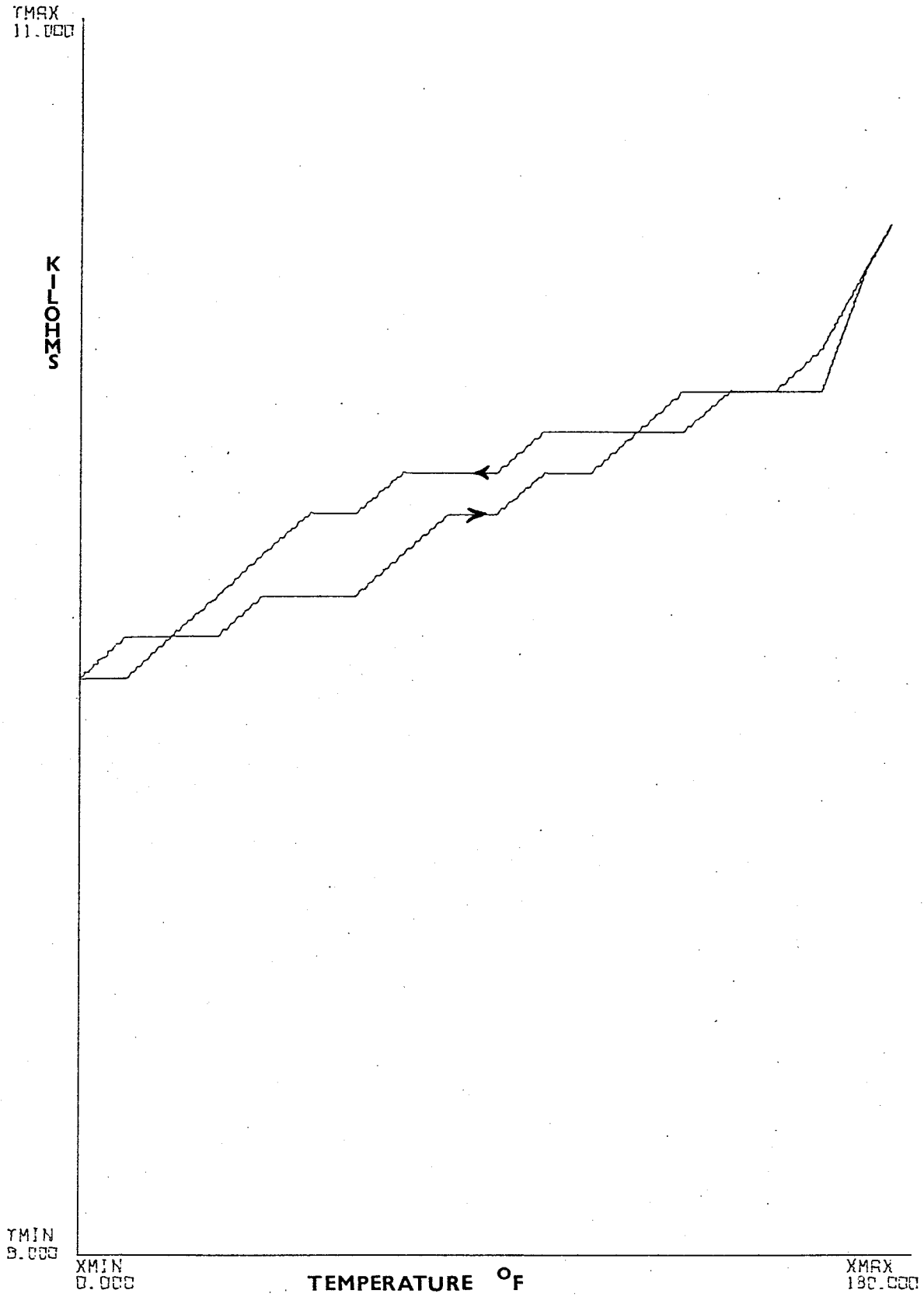

only changing by approximately 1 KΩ as demonstrated in the previous examples. It is therefore obvious that the temperature compensator is a novel scheme which operates in a satisfactory manner under laboratory test conditions.

While Figs. 5.2 to 5.7 illustrate how the pulses control the temperature of the compensating Moxie MX1, Fig. 5.8 shows how the converted pulses control the temperature of the metering Moxies MX2 and MX3 (note only response of MX2 is illustrated due to similiarity with MX3). To achieve this, MX1 was biased with a Mq of 60 KΩ resulting in a pulse train of frequency fp with average power Pq. In order to convert Pq to a dc level, the gain and offset control of the low pass filter OP10 were adjusted so that M2 equaled 60 KΩ at room temperature (70 °F). In addition the first derivative (dv/dfp) is another requirement which must be set so as to give minimum variance of M2 for ambient temperature changes around the quiescent temperature (T_o). As previously stated, due to the nonlinear frequency to temperature response of the compensating pulses and the linear response of the frequency to voltage converter, the compensator could not be adjusted to give complete compensation throughout the total temperature range. When sub-

FIGURE 5.8 TEMPERATURE COMPENSATION-60K

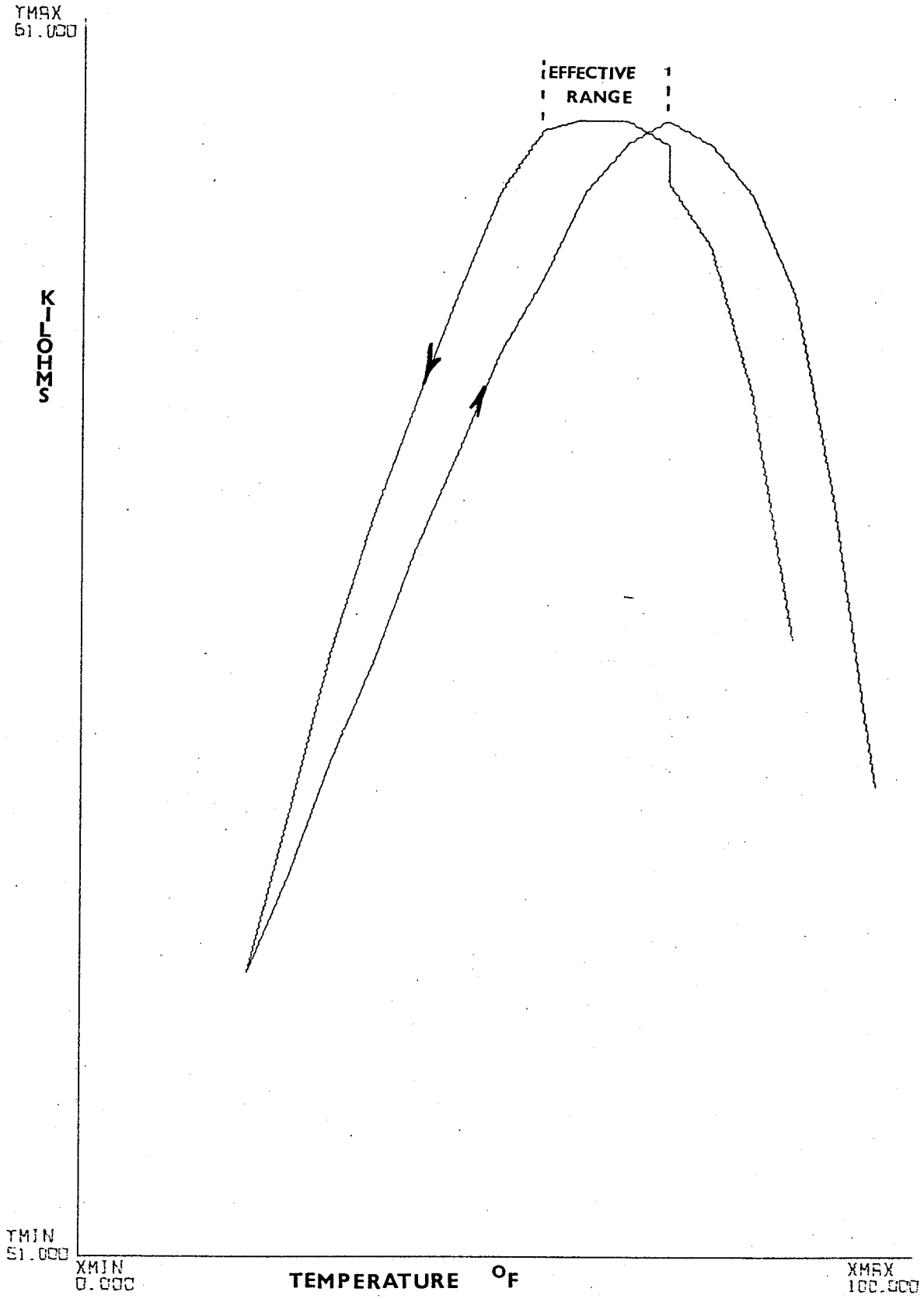

jected to a temperature variation of 75°F (20 to 95°F) M2 varied from 60.2 to 54.8, a 5.4 KΩ range which corresponds to a 40% reduction in Mq between the compensated and uncompensated cases. In order to plot Fig. 5.9 the settings on the temperature compensator were identical to those for the Mq of 60 KΩ and a processed signal was applied to increase M2 to 30 KΩ. The temperature was then varied to obtain a resistive excursion of M2 shown by the curve in Fig. 5.9 (32.7 to 24.1 KΩ) through a temperature range of 20°F to 95°F. The monotonic nature of the curve suggests that a lower gain would be more suitable to produce a better compensation for operation of MX2 at higher transition (i.e. a better choice of dV5/dfp in view of the non-linear fp vs T characteristic as may be seen from Fig. 4.8 and Fig. 4.9).

In general the compensation proved to be satisfactory and its best realigation would come when dual heater Moxies become available thus eliminating the need for the error introduced by using a frequency to voltage convertor.

It should be noted that the pulsed temperature compensation has a tendency to over correct (i.e. remove or replace more Pq than necessary). This phenomenon seems to occur as the temperature Tq of MX1 is

FIGURE 5.9 TEMPERATURE COMPENSATION-30K

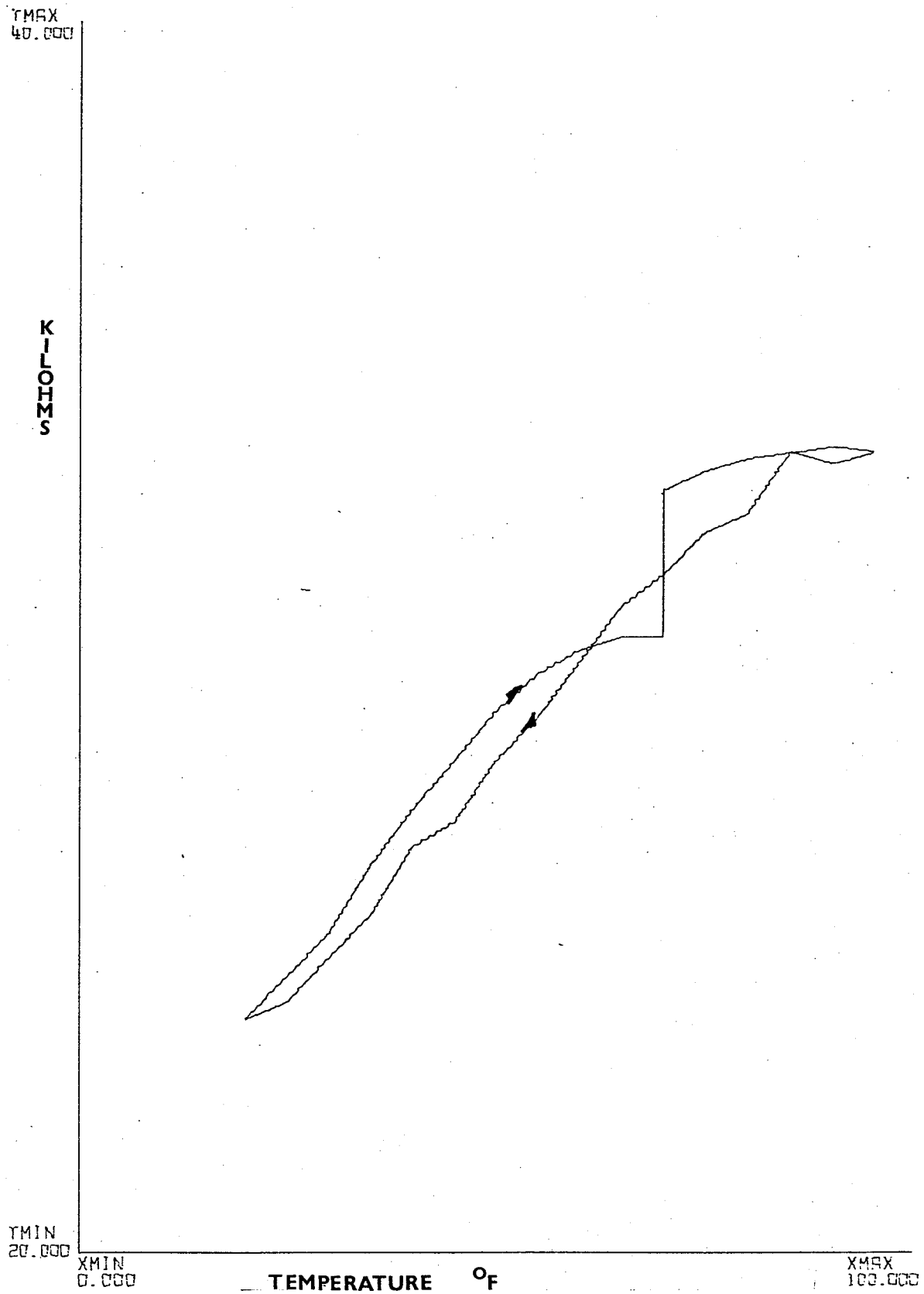

fluctuating between an upper and a lower level determined by V6 and V3 and as the frequency of the pulses increases the Moxie averages out a power level nearer to the upper limit and conversly, as the pulse frequency decreases the VO_2 film resistance hovers close to the lower limit.

5.2 Power Sensing Circuit

5.2.1 Experimental Layout

The wattmeter performance was tested under various simulated load conditions in the laboratory generated using a General Radio Low Frequency Oscillator which produces a variable phase shifted signal with respect to a reference voltage signal (see circuit diagram in Fig. 5.10). The latter represented V2 and was fed into OP2 while the former represented V1 and was fed into OP1. The signal generator has continuous phase adjustment, thus enabling good simulation of any power factor loading condition. The power supplies for the wattmeter were two Lambda regulated power supplies, Model LP411-FM. The processed signals (V1 + V2 and V1 - V2) were observed on a type 516 A Tektronix Oscilloscope. The voltage and terminal resistance

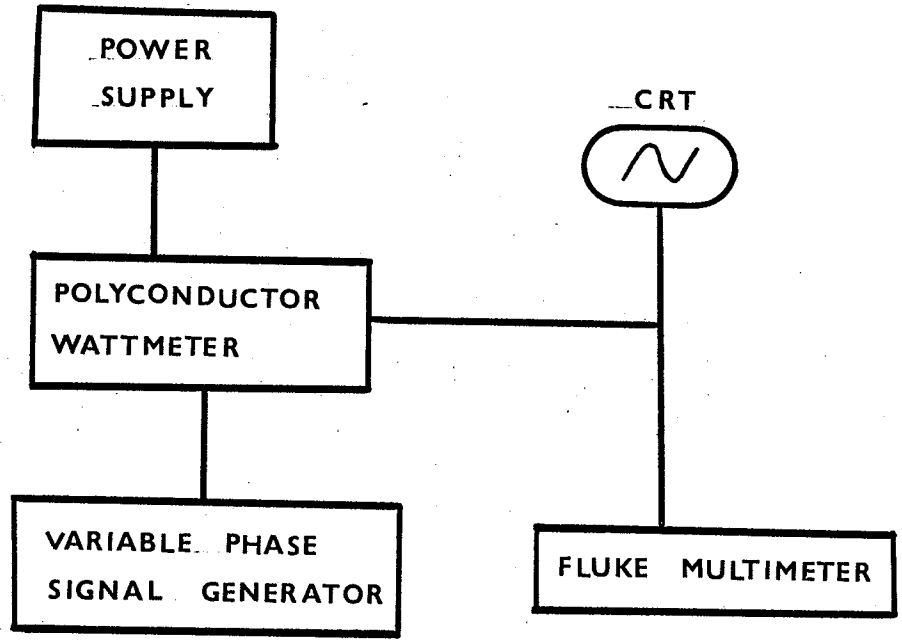

FIGURE 5.10 CIRCUIT DIAGRAM FOR POWER RESPONSE MEASUREMENTS

readings were displayed by a Fluke Model 8000-A Digital Multimeter. The polyconductor wattmeter circuit is fully described in Chapter 4 and Appendix B.

5.2.2 Power Response Curves - Procedure And Results

The wattmeter response curves presented in this sub-section were attained by synthetically introducing various load power facter conditions, thus enabling the voltages V1 and V2 to be varied both in magnitude and relative phase angle ($\emptyset$) with continuous resolution, something not easily generated with variable impedence loads.

Fig. 5.11 illustrates M3 - M2 as a unity power factor load curve (M3 - M2 being the proportional measure of load power as explained in Section 4.1.1). This graph was generated by the polyconductor wattmeter by setting V2 at the rated voltage of 2.75 V. and varying V1 from 0 to 2.75 V and back to 0 V. The lower curve depicts the increasing power condition (monotonically and at a rate slower than the thermal time constant of both Moxies) while the upper depicts the decreasing power condition. The maximum power sensed by the simulation occurs when V1 and V2 equal

FIGURE 5.11 RESISTANCE VS POWER

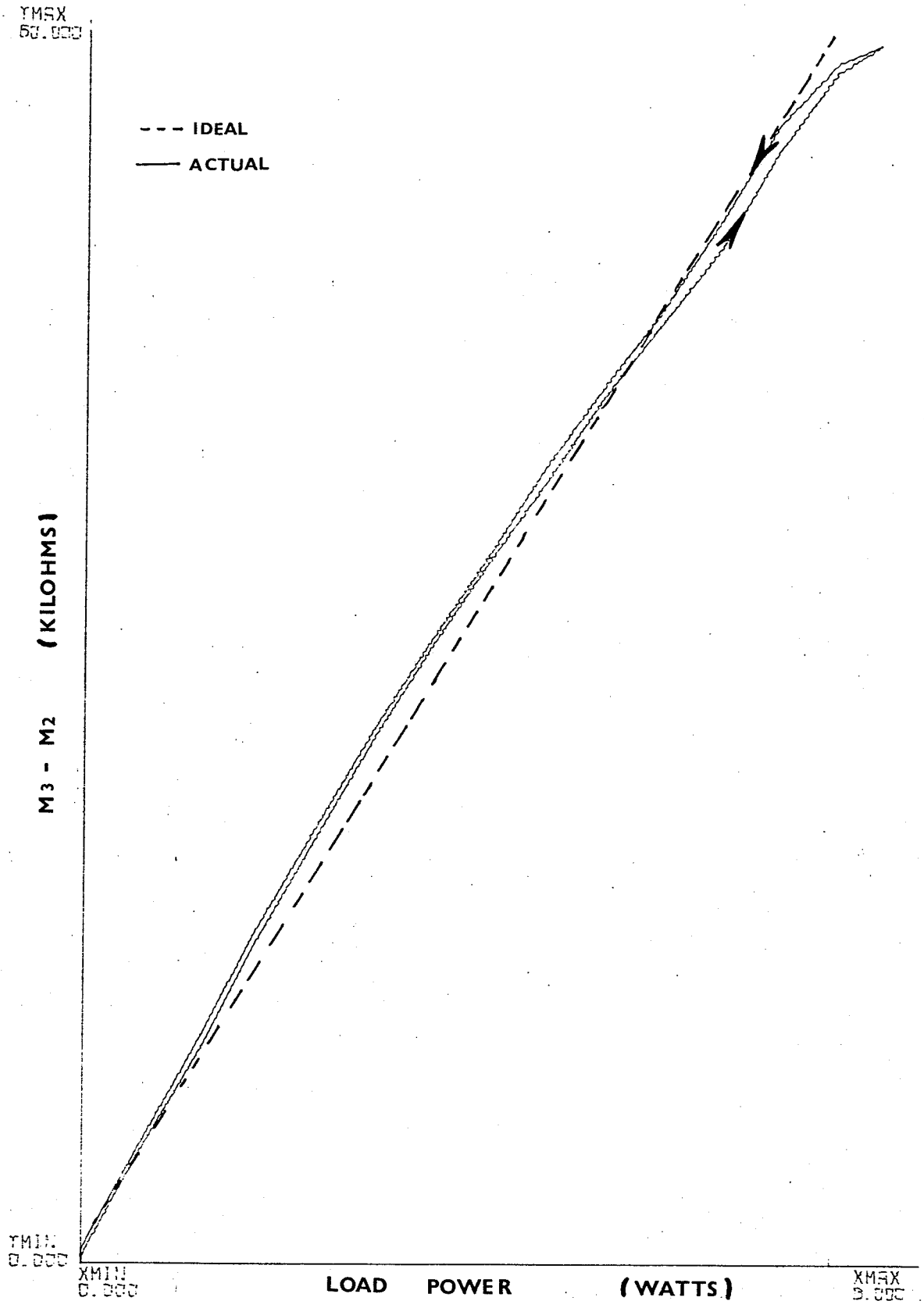

2.75 V, which corresponds to a load of 7.56 watts (since $\frac{V1V2}{R1}\cos\phi = 2.75^2$ for R1 = 1Ω where V1 and V2 are proportional to the line current and line voltage, respectively) which corresponds to the basic power condition necessary to produce a full excursion of the monitoring or dynamic range of the wattmeter for the Moxies employed in the circuit (i.e. V1 + V2 = 5.5 V and V1 - V2 = 0 V). Whole and fractional multiple of the dynamic range can be accomodated by corresponding reduction or enlargement (i.e. scaling with the appropriate factors) of the current shunt (R1) and the voltage divider ($\frac{R3}{R2 \times R3}$ which is equivalent to the ration $\frac{V2}{V_{phase}}$). The maximum hysteresis is illustrated by the major loop in Fig. 5.11 since a full transition of the dynamic range is simulated as MX2 will have maximum voltage (5.5 V) applied when V1 = 2.75 V and is in phase with V2. Smaller excursion of V1 would produce smaller minor hystersis loops with this major loop. One problem associated with this hystersis effect is that it necessitates readjustment of the bias points of MX2 and MX1 (adjustment of dc offset control R49 of OP10) after a complete power range had been simulated. This is because when the load power

was reduced to zero an erroneous bias point existed.

Fig. 5.12 illustrates how the sensing Moxies (MX2 and MX3) follow a square law response keeping in mind that curve A is generated by varying V1 and V2 simultaneously and curve B is identical to the curve in Fig. 5.11. In this comparison, if MX2 and MX3 had obeyed perfect square law relationship throughout the dynamic range, both curves would be identical and linear but it can be noticed that they in fact are dissmilar and nonlinear, thus indicative of a non perfect square law relationship. It should be noted that the most common use of a wattmeter is in a relatively constant line voltage and fluctuating current mode and thus the polyconductor wattmeter could be calibrated for this type of operation.

To determine the sensitivity of the wattmeter to real power, various load power factor conditions were simulated. Fig. 5.13 illustrates the meter response to volt amperes at selected power factors. These curves illustrate that the minimum value of VH3 (voltage V1 - V2 applied to H3 of MX3) was zero only at unity power factor. The minimum value reached of VH3 increases with increasing power factor, thus the maximum value of M3 - M2 decreases to zero for

FIGURE 5.12 RESISTANCE VS POWER

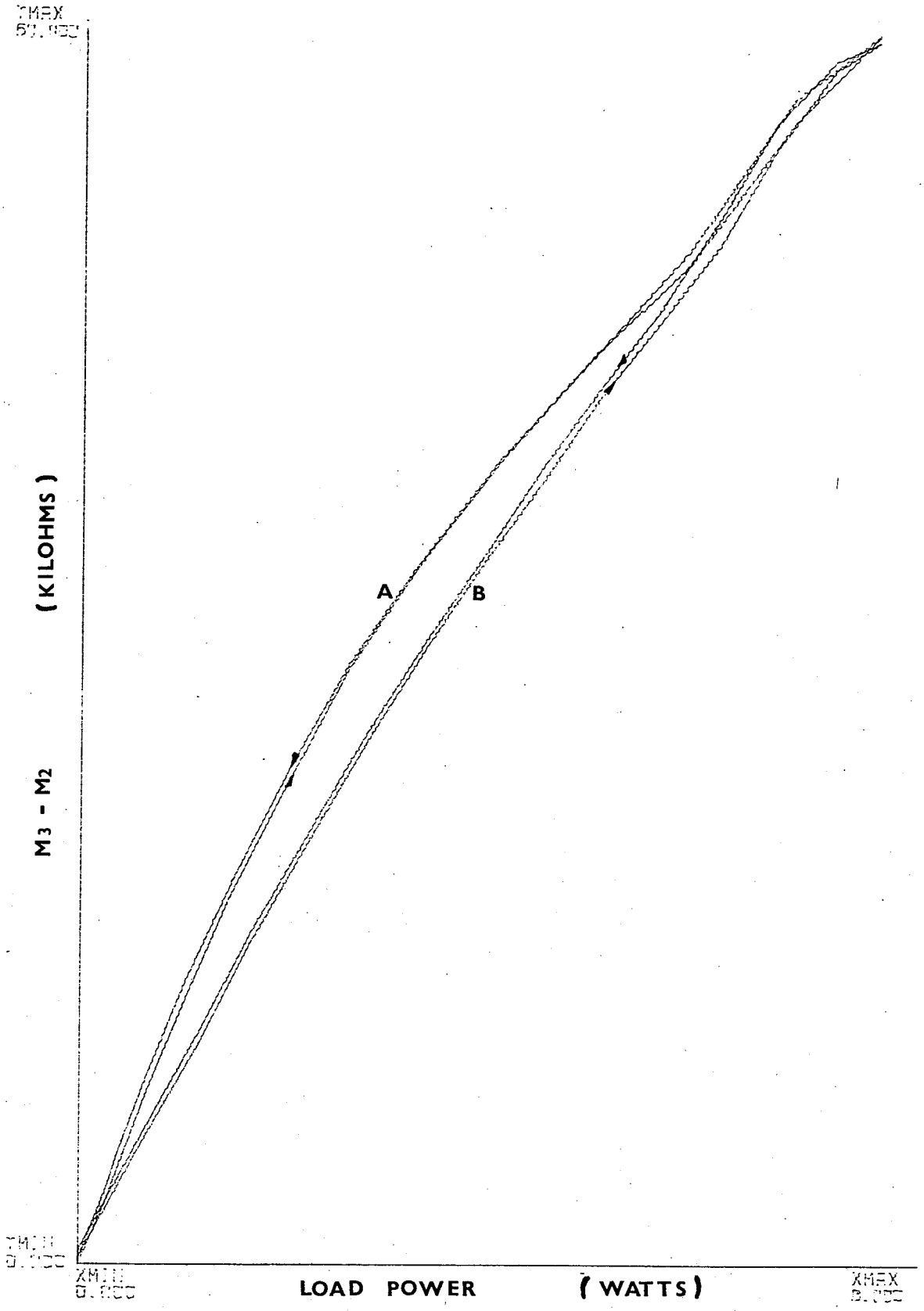

FIGURE 5.13 RESISTANCE VS VOLT-AMPERES

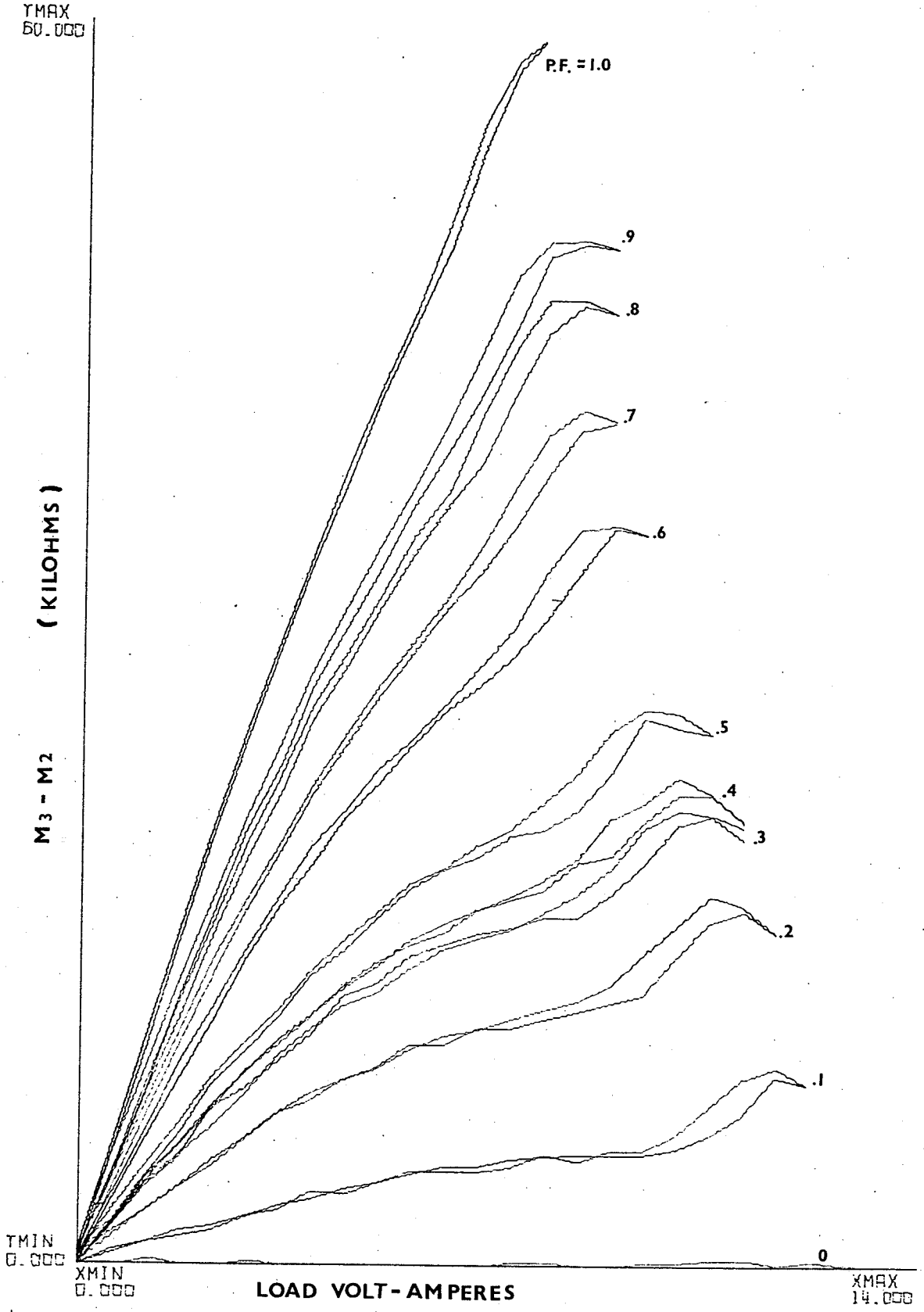

zero power factor. In Fig. 5.14 the abscissa is changed from volt amperes to real power (watts) to illustrate the meter's ability to sense real power under selected power factors. The unity power factor curve illustrates the maximum dynamic range which decreases with decreasing power factor as explained. Commercial wattmeter must accomodate power factors as low as .5 which in this case corresponds to an approximate 50% reduction in the dynamic range of the meter.

The graphs presented in this sub-section indicate that the meter is capable of sensing real load power within certain restrictions (primarily dynamic range). Accurate calibration of the meter would prove difficult as a result of the uncertainty of a reading of an unknown load power due to the hysteresis effect. This and other Moxie associated conditions affecting accuracy are discussed in part in the next chapter.

It should be noted that reactive power could be measured by first phase shifting V1 (the voltage proportional to line current) by 90° and feeding the resultant to be processed (added and subtracted) with V2.

FIGURE 5.14 RESISTANCE VS POWER

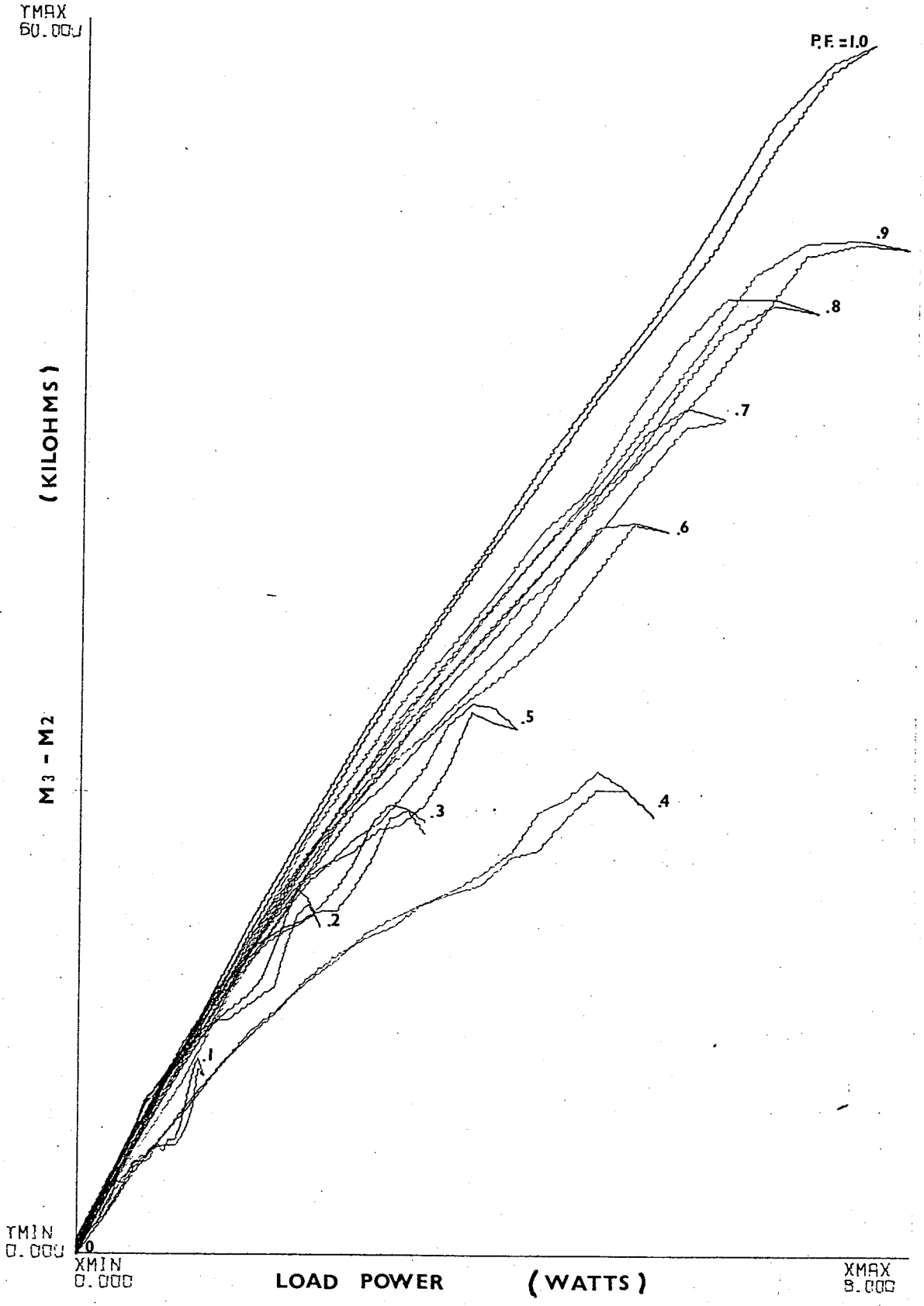

CHAPTER 6

SYSTEM ERRORS AND RESOLUTION

In this chapter a brief error analysis of the polyconductor wattmeter is presented to achieve an approximate error estimation due to circuit component tolerances and variation, temperature compensation and hysteresis, thermal and frequency response.

The possibilty of error magnification in the two main areas of the signal processing circuit is examined along with the effectiveness of both the temperature compensating schemes (pulsed and frequency to voltage conversion). The error due to the hysteresis phenomonon is calculated with the maximum hystersis loop. A minimum resolution or threshold is given with reference to the digital multimeter used in the experimental procedure. The same multimeter was in fact used as the standard for the power, voltage, current and resistance measurement throughout this experiment.

Errors associated with the thermal response of the Moxies are briefly discussed as well as a comment on the linearity of the meter.

6.1 Component Tolerance Effecting Output Error

In order to estimate the effect of components, tolerances or variations, a linear curve is approximated from the response curve in Fig. 4.4. This curve is approximated by a straight line extending from 50KΩ to 1KΩ and illustrated by curve C (dotted line). The slope of the linearized curve is -13.0KΩ per volt. The wattmeter output (M3-M2) vs load power can be approximated from the solid line of Fig. 5.11 by the dotted line whose slope is 8.45KΩ per watt. These two linearized response slope enable the approximation of the effect of component variation on the output.

To analyze the signal processing circuit the temperature compensation level is assumed to be ideal. As defined in Chapter 4, the voltages of interest VH3' and VH2',being V1-V2 and V1+V2, respectively. The tolerance conditions are investigated in the two main areas. First, an error may occur in either the value of R1 or R4 which will contribute to an error in V1 or similarily a variation may occur in R2 or R5 which will lead to an error in V2. The second type of error will occur in either addition or subtraction yeilding an

error in V1 or V2 at this stage of processing. An error may occur in the adder OP4 or OP5 but is of no particular concern since these adders will hopefully be eliminated when dual heater hysteresis free Moxies become available.

To analyze the first type of error, assume that V1 is represented as V1+δV1 and V2 is unchanged (no error). This error will be carried through to H2 and H3 and results in

$$VH2' = (V1+\delta V1+V2) \tag{6.1}$$

and

$$VH3' = (V1+\delta V1-V2) \tag{6.2}$$

To illustrate through a numerical example, assume this error to be 1% (i.e. $\delta V1/V1 = .01$) and V2 equals rated voltage. The linear approximation of M2(and M3 due to similiarity) in Fig. 4.4 lead to

$$M2 = (72.5-13.0(V1+V2))\ K\Omega \tag{6.3}$$

$$M3 = (72.5-13.0(V1-V2))\ K\Omega \tag{6.4}$$

V2 being 2.75 volts and current flowing to produce V1 = 1.00V. Note that M2 and M3 must equal 1KΩ when either V1+V2 or V1-V2 equal 5.50V. Substitution of these values of V1 and V2 into (6.3) and (6.4) yields

$$M2 = 23.75\ K\Omega$$

$$M3 = 49.75\ K\Omega$$

and hence

$$M3-M2 = 26.0\ K\Omega$$

Since V1 has increased by +1% it is now 1.01V giving new results for M2 and M3, i.e.

$$M2 = 23.62\ K\Omega$$

$$M3 = 49.88\ K\Omega$$

and hence

$$M3-M2 = 26.26$$

It is therefore obvious that a +1% error in the input produces a 1% error in the output and no error multiplication is evident.

In the second case the same error ($\delta V1$) will be assumed to take place in the adder and thus the heater voltages are:

$$VH2' = V1+\delta V1+V2 \qquad (6.5)$$

$$VH3' = V1-V2 \qquad (6.6)$$

Since the conditions before the error takes place are the same as the first case, we have

$$M3-M2 = 26.0\ K\Omega$$

and since VH3' remains the same, we also have

$$M3 = 49.75\ K\Omega$$

as before. Since V1 has changed by +1% the new value will be,as before

$$M2 = 23.62\ K\Omega$$

and thus

$$M3-M2 = 26.13\ K\Omega$$

which gives an output error of .5% indicating that the circuit has an inherent error reducing capability if an error occurs within the second region mentioned.

6.2 Temperature Compensation Error

The temperature compensation method consists of the pulsed scheme outlined in Chapter 4. A "trade off" compensation network is used in the wattmeter due to the unavailability of a dual heater Moxie in which the pulses V5 could be applied to one heater and the processed signal applied to the other heater. The "trade off" scheme is the frequency to voltage convertor described in Chapter 4. The error introduced by either scheme would be negligible if M2 and M3 remain within the linear range (1-50KΩ) as will now be explaned.

Assuming the availability of the dual heater Moxies and the linear curve of Fig. 4.4 it can be illustrated that negligible error results with limited temperature range (32-100°F) of the ambient temperature. The error is negligible so

long as M2 and M3 are kept within the ideal linear dynamic range. The pulsed compensation was tested at three different transition regions illustrated by Figs. 5.1, 5.3 and 5.5. If a straight line approximation is applied to these three curves the resulting slopes are approximately 12.5, 6.0 and 5.0 Ω/°F for the 60, 40 and 10KΩ bias settings, respectively. The temperature compensation seems to perform better at lower values of Mq (40KΩ and 10KΩ) than at the higher value (60KΩ). This is not necessarily true as the compensation will limit the temperature variance within the Moxie to similar limits but since at lower regions the incremental resistance change per °F ($d\overline{MI}/dT$) is less than at the higher regions, a smaller resistance change will be observed.

In practice the compensator will be set at the bias point of 60KΩ and the corresponding curve slope of 12.5Ω/°F should then be used in the analysis. The dynamic linear range is 1 to 50 KΩ, therefore assume that M3 equals 40KΩ when an ambient temperature variance is observed. The Moxie must increase its resistance by 10KΩ to break away from the aforementioned linear range. Fig. 5.3 illustrates that an increase in temperature is

required to increase the resistance of the device (an over correcting phenemonon). Therefore to increase M3 by 10KΩ an 800 F increase in ambient temperature would be required, but due to the fact that above 100 F the compensator reaches its upper limit, the device will rapidly decrease in resistance and the error becomes significant. The error is negligible until this upper limit is reached if both M3 and M2 will increase by similar amounts and the difference will remain approximately the same. On the other hand if M2 is 11KΩ it also has a 10KΩ region of deviation before it falls from the linear range. This 10KΩ decrease in resistance corresponds to an 800 F decrease in temperature if the curve of Fig. 5.3 is extrapolated linearly. This would not be the case because the lower limit will probably be observed (no limit was experimentally observed due to inadequate controlled temperature chambers available). This lower limit will be observed if the electronic components could tolerate such extreme temperature variations. The operational amplifiers are designed to operate above the lower limit of 32°F.

Fig. 5.8 illustrates the dc temperature compensator response. This curve (M2 or M3 vs T) is much inferior to the curve of Fig. 5.4 and has an

effective region from 50°F to 70°F where a relatively flat response is observed. Outside this region, the errors become significant as the compensator rapidly loses effectiveness.

6.3 Calibration Error Due To Hysteresis

The Moxies used in the polyconductor wattmeter have an inherent hysteresis loop which produces an uncertainity in a load power reading. The major hysteresis loop from the dual TC1-F 5V Moxie is illustrated in Fig. 2.6 in which a complete transition occured. The amount of hysteresis may be reduced if the polyconductor is not "pushed" through total transition but only operated in a dynamic range which includes a partial transition of the polyconductor. This phenomenon can numerically be illustrated by examining similar regions of two hysteresis curves, one curve being Fig. 2.6 where total transition is incured and the second being Fig. 4.4 where the polyconductor is limited to a partial transition dynamic range (i.e. 60KΩ to 1KΩ). An average difference of 3.08KΩ is the amount of hysteresis calculated from the total transition curve of Fig. 2.6, while an average

difference of 0.688KΩ represents the hysteresis of Fig. 4.4. It is thus shown that the hysteresis effect is reduced by 77.7% by limiting the dynamic range of partial transition of the polyconductors. This numerical result was obtained by calculating the average hysteresis between 60KΩ and 1KΩ and thus the 0.688KΩ hysteresis of Fig. 4.4 introduces an error of 1.17%. The average difference in the M3-M2 value at a particular power reading is calculated from Fig. 5.12 as 0.564KΩ which corresponds to 0.96% of the total range of 59KΩ which is approximately equal to the error calculated from the Fig. 4.4. A reason for the power hysteresis error being slightly smaller is that the difference (M3-M2) is calculated indicating an inherent partial cancellation of the hysteresis phenomenon.

An illustration of calibration error is shown in Fig. 6.1. Fig. 6.1A illustrates the critically damped case when the power is raised to the steady state point B from point A. The hysteresis curve is shown in Fig. 6.1B. The course traced out shows no minor hysteresis loop, the difference M3-M2 reached point B from point A. The slightly under damped case of Fig. 6.1C shows an over shoot of the final power level. In this case the minor partial hysteresis

FIGURE 6.1 CALIBRATION ERROR DUE TO HYSTERESIS

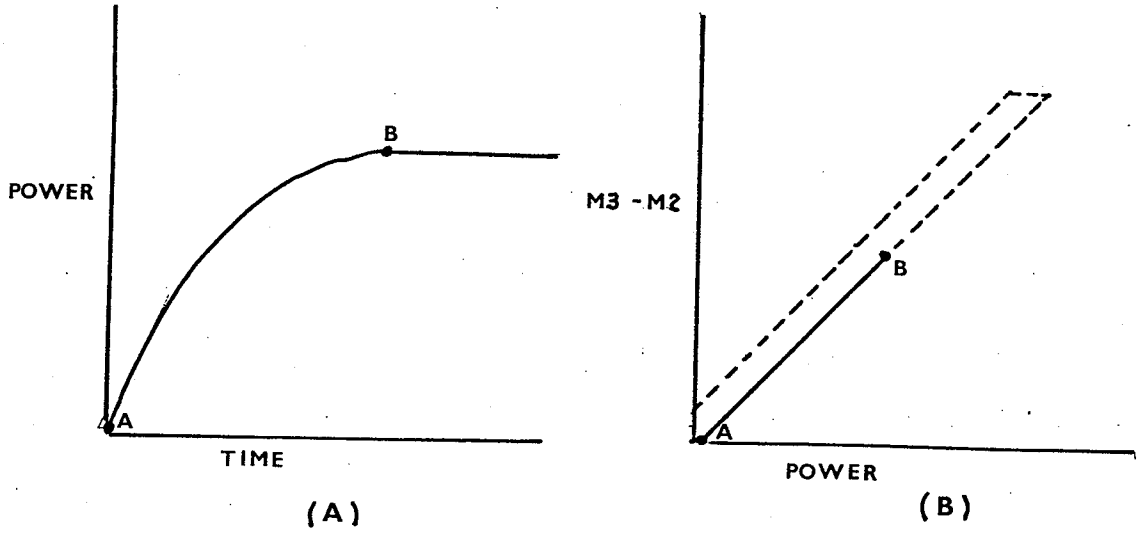

-----COMPLETE HYSTERESIS CURVE

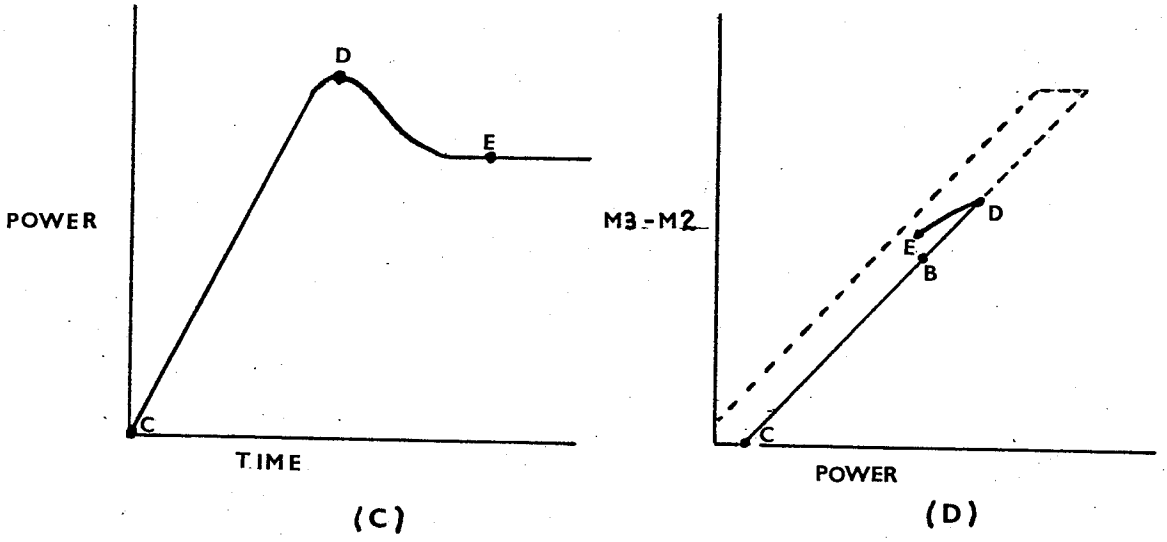

loop CDE illustrates how an erroneous reading is attained even though the final power reading is the same as in Fig. 6.1A. The maximum attainable error is .96% as stated previously.

6.4 Wattmeter Resolution Error

The wattmeter output was read from a digital multimeter which was capable of reading 1 part in 2,000. For experimental results in this study, the resolution on the wattmeter was the resolution of the resistance measuring device, in this case 0.05% of full scale. When full scale deflection was set at 200KΩ, the smallest increment observed is 100Ω. The slope of the differential resistance vs power curve of Fig. 5.11 is approximately 8.45KΩ per watt. Therefore, the load must change by at least 0.01 watt before a change in load is noticed if the voltage and current are varied simultaneously. If the meter is operating at rated voltage and the current is varied, a 100Ω output change is represented by a 50Ω decrease in M3 and a 50Ω increase in M2. Therefore no load change would be noticed as the individual readings changed by only 50Ω. In the case where current and voltage are varied simultaneously

M3 would remain at the bias point of 60KΩ and M2 would vary 100Ω and load change would be evident. The case of the rated voltage and variable current load, which is the most common one, a load change of .02 watt must occur before a load variation is experimentally sensed (without changing the meter range). This resolution error is approximately 0.26% (full scale deflection at unity power factor is 7.56 watts), whereas a simultaneous variance of load current and voltage produces an experimental resolution error of 0.13%. This error is quite small compared to the 0.96% hysteresis error, but would deserve more attention when the hysteresis free Moxies TS3-140 (see Fig.6.2) are available with dual heater elements.

6.5 Frequency And Thermal Response Error

The wattmeter frequency and thermal response are presented in this section in relation to two external variations, one being transient power while the other step ambient temperature variations.

6.5.1 Transient Power Variations

The frequency and thermal response of the wattmeter could introduce an error in the metering of transient energy once an integration is developed but due to

FIGURE 6.2

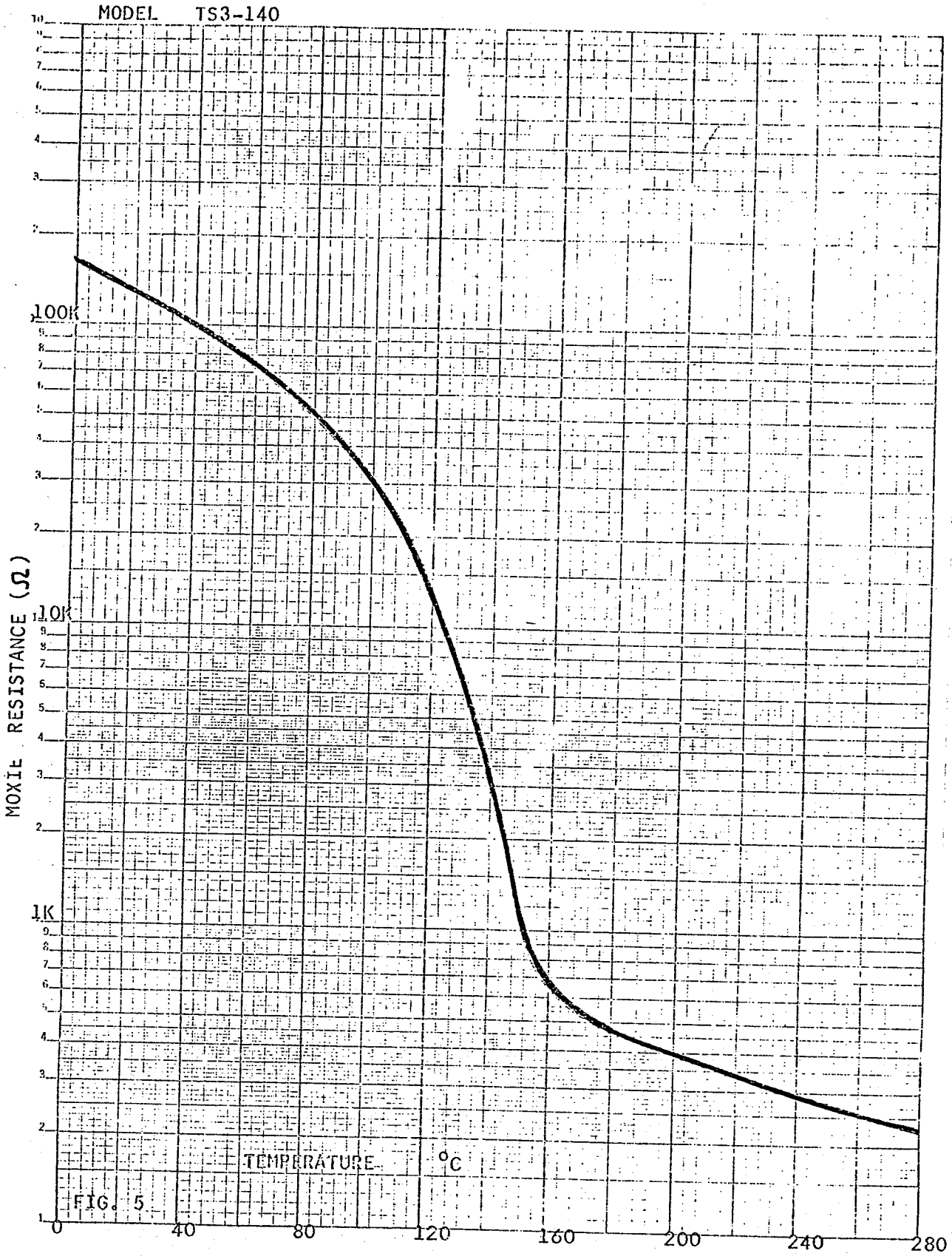
MODEL TS3-140
MOXIE RESISTANCE (Ω)
100K
10K
1K
TEMPERATURE °C
0
40
80
120
160
200
240
280
FIG. 5

the fact that energy metering personnel do not concern themselves with transient energy (14), this error would be of little importance. The ability of the meter to accurately sense transient power could correspond to how a polyconductor watthour meter responds to a narrow high amplitude energy pulse as compared to a wide low amplitude pulse of equal energy content (8).

In an ideal wattmeter the frequency spectrum with the energy pulse would be applied to the Moxie heater and the corresponding thermal energy would be applied to the polyconductor film, thus the shape of the pulse would have no effect on the accuracy of the meter. This ideal situation, however, does not exist and thus the transient energy sensitivity of the meter would depend upon the frequency response of the operational amplifiers and the thermal energy dissipation of the Moxie device.

Operational amplifiers act as low pass filters and the corresponding effect on accurately sensing the aforementioned energy pulses is illustrated in Fig. 6.3. The energy pulses could occur as current pulses thus voltage pulses would occur across the current shunt. For the purpose of this analysis the voltage pulses are assigned an equal area of

FIGURE 6.3 OPERATIONAL AMPLIFIER LOW PASS FILTER EFFECT ON VOLTAGE PULSES OF EQUAL ENERGY CONTENT

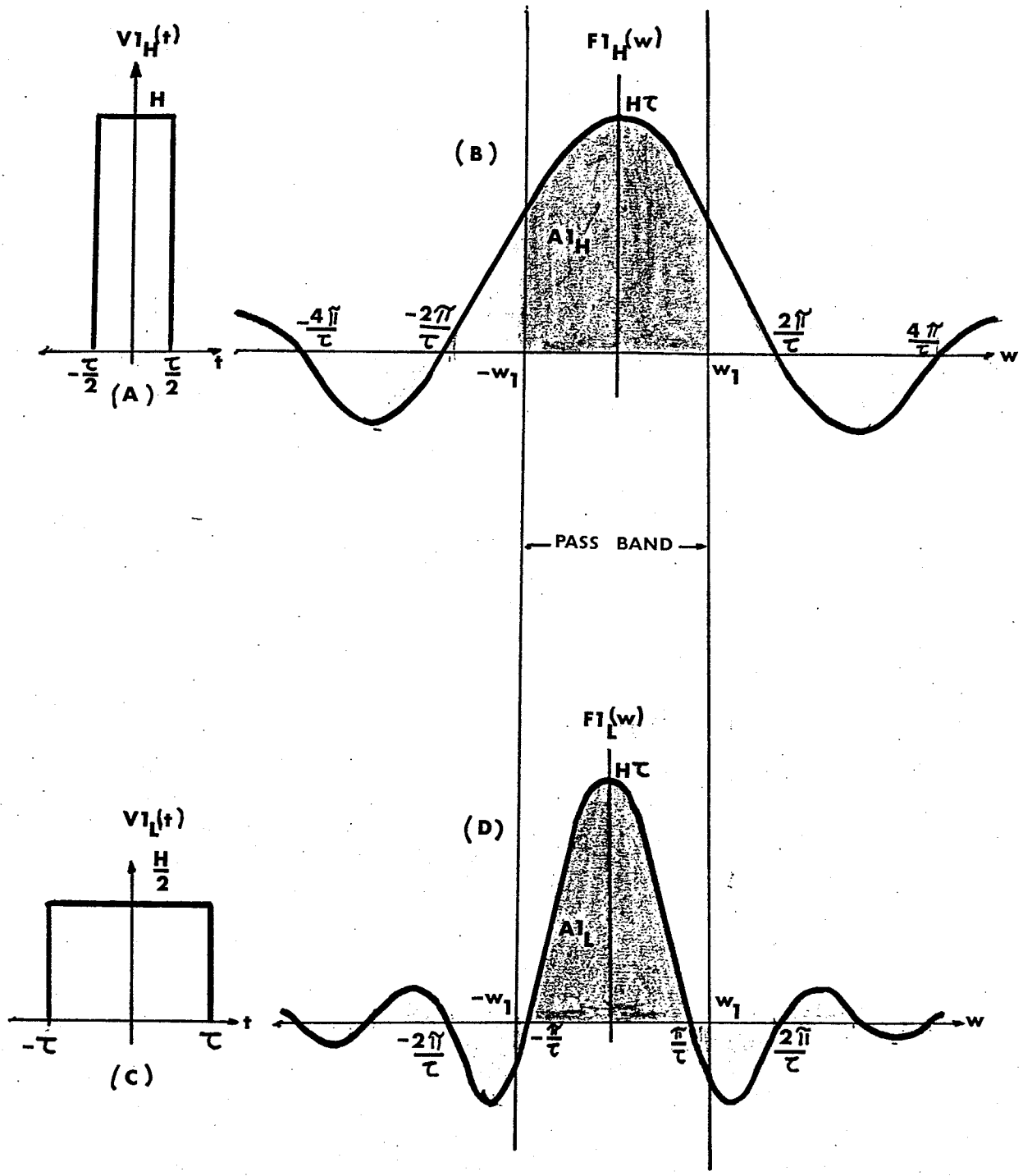

H volt-seconds which would correspond to an equal energy content condition as the wattmeter is to be operated at rated line voltage. The narrow high pulse $Vl_H(t)$ (Fig. 6.3A) is defined by

$$Vl_H(t) = \begin{cases} H & |t| < \frac{\tau}{2} \\ 0 & |t| > \frac{\tau}{2} \end{cases} \quad \text{VOLTS} \qquad (6.1)$$

in the time domain and has a spectral density (Fig. 6.3D) defined by the Fourier transform

$$Fl_H(\omega) = A\ Sa\left(\frac{\omega\tau}{2}\right) \quad \text{VOLTS} \qquad (6.2)$$

The wide low amplitude pulse (Fig. 6.3C) is defined by

$$Vl_L(t) = \begin{cases} \frac{H}{2} < |t| \\ 0 > |t| \end{cases} \quad \text{VOLTS} \qquad (6.3)$$

with a corresponding spectral density (Fig. 6.3D) defined by the Fourier transform

$$Fl_L(\omega) = A\ Sa(\omega\tau) \quad \text{VOLTS} \qquad (6.4)$$

The operational amplifiers have a corresponding pass band ($-\omega_1$ to ω_1) which consists of the heavily shaded areas of $Fl_H(\omega)$ and $Fl_L(\omega)$ represented as Al_H and Al_L

respectively. If Al_H doesn't equal Al_L there would be an error associated with the frequency response of the operational amplifiers as will be shown next. Since the spectral densities are symetric the area Al_H can be defined as

$$Al_H = 2 \int_0^{\omega_1} Fl_H(\omega)d\omega \tag{6.5}$$

$$= 2 \int_0^{\omega_1} A\ Sa(\frac{\omega\tau}{2}) \tag{6.6}$$

and similiarily Al_L can be defined as

$$Al_L = 2 \int_0^{\omega_1} Fl_L(\omega)d\omega \tag{6.7}$$

$$= 2 \int_0^{\omega_1} A\ Sa(\omega\tau)d\omega \tag{6.8}$$

The integrals (6.6) and (6.8) can be evaluated with use of the Si(x) function which is evaluated in tables (13) and defined by

$$Si(z) = \int_0^z Sa(x)dx \tag{6.9}$$

Substitution of (6.9) in (6.6) yields

$$Al_H = 4H\ Si(z)\Big|^{z_1} \tag{6.10}$$

where $z = \frac{\omega\tau}{2}$ and $z_1 = \frac{\omega_1\tau}{2}$

and similar substitution of (6.9) into (6.8) yield

$$Al_L = 2H\ Si(z)\Big|^{2z_1} \qquad (6.11)$$

where z and z_1 are as in (6.11). Two sample substitutions of $z_1 = 2.0$ and $z = 3.0$ yield

$$Al_H\Big|_{z_1=2.0} = 4H(1.605) = 6.42H \text{ VOLT-RADIANS}$$

$$A2_H\Big|_{z_1=2.0} = 2H(1.76) = 3.52H \text{ VOLT-RADIANS}$$

$$Al_H\Big|_{z_1=3.0} = 4H(1.85) = 7.4H \text{ VOLT-RADIANS}$$

$$Al_L\Big|_{z_1=3.0} = 2H(1.42) = 2.84H \text{ VOLT-RADIANS}$$

Similar substitutions yeild numerical values of Al_H greater than Al_L due to the factor of 2(ie 4H and 2H in(6.10) and (6.11), respectively) between Al_H and Al_L.

It can be concluded from this numerical analysis that more energy would be applied to the heater due to a high amplitude, narrow pulse of energy with respect to a low amplitude, wide pulse of equal energy content thus an erroneous output reading would result from the low pass filter characteristics of operational amplifiers.

The possibility of error due to different thermal

energy dissipation to the surrounding medium corresponding to the aforementioned equal energy content related pulses $Vl_H(t)$ and $Vl_L(t)$ can be discussed as follows. A narrow high voltage pulse $Vl_H(t)$ would generate a higher temperature and thus higher rate of heat dissipation than the wider pulse of lower amplitude, $Vl_L(t)$, but the wider pulse would dissipate heat for a longer period than narrow pulse. The accuracy of the system in relation to heat dissipation would depend on whether equal amounts of thermal energy were dissipated in the Moxie film in these two cases. Calculation of the energy dissipations is deemed almost impossible and the only practical way of determining transient energy sensitivity would be under actual test conditions when an integrating scheme is developed for this meter (15).

Once this energy pulse occured the output of the meter would reach .6 of its final value in approximately 2.5 msec. later. This value was experimentally obtained by comparison of the pulse train V5 and voltage V3. Approximately .5 msec. (lag time) is required for the pulse to heat the heater and initiate heating of the polyconductor film (causing a reduction in V3). Once the heating

of the film is initiated 2.0 msec. are required before V3 decreases .6 of the total variation resulting from the input pulse (ie a thermal time constant of 2.0 msec. when measured under aforementioned conditions). Since both sensing Moxies have the results of the energy pulse applied simultaneously, any variation in the load would be sensed .5 msec. later and complete .6 of the output response 2.0 msec. after the time lag passed (the time lag associated with the operational amplifiers is negligible). It should be noted that the fast thermal time constant enables design of the pulsed temperature compensation as if this time constant was slow,(ie .05 sec. which corresponds to the lower frequency limit of the Thermal Couplers), the temperature fluctuation within the reference Moxie MX1 would be too large and cause a fluctuating bias point for the reference Moxies.

6.5.2 Temperature Compensator Response To Step Ambient Temperature Change

A properly designed temperature compensator should be able to respond to step changes in ambient temperature without producing errors. Fig. 6.4 illustrates what would occur when the reference Moxie MX1 senses a step variation (ΔTo) in ambient temperature To.

FIGURE 6.4

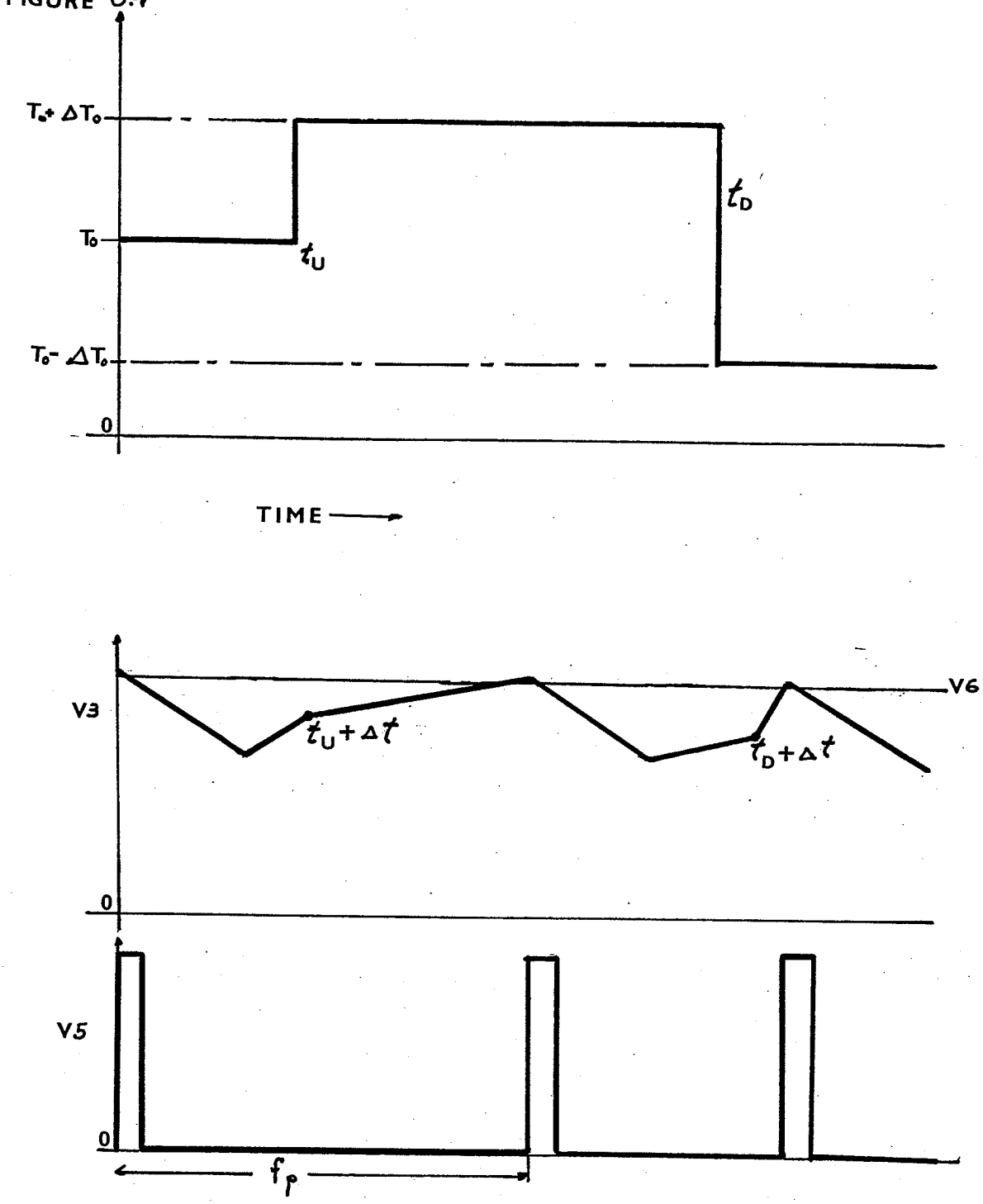

TEMPERATURE COMPENSATOR SENSITIVITY TO STEP AMBIENT TEMPERATURE CHANGES

These curves illustrate how the pulse frequency would change almost instantaneously once the temperature change is sensed. This is because the thermal time constant of MX1 is quite small and the thermal hysteresis involved is negligible. This change could occur during the heating or cooling region of the temperature compensator curve V3 but the frequency is mainly altered by variations in the cooling time thus the temperature disturbances are introduced during the cooling cycle in these graphs to illustrate the almost instant frequency shift. A temperature increase To is applied at a time t_u and the temperature controlled voltage V3 (ie Moxie resistance M1 senses temperature variations and in turn varies voltage V3) responds to the disturbance at a time $t_u+\Delta t$, time lag Δt being due to the thermal transportation time of the Thermal Coupler. This time lag is approximately 60 seconds which represents the time for a Thermal Sensor to change its temperature 63% in response to a step change in ambient air temperature (16). With the increase in temperature sensed, the rate of cooling is immediately decreased and thus the frequency fp is decreased. Similiarily a step decrease in temperature 2ΔTo is introduced at a time t_D and sensed by the reference Moxie at a time $t_D+\Delta t$.

Once the temperature decrease is sensed, the cooling rate of MX1, illustrated by V3, is increased and thus the frequency fp of V5 is increased to compensate for this temperature variation.

A frequency change is noted in both cases without losing the effect of the temperature compensator conditions before the disturbance occurs. If the disturbance is felt initially during the heating region, the pulse width would be effected accordingly (ie shorter for an increase in temperature and longer for a decrease in temperature) and the frequency fp would be changed since a different heat dissipation condition would already exist once the cooling region starts.

This almost instant temperature sensitivity is destroyed when the pulses are converted to a dc level as the low pass filter involved in the conversion has an electrical time constant of 1.0 second. The corrective voltage V7 would not be applied instantly and thus the sensing Moxies would first be subjected to a temperature variation due to the surrounding ambient temperature which produced the step variation initially, then subjected to another temperature variation as V7 corrects the effects of the variation and thus the small hysteresis affect would produce a negligible error as long as the effective dc temperature compensation range of 20 °F is not exceeded (see Fig. 5.7).

6.6 Meter Linearity

The ideal power response curve would be a linear relationship between the output response (M3-M2) and the input power (in watts) but unfortunately the meter does not respond in a perfectly linear fashion as illustrated by the deviation between the actual and the ideal curves of Fig. 5.11. The reason for this non-linearity of the output is due to the fact that the only available region of operation of the Moxies used in this study did not illustrate a perfect uniform square law relationship as illustrated by the difference in the two curves of Fig. 5.12 (as explained earlier in this study.

When the hysteresis free TS-140 Moxies (see Fig. 6.2) are available in a Thermal Coupler configuration a region which displays the best relationship could be selected for the dynamic range of the sensing Moxies as the transition temperature is 140°C, thus a larger above room temperature range is available in comparison with the TS-57 type polyconductor films used in this study.

CHAPTER 7

CONCLUSIONS AND SUGGESTIONS FOR RESEARCH

7.1 Conclusion

In this thesis an experimental wattmeter is presented in an attempt to overcome the mechanical and electrical difficulties with which induction type meters are associated. The polyconductor wattmeter has no associated mechanical problems but has a limited frequency response (due to operational amplifiers) but nevertheless this frequency range is larger than the induction type meter which is designed for specific frequency (ie 60 cycles per second). The polyconductors utilized in this meter have an inherent hysteresis loop which introduces an approximate 1% uncertainty as illustrated in the actual power response curve of Fig. 5.11. A novel pulsed temperature compensation scheme was presented and performed well under slow and fast switching transition regions, a characteristic not offered with a commercial compensator built by the Moxie manufacturer. In order to utilize it the pulsed compensation scheme was converted to a dc scheme in

which much of the effectiveness of the pulse type compensation was destroyed.

Although the total power factor response curves of Fig. 5.14 illustrate that the effective dynamic range of the polyconductor is reduced with decreasing power factor, this phenomenon could be accomodated by under rating the wattmeter to enable accurate measurement within specified power factor limits as is the case in domestic and industrial installations for which the basic idea of this wattmeter is intended.

The polyconductor wattmeter offers no inherent mechanical difficulties and an electrical type output. This electrical output (resistance) makes the meter suitable for remote meter readings applications for which it is intended.

7.2 Suggestions For Research

The two main difficulties with the polyconductor wattmeter are the hysteresis effect and the dc compensation scheme. At present there exists a hysteresis free Moxie TS3-140, whose terminal resistance vs temperature characteristic is illustrated in Fig. 6.2, but unfortunately is not manufactured in Thermal Coupler configuration. When this Moxie becomes available with a heating element and is utilized in the

polyconductor wattmeter, the hysteresis problem would dissappear. Similiarily if this TS3-140 Moxie was available with two heaters the pulse temperature compensation could be applied to one heater and the processed signal to the remainder thus eliminating the relatively ineffective dc compensation scheme.

Although operational amplifiers were employed to process the phase voltage and line current in the polyconductor wattmeter, a transformer type meter would be reasonable for a specific frequency range application (17). When the hysteresis free Thermal Couplers become available a watthour meter of this type would be a useful investigation experimentally since currently used domestic watthour meters do not read true power under certain conditions (14).

An integration scheme might be developed using a metal-nitride-oxide IC memory (18). This scheme would be especially attractive as it has a long term temperature independent charge retention ability associated with it.

Newly developed current transformers which use Yig tuned oscillators and transmit a frequency modulated signal to an isolated receiver (19) suggest a possible incorporation of a polyconductor meter in monitoring EHV and UHV loads as the analogue signal from the receiver could be fed into the signal pro-

cessing section out of the polyconductor meter.

The pulsed temperature compensator scheme could also be incorporated to develope new type meters or possibly improve the behavion of existing ones. The frequency fp of V5 corresponds to the ambient temperature thus if thermal power due to an unknown current was applied, the shift in frequency fp generated would indicate a value proportional to that current. The compensator could also be used in a digital ohmmeter scheme. The voltage V6 determines what value V3 will fluctuate around, R44 determines the degree of transition required to maintain V3 and this degree of transition dictates the pulse frequency fp as explained in Chapter 4. Therefore, with a constant V6 and substitution of R44 with an unknown resistance, the value of which is within the terminal resistance range of the Moxie, the pulse frequency fp will be dependent on the unknown resistance and thus a digital ohmmeter is conceived.

The meter presented in this study is believed to be the first wattmeter of this type to be built and serves as a basic prototype which could be developed in remote meter reading applications of on line power loads as referred to in Chapter 1.

BIBLIOGRAPHY

(1) Techniques Applied, "Remote Meter Reading", Control and Instrumentation, pp. 25, Oct. 1970.

(2) Davey, J., Campbell, C.A., Miltz, G.O., "Meters Remotely Read on 80 House Loop", Electrical World, pp. 62-65, May 6, 1973.

(3) Hellar, Martin W. Jr., "Automatic Meter Reading Not 'Just Around Corner' ", Electrical World, pp. 42-44, 126, Dec. 18, 1961.

(4) Hagan, William A., "A .1% Thermal Wattmeter to 20 KHz" 20th Annual ISA Conference and Exhibit, Oct. 4-7, 1965, Los Angeles.

(5) McAuliff, Dan, "Thermal Measurement of Electrical Quantities", Instruments and Control System, Vol. 37, pp. 102-105, Jan. 1965.

(6) Johnson, F:A: "Internal Pulse Power Dissipation in a VO_2 Polyconductor Film and Its Effect On Switching Speed", DREO Technical Note NO. 73-2.

(7) Multi-State Transition Metal Polyconductors "Thermal Coupler", Data Sheet TC, Issue 2.

(8) Private Communication with Dr. M.A.K. Hamid, University of Manitoba.

(9) Ferns "Where is Cheap Watthour Solid-State Meter", Electrical World, pp. 37, 38, Oct. 20, 1969.

(10) Karsa, Bela, E.F., "Electrical Measuring Instruments and Measurements.

(11) Alexander, "Instruments and Measurements " NO. 5., Cleaver - Hume Electrical Series, 1951.

(12) Multi-State Devices Ltd., "Moxie Applications".

(13) Abramowitz, M., Stegun, I.A., "Handbook of Mathematical Functions", Dover Publications, Inc, New York, 1968.

(14) Private Communication with Mr. Joe Taylor, Department of Consumer and Corporate Affairs of Canada.

(15) Private Communication with J.P. McMath, University of Manitoba.

(16) Multi-State Moxie Thermal Sensors (Preliminary TS3 Specifications) Multi-State Devices Ltd., Dec. 3, 1973.

(17) Private Communication with C. Ward, Manitoba Hydro.

(18) Britton, James, Cricchi, J.R., Ottobre, L.G., "Metal-nitride-oxide IC memory retains data for meter reader", Electronics, pp. 119-123, Oct. 23, 1972.

(19) Stuckly, S.S., Tarnawecky, M.Z., "A Microwave Current Transformer", IEEE PES Seminar, Dec. 4, 1974, University of Manitoba.

APPENDIX A

AC AND DC POWER SUMMATION IN A MOXIE HEATER

Since a dual heater Moxie device was unavailable the temperature compensation pulses were converted to a dc level using a frequency to voltage convertor. The desired result is that the temperature compensating dc power level would not be altered when the ac processed signal was applied. The sum of the two voltages (ac and dc) is

$$V_H = E_{dc} + E_m \sin(\omega t) \qquad (A.1)$$

where V_H is the total voltage applied to the heater, E_{dc} is the dc voltage and E_m is the peak value of the ac voltage. The instantaneous power dissipated in the heater is proportional to the square of V_H

$$p = \frac{V_H^2}{H} = \frac{1}{H}(E_{dc} + E_m \sin(\omega t))^2 \qquad (A.2)$$

where p is the dissipated instantaneous power and H is the resistance of the heater. The Moxie device responds to the average power dissipated in the heater which can be determined by averaging over a over a period as follows

$$\frac{\omega}{2\pi}\int_0^{\frac{2\pi}{\omega}} p\,dt = \frac{\omega}{2\pi H}\int_0^{\frac{2\pi}{\omega}} (E_{dc}+E_m\sin(\omega t)^2 dt$$

$$= \frac{\omega}{2\pi H}\int_0^{\frac{2\pi}{\omega}} (E_{dc}^2+\frac{E_m^2}{2}+2E_{dc}E_m\sin(\omega t)-\frac{E_m}{2}\cos(2\omega t))dt \quad (A.3)$$

s

and since the average of the ac terms are zero, we have

$$Pav = \frac{E_{dc}^2}{H} + \frac{E_m^2}{2H}$$

$$= \frac{E_{dc}^2}{H} + \frac{E_{rms}^2}{H} \quad (A.4)$$

where E_{rms} is the rms ac voltage and Pav is the average power dissipated in the heater. Thus the temperature compensation is retained and as referred to in Chapter 4 the terminal resistance vs applied voltage curves will vary (from ac to dc) but the total power applied remains the same.

APPENDIX B

DESCRIPTION OF PHYSICAL CONSTRUCTION

The wattmeter was built on copper backed Vero boards, mounted on removeable front and back panels of a Hammond enclosure. There are three Vero boards mounted on the front panel (see photograph Fig. B.1), one board containing the 9 of the 10 operational amplifiers and associated circuitry, joined by Jumper 1 to the second board which acts as junction panel for Jumper 2 which electrically joins the front panel to the back panel. The third board on the front panel contains the complete voltage to frequency converter. The single board on the back panel acts as a junction panel for Jumper 2 on the rear panel side. Moxies MX1, MX2, MX3 and transistor Q1 are mounted on seperate heat sinks attached to the rear panel while transistors Q2, Q3, Q4 and Q5 are mounted on a common heat sink and since transistors Q6, Q7 and Q9 are used in a low power mode there are no heat sinks required.

The photograph in Fig. B.2 illustrates the various quantities associated with the binding posts mounted on the front panel.

FIGURE B.1 ACTUAL CIRCUITRY

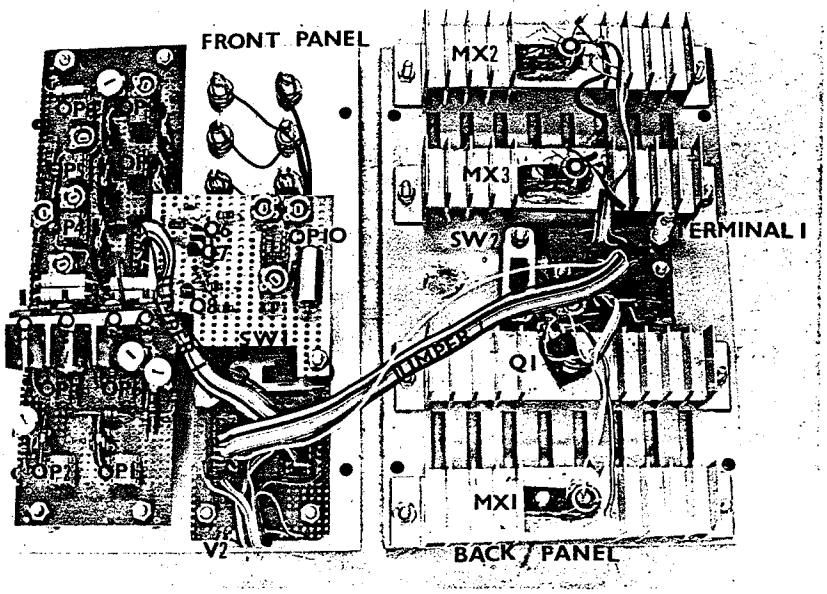

FIGURE B.2

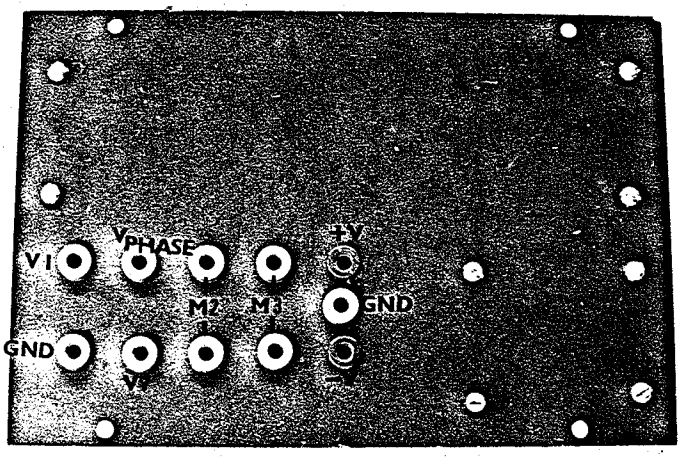

FRONT PANEL

The circuit diagram of the two jumpers used in connection of the various Vero boards previously mentioned is shown in the photograph Fig. B.3 with colour coding information given in Table B.1.

The electronic components description is given in Table B.2.

The complete polyconductor wattmeter assembly is shown in photograph Fig. B.4.

FIGURE B.3

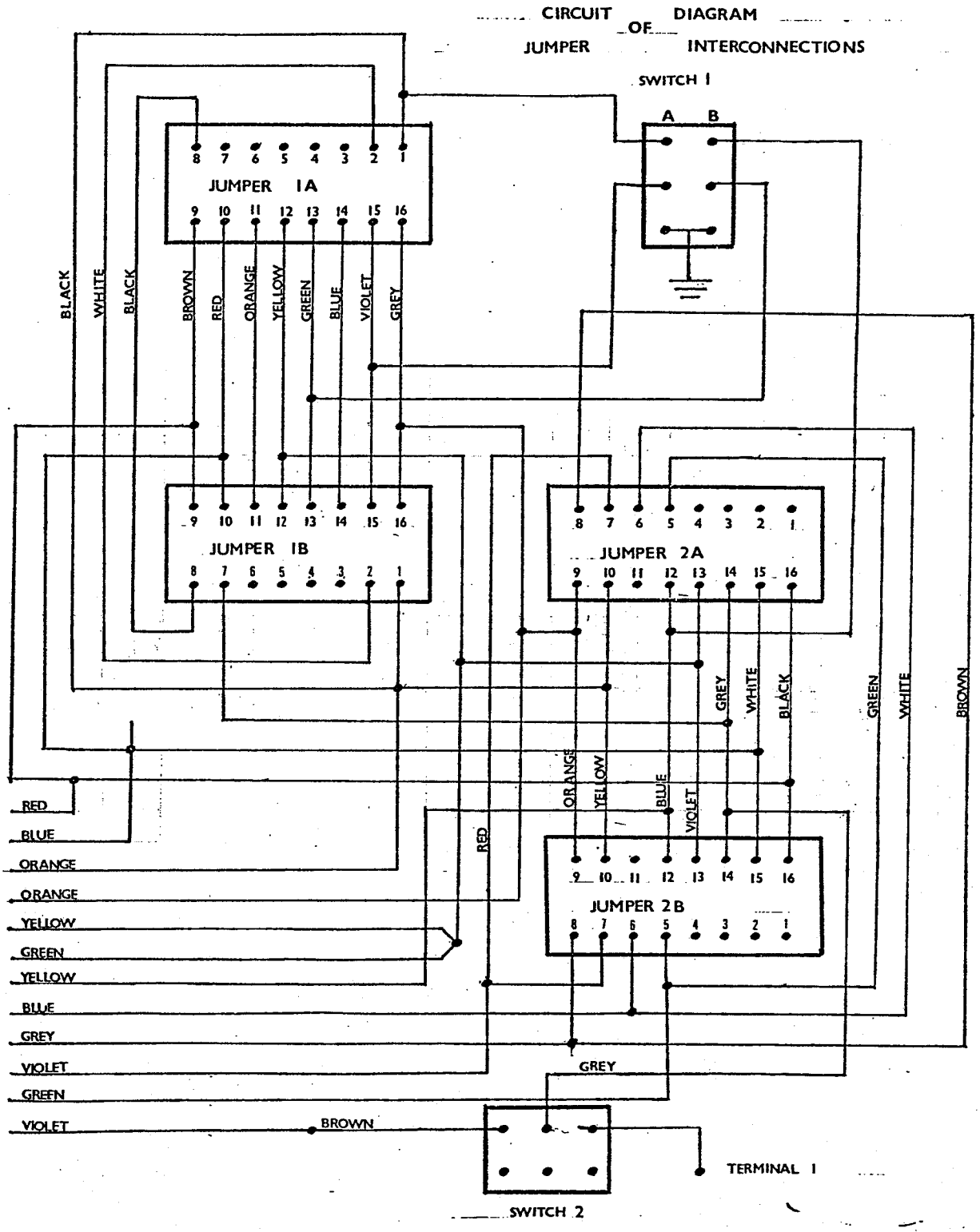
CIRCUIT DIAGRAM OF JUMPER INTERCONNECTIONS
SWITCH 1
A
B
JUMPER 1A
JUMPER 1B
JUMPER 2A
JUMPER 2B
BLACK
WHITE
BLACK
BROWN
RED
ORANGE
YELLOW
GREEN
BLUE
VIOLET
GREY
RED
BLUE
ORANGE
ORANGE
YELLOW
GREEN
YELLOW
BLUE
GREY
VIOLET
GREEN
VIOLET
BROWN
GREY
WHITE
BLACK
GREEN
WHITE
BROWN
TERMINAL 1
SWITCH 2

TABLE B.1 COLOUR CODE OF JUMPERS

Pin No.	Colour	Description
Jumper No. 1		
1	Black	+V
2	White	V1
8	Black	Base of Q1
9	Brown	Heater H3 of MX3
10	Red	Frequency to voltage output V7
11	Orange	-V
12	Yellow	Ground
13	Green	Temperature Compensation voltage V3
14	Blue	V2
15	Violet	Reference voltage of OP9 (+V or OV
16	Grey	Heater H2 of MX2
Jumper No. 2		
5	Green	Resistance of Moxie MX3 (M3)
6	White	
7	Red	Resistance of Moxie MX2 (M2)
8	Brown	
9	Orange	Heater H2 of MX2
10	Yellow	+V
12	Blue	Temperature Compensation voltage V3
13	Violet	Ground
14	Grey	Base of Q1
15	White	Temperature Compensation Pulses V5
16	Black	Heater H3 of MX3

TABLE B.2 COMPONENT DESCRIPTION

Resistors:

R1	- chosen to give 2.75 voltage drop across it at rated current
R2	- 1KΩ 1/2 watt trimmer pot
R3	- 100KΩ 1/4 watt 5%
R4, R5, R11, R13, R22 R36, R41, R42, R45	- 10KΩ 1/2 watt trimmer pot
R6, R8, R9, R12, R15, R28, R29, R32, R33, R35, R37, R39, R40, R52, R54	- 10KΩ 1/4 watt 5%
R7, R10, R21, R30, R38	- 470Ω 1/2 watt trimmer pot
R20, R27	- 4.7KΩ 1/2 watt trimmer pot
R16, R19, R23, R26,	- 3.3KΩ 1/4 watt 5%
R31	- 1KΩ 1/2 watt 5%
R17, R18, R24, R25	- 5Ω 1 watt 5%
R43	- 120KΩ 1/4 watt 5%
R44	- 470KΩ 1/2 watt trimmer pot
R46	- 47KΩ 1/2 watt 5%
R47	- 4.7KΩ 1/2 watt trimmer pot
R48	- 100KΩ 1/2 watt trimmer pot
R49, R50	- 1KΩ 1/2 watt trimmer pot
R51	- 100Ω 1/2 watt trimmer pot
R53	- 39KΩ 1/4 watt 5%
R55	- 680Ω 1/4 watt 5%

Polyconductors:

MX1, MX2, MX3	- Dual TC1-F 5V

Transistors:

Q1	- MJE 3055 BJT
Q2, Q4	- MJE 180 BJT
Q3, Q5	- MJE 170 BJT
Q6, Q7, Q8	- 2N2495

Diodes:

D1, D2, D3, D4, D5, D6	- IN 4005

Operational Amplifiers:

OP1, OP2, OP3, OP4, OP5. OP6, OP7, OP8, OP9	- ML741 CS 7340
OP10	- ML307

Capacitors:

C1	- .1μf
C2	- 100μf
C3	- 2200pf

FIGURE 8.4 POLYCONDUCTOR WATTMETER